Separation of Liquid Mixtures by Membranes

Yi Fang

A thesis submitted to the School of Graduate Studies and Research

in partial fulfilment of the requirements for the

degree of

DOCTOR OF PHILOSOPHY

in the Department of Chemical Engineering

University of Ottawa

Yi Fang
Ottawa, Ontario

1996

National Library of Canada

Acquisitions and Bibliographic Services Branch

395 Wellington Street
Ottawa, Ontario
K1A 0N4

Bibliothèque nationale du Canada

Direction des acquisitions et des services bibliographiques

395, rue Wellington
Ottawa (Ontario)
K1A 0N4

Your file Votre référence

Our file Notre référence

ISBN 0-612-19956-8

Canada

UNIVERSITÉ D'OTTAWA
UNIVERSITY OF OTTAWA

Abstract

Membrane separation of liquid mixtures was attempted by pervaporation and reverse osmosis. The study focused on the interface, morphology and transport involved in pervaporation and reverse osmosis separation of liquid mixtures.

The first part of this study concerns pervaporation separation of liquid mixtures. A novel method to modify a membrane surface is proposed. A fluorine-containing surface modifying macromolecule (SMM) was added into a polyethersulfone (PES) membrane casting solution. Because of its lower surface energy, SMM is expected to move up to the top surface of the membrane. The resulting membrane is to have a layer of SMM at the top surface and a PES rich bulk substrate underneath. Asymmetric PES/SMM membranes were fabricated by the phase inversion method under various conditions and tested in pervaporation separation of chloroform/water mixtures. Membrane surface was characterized by contact angle and X-ray photoelectron spectroscopy (XPS) measurements.

The principal findings are: (i) The contact angles of water on the surface of PES/SMM membranes were significantly larger than those of PES membranes. (ii) The XPS results indicate a much higher fluorine concentration at the membrane surface than in the bulk and upwards orientation of SMM's fluorine tail at the membrane surface. It is concluded that SMM migrates to and accumulates at the membrane-air interface. The membrane surface can be covered by a layer of SMM. (iii) A PES/SMM membrane has a superior performance to a PES membrane for pervaporation separation of chloroform/water mixtures, since the former has a much higher water selectivity than the latter. (iv) A PES/SMM membrane has a higher permeation rate of n-heptane and a lower permeation rate of ethyl alcohol than a PES membrane in pervaporation separation of ethyl alcohol/n-heptane mixtures.

The second part of this study concerns reverse osmosis of liquid mixtures. A new method to determine the preferential sorption in binary mixtures based on liquid chromatography is presented. Liquid chromatography and liquid sorption experiments were performed for cellulose acetate butyrate (CAB)/ethyl alcohol/n-heptane system. An interaction force constant characterizing the interaction between the feed species and the membrane was generated and incorporated in the transport equations based on a pore model. Transport simulation was performed for reverse osmosis separation of ethyl alcohol and n-heptane by the CAB membrane.

It was found that (i) Both CAB powder and homogenous membrane preferentially sorbed ethyl alcohol from the binary liquid mixtures of ethyl alcohol and n-heptane; (ii) Sorption data can be calculated based on the liquid chromatography data. The calculated values are well in line with the data from the homogeneous CAB membrane. The good agreement between the two indicates the validity of the proposed approach; (iii) The binary liquid mixtures can be separated by reverse osmosis, and its performance can be calculated using the transport equations based on a pore model. The calculated data represent the experimental ones reasonably well. Thus, the proposed approach can be considered as a valuable one.

In the last part of this study, reverse osmosis and pervaporation experiments were performed and their results were compared for two cases, namely, separation of ethyl alcohol/n-heptane mixtures by the CAB membrane, and separation of a vinyl acetate/hexane mixture by four different membranes. It was found that pervaporation had a higher separation than reverse osmosis in the separation of ethyl alcohol/n-heptane mixture and vinyl acetate/hexane mixture. For both reverse osmosis and pervaporation, ethyl alcohol was enriched in the permeate by the CAB membrane, and vinyl acetate permeated preferentially through the laboratory made CAB membrane and aromatic polyamide membrane, although vinyl acetate was only slightly concentrated in the permeate for FT-30 and silicone rubber membranes.

Acknowledgement

I wish to express my sincere appreciation and gratitude to Professor T. Matsuura for his invaluable guidance, continued encouragement and constructive criticism throughout the course of this study including the preparation of the thesis.

My sincere thanks are due to Professor J. P. Santerre and his research group including Mr. V. A. Pham of Department of Biomaterials, University of Toronto, and Professor R. M. Narbaitz and his research group including Mr. J. Minnery and Mr. H. Mahmud of Department of Civil Engineering, University of Ottawa for their helpful suggestions and help. The equipment and technical support provided by the Machine Shop in the Department of Chemical Engineering at the University of Ottawa are deeply appreciated as well.

I also would like to thank people at the Industrial Membrane Research Institute, my parents and family, and all those who helped me directly and indirectly in the course of study.

The financial support of the Natural Science and Engineering Research Council of Canada is gratefully acknowledged.

Nomenclature

a_A	activity of component A
Λ_m	the area covered by each adsorbate molecule, m^2/molecule
b_A	the friction constant defined in Equation (29)
$\underline{B}$	constant characterizing the van der Waals force, m^3
C	total concentration, mol/m^3, or constant related to heat of adsorption
$\overline{C}_A$, $\overline{C}_B$	average concentrations of component A and B in the pore, respectively, mol/m^3
$C_{A,b}$	concentration of component A in the bulk, mol/m^3
C_t	total molar concentration of the mobile phase, mol/m^3
d	distance on the chromatography chart, m
$\underline{d}$	distance between polymer surface and the center of the solute molecule, m
d_a	distance on the chromatography chart of a peak, m
d_u	gas hold-up distance, m
D_A, D_B	Stokes' radius of component A and B, respectively, m
D_{AB}	diffusivity of component A in solvent B, m^2/s
F	area fraction of SMM additive in surface (m^2/m^2)
G	SMM monolayer thickness (m).
h	recorder response, m
H	original bulk volume fraction of an SMM (m^3/m^3)
K	equilibrium distribution coefficient
L	length, m
m	amount of polymer packed in a column, kg, or number of repeat unit
M	molecular weight, kg/mol
N	the amount of adsorbate vapor injected into the column, mol
N_0	Avogadro's number
N_a	the amount of adsorbed vapor in unit weight of polymer, mol/kg
N_{am}	N corresponding to a monolayer coverage, mol/kg
p	vapor pressure, Pa
p_0	saturation vapor pressure, Pa
$P_2 - P_3$	effective driving pressure, Pa
P_i, P_o	pressure at the pore inlet and at the pore outlet, respectively, Pa
[PR]	membrane permeated product rate for given area of membrane surface, kg/h
$[PSP]_B$	pure solvent (of component B) permeation rate for given membrane area, kg/h
q	recorder chart speed, m/s
Q	carrier gas flow rate, m^3/s

r	radial distance in cylindrical coordinate, m
R	gas constant, or pore radius, m
R_a	$= R_b - D_A$, m
R_b	membrane pore radius, m
S	area, m^2
S_{locus}	the area bounded by the common curve along the peak height maxima, the gas hold-up distance, and a given recorder response h, m^2
S_P	the area of the adsorbate peak, m^2
S_{sp}	specific surface area of the polymer, m^2/kg
t_i	thickness of sorbed layer, m
T	absolute temperature, K
u	velocity, m/s
v_μ	mean molar volume of the mobile phase, m^3/mol
V_m	volume of the mobile phase, m^3
$V_{R,i}$	retention volume of component i, m^3
$(V_R')_u$	retention volume of the unadsorbed gas, m^3
V_s	volume of the stationary phase, m^3
V_μ	bulk liquid volume with a boundary parallel to the interface plane, m^3
$\overline{V}_A$, $\overline{V}_B$	average molar volume of the component A and B, respectively, m^3/mol
X	mole fraction
$X_{\mu,A}$	mole fraction of component A in mobile phase
$X_{\mu,i}$	individual mole fraction in the mobile phase
$X_{k,A}$	mole fraction of component A in sorbed phase
Y	the ratio of the area formed by SMM to the bulk volume (m^2/m^3)
z	axial distance, m

Greek letters

γ	ratio of the volumetric flow rate of the carrier gas to the recorder chart speed, m^2
Γ	surface excess, mol/m^2
δ	length of the cylindrical pore, m
λ_f	$\lambda_f = D_A / R_b$
η	solution viscosity, Pa·s
ρ	density, kg/m^3
π	osmotic pressure, Pa
ϕ	potential function of interaction force, J/mol
χ	friction constant, $J \cdot s/m^2 \cdot mol$

Subscripts and superscripts:

M	membrane
μ	mobile phase
i	component i
i*	a labelled solute as defined in Section 2.2.2
0	before the beginning of the chromatographic process
A, B	component A and B, respectively
1	bulk feed solution on the high pressure side of membrane
2	concentrated boundary solution on the high pressure side of membrane or pore inlet outside the pore
3	membrane permeated product solution on the atmospheric side of the membrane or pore outlet outside the pore

Abbreviations

BA-L	fluorotelomer, Zonyl BA-L™ from DuPont Chemical Co.
CAB	cellulose acetate butyrate
DMAc	N,N-dimethylacetamide
DMF	dimethylformamide
DMSO	dimethyl sulfoxide
LC	liquid chromatography
MDI	methylene bis-phenyl diisocyanate
MWCO	molecular weight cutoff
NMP	N-methyl-2-pyrrolidone
PA	aromatic polyamide
PDMS	polydimethylsiloxane
PEBA	polyether block amide
PEG	polyethylene glycol
PES	polyethersulfone
PPO	polypropylene diol
PV	pervaporation
PVA	polyvinyl alcohol
RO	reverse osmosis
SMM	surface modifying macromolecule
VOC	volatile organic compound
XPS	X-ray photoelectron spectroscopy

Table of Contents

List of Tables

List of Figures

1. Introduction

1.1 Background and an Introduction to Reverse Osmosis and Pervaporation

The membrane separation of liquid mixtures can be attempted in two ways: reverse osmosis and pervaporation. Since these two processes are studied in this work, a brief introduction to reverse osmosis and pervaporation is given as follows.

Reverse osmosis separates a particular species partially or completely from a solution by forcing the solution to flow through a membrane by applying a pressure greater than the osmotic pressure. It can operate at ambient temperature without a phase change.

Pervaporation is a membrane separation process in which the upstream side of a membrane is in contact with a feed liquid while vacuum is applied on the downstream side of the membrane. The permeate, vaporized somewhere between the upstream and the downstream side of the membrane, is obtained as a vapor. Since different species permeate through a membrane at different rates, a substance at a low concentration in a feed can be concentrated in the permeate. Thus, volatile organic compounds (VOCs) in dilute aqueous solutions can be enriched in a permeate. It is a potential industrial process to remove VOCs from polluted waters.

Figure 1 is a schematic diagram of reverse osmosis and pervaporation. A comparison between the two is given in Table 1.

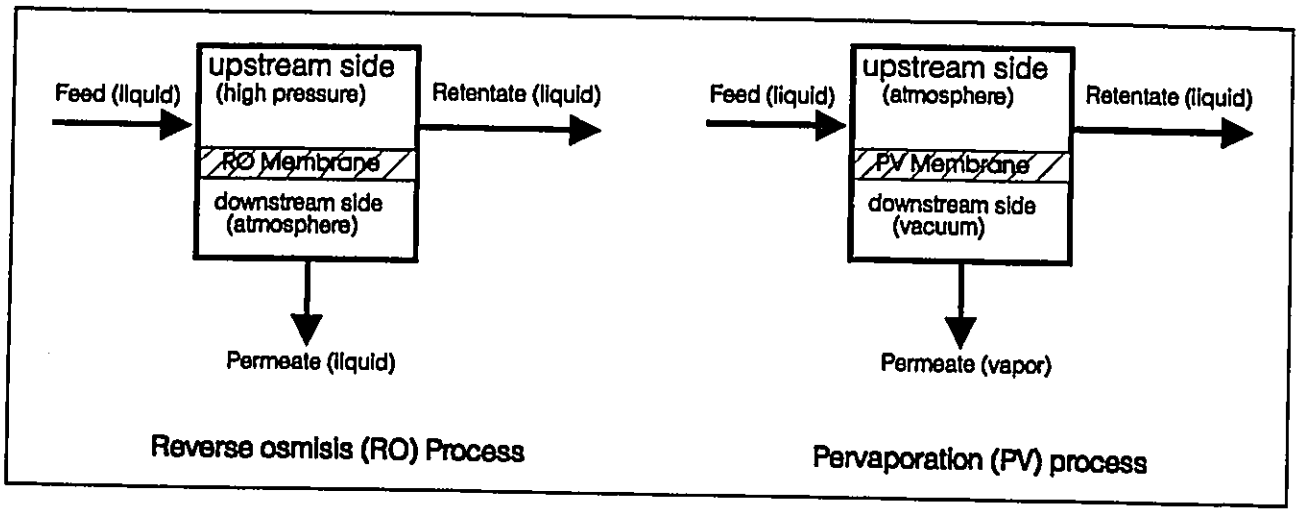

Figure 1 A schematic diagram of reverse osmosis and pervaporation processes.

Table 1 A comparison between reverse osmosis and pervaporation

Comparing items	Reverse osmosis	Pervaporation
Pressure driven process	Yes	Yes
Phase change	No	Yes
Typical upstream pressure	~ 50 atm	1 atm
Typical downstream pressure	1 atm	≤ 3 mmHg
State of feed	liquid	liquid
State of permeate	liquid	vapor
Separation mechanism	1) preferential sorption of one species to the membrane 2) differing rates of transport through the membrane	
Current main applications	water & wastewater treatment including desalination	dehydration of organic solvents like ethyl alcohol

1.2 Scope of Research

Membrane separation processes are relatively new additions to chemical engineering practices. Based on the literature survey, the general objective of this work is to study membrane separations involving organic liquids, using the concept that membranes have pores. Two of the membrane processes, namely, reverse osmosis (RO) and pervaporation (PV), are deemed to be effective in liquid separations involving organics. Therefore, the particular objectives were:

- to characterize the preferential sorption property of a membrane material used in RO,
- to determine the interaction between feed molecules and membranes in RO,
- to test the established transport equations using the above results,
- to study the feasibility of the removal of organics from aqueous solutions by PV,
- to explore the possibility of a new method to fabricate composite membranes.

The above objectives are set because a) they are of industrial significance; b) the accomplishment of these objectives will provide improved understanding in the fundamentals and applications of reverse osmosis and pervaporation processes, which is a contribution to membrane science and technology.

The approaches to achieve the objectives can be described as follows.

--Cellulose acetate butyrate membrane/ethyl alcohol/n-heptane is chosen as a model system for reverse osmosis study;

--Liquid chromatography is used to study feed compounds/membrane materials interaction;

--A new model is developed to characterize the preferential sorption of membrane materials using liquid chromatography data;

--Reverse osmosis separation results are predicted using transport equations and compare with experimental values;

--For pervaporation, polyethersulfone membrane/water/chloroform is chosen as the model system;

--A newly formulated, hydrophobic, surface modifying macromolecule is incorporated in the membrane preparation;

--Membranes so prepared are evaluated in terms of separation and permeation rate;

--Possible validation of the potentially new membrane preparation method by experimental evidence, such as X-ray photoelectron spectroscopy (XPS) method.

1.3 A Survey of Literature

The following three subsections cover a survey of literature pertinent to this study.

1.3.1 Reverse Osmosis Applications in Organic Separations

The reverse osmosis separation of organic liquids was first attempted and illustrated in principle by Sourirajan (1964). Cellulose acetate and polyethylene films were tested for the separation of xylene/ethanol and xylene/heptane mixtures, including their azeotropic mixtures. More data were reported (Kopecek and Sourirajan, 1969, 1970) on the separation of binary azeotropic mixtures and isomers in 1969-70. Various mixtures were tested afterwards.

During 1980-84, Farnand et al. (1980, 1982, 1984a) extended their work and further illustrated the applicability of the reverse osmosis technique for the separation of organic liquid mixtures. In 1986, Kulkarni et al. (1986) reported hydrocarbon separations with polymeric membranes. The hydrocarbons separated were chemically similar but differed significantly in molecular weight. Adam et al. (1983) explored the factors governing membrane selectivity.

As for membrane material research and development, membranes made from

various materials, such as regenerated cellulose, modified polysulfone, aromatic polyamide, polyimide, polycarbonate, cellulose acetate, cellulose acetate butyrate, copolymer, and inorganic glass membranes were reported by different research groups (Martin, 1964; Uragami, 1982; Wan, 1985; Hafez and Koenitzer, 1985; Chang et al., 1986; Farnand, 1983; Black and Boucher, 1986; Thompson, 1987; Wernick, 1985; Matsui et al., 1986; Bitter and Haan, 1988) with various applications. Evaluations of various polymers as membrane materials were reported (Farnand, 1984b; Hazlett et al., 1989; Fang et al., 1992). It was found that there were more and more reports/patents concentrated on two areas -- the hydrocarbon separation industry and oil refining processes. Two examples were fractionation of aromatic from non-aromatic components in naphtha and crude oil distillates (Farnand and Sawatzky, 1989), and dewaxing of lubricating oil (Bitter et al., 1989).

Kuk et al. (1989) conducted reverse osmosis fractionation of triglyceride/solvent mixtures. Cellulose acetate membranes with nominal molecular weight cutoff (MWCO) values between 500 and 1000, and aromatic polyamide membranes with a MWCO value of 1000 were tested. They were found to be efficient in fractionating cottonseed triglycerides from the base solvent, ethanol. Experimental results indicated the potential use of reverse osmosis membranes for the regeneration of ethanol from the ethanol miscellas.

Exxon Research and Engineering Company has had a major effort underway on composite membranes for fractionation of hydrocarbon streams (Petersen, 1993). For example, Black (1991) used interfacial membranes made from interfacial condensation of 1,3-benzenediamine with trimesoyl chloride, or of polyethylenimine with methylenediphenyl diisocyanate, to separate aromatic extraction solvents (N-methyl-2-pyrrolidone (NMP), N,N-dimethylacetamide (DMAc), dimethylformamide (DMF), dimethyl sulfoxide (DMSO)) from oils by reverse osmosis.

In brief, efforts were made towards applications using organic polymeric membranes. The choice of membrane polymer presented crucial problems because the membrane must resist dissolution or excessive swelling in the liquids, have a good permeability and show a high selectivity (Brass and Meares, 1980). It is expected that the development of inorganic reverse osmosis membranes will have a major impact on the field (Matsuura, 1994).

1.3.2 Pervaporation Applications in Liquid Separations Involving Organics

The adoption of pervaporation as a viable and economical industrial separation process has occurred fairly recently--within the last ten years. Today, the biggest application is the dehydration of 90% ethanol/water solution to yield 99.5% pure ethanol (Rautenbach, 1992; Brüschke, 1988; Tusel and Brüschke, 1988). Since dehydration of

organics by pervaporation is considered as a relatively developed process, this survey puts focus on the other two important topics of pervaporation research, namely, separation of organic liquid mixtures, and removal of organic molecules from aqueous solutions.

The importance of pervaporation separation of organic liquid mixtures was best illustrated in the findings in a recent report (Baker, 1991) commissioned by the US Department of Energy. The report evaluated the recent developments and future directions of the membrane separation systems identified, and prioritized the research topics. As shown in Table 2, developing pervaporation membranes for organic/organic separations was ranked as the number one research topic (the highest rank). This ranking reflects the promise of this developing technology. It is the least developed, yet has the largest potential impact on the chemical industry. The early work was for benzene/cyclohexane separation (Binning and James, 1958a, b). Since then, various organic liquid mixtures have been tested with different membranes. Table 3 is a representative list of these efforts.

Table 2 Priority in membrane separation systems (Baker et al., 1991)

Rank	Research Topics	Comments
1	***Pervaporation*** membranes for organic/organic separation	If sufficiently selective membranes could be made, pervaporation could replace distillation in many separations
2	***Reverse Osmosis*** oxidation-resistant membranes	Commercial polyamide reverse osmosis membranes rapidly deteriorate in the presence of oxidizing agents such as chlorine, hydrogen peroxide, etc. This deficiency has slowed the acceptance of the progress in some areas.
3	***Gas Separation*** development of generally applicable method for producing membranes with <500Å skins	Would allow broad usage of advanced materials - even better if done in hollow fibers
4	***Facilitated Transport*** oxygen-selective solid facilitated transport membranes	Air separations of higher selectivity are a target common to all types of membranes
5	***Gas Separation*** higher O_2/N_2 selectivity productivity polymer	Selectivity of 8-10 and permeability of 10 Barrer is required. Experimental materials approach these, but no ability to spin them in hollow-fiber form has been reported. Most valuable as hollow fibers.
6	***Ultrafiltration*** (UF) fouling-resistant membranes	Fouling is a ubiquitous problem in UF. Its elimination would boost total throughput >30% and reduce capital costs by 15% on top of eliminating cleaning. Better fractionation would also result, expanding UF use significantly.
7	***Pervaporation*** better solvent-resistant modules	Current modules cannot be used with organic solvents and are also very expensive
8	***Gas Separation*** development of generally applicable method for forming composite hollow fibers with <500Å skins	Only small amounts of the valuable selective material are required
9	***Microfiltration*** high temperature, solvent-resistant membranes and modules	Opportunity for ceramic or inorganic membranes. Potential uses include removal of particulates from coal liquids and replacement of bag houses in flue gas treatment
10	***Microfiltration*** low-cost membrane modules	Huge potential applications will require commodity pricing, far from today's reality.

Table 3 A list of selected membrane materials and organic mixtures separated by pervaporation

Membrane material	Organic mixtures	Reference
Polyethylene, polypropylene	Saturated hydrocarbons isomer (xylenes)	Binning (1961) Huang (1968)
Ethylene-styrene copolymers	Unsaturated/saturated hydrocarbons	Huang (1969)
Butadiene-acrylonitrile copolymers	Aromatics/saturated hydrocarbons	Brun (1985a)
Aromatic polyimide	Diene/alkanes	Perry (1974)
Polyvinylidenefluoride (PVF_2)	Isomeric xylenes	Sikonia (1978)
Copolymers containing vinylpyridine units	Alcohols/alkanes chlorinated solvents	Aptel (1976) Shimidzu (1988)
Cellulose	Alcohol/alkane	Okada (1991,1992)
Modified poly (phenylene oxide)	Methanol/methyl-tert-butyl ether (MTBE)	Doghieri (1994)
Cellulose acetate	Alcohols/alkanes aromatics/alkanes methanol/ethanol methanol/(MTBE)	Cabasso (1983) Laatikainen (1986) Chen (1989)

It is worth pointing out that the focus has shifted from using commercially available polymers to the exploration of modified and/or newly developed polymers (Koops and Smolders, 1991). For instance, polyvinyl alcohol (PVA) membranes were modified by introducing cyclodextrin (Yamasaki and Mizoguchi, 1994). They reported that membrane selectivity changed from ethanol selective to water selective when the cross-link time changed from 1 hour to 8 hours. PVA membranes containing cyclodextrin were also investigated (Miyata et al., 1994) for the separation of propanol isomers. The study found that n-propanol could be concentrated in the permeate from normal and iso-propanol mixtures.

A recent study (Yanagishita et al., 1994) reported that asymmetric polyimide membranes, made from a casting solution composed of 25 wt % polyimide, 37.5 wt % N,N'-dimethylformamide (DMF) and 37.5 wt % dioxane, showed a molecular weight cutoff of 600. The membranes annealed at 300°C for 3 hours exhibited a separation factor (water/ethanol) of 900 with a flux of 1.0 kg/m^2 h for an aqueous 95 vol % ethanol solution at 60°C. It enabled a much lower ethanol concentration in the feed than that of current commercial membranes.

Inorganic membranes prepared by the sol-gel method using colloidal silica sols were experimentally studied (Asaeda and Kitao, 1991) for the separation of ethanol/ cyclohexane mixtures. High separation factors (200-4200) were reported and the

separation was almost complete. Membranes composed of inorganic main chains were studied by other researchers, too. For example, Suzuki et al. (1987) investigated poly [bis(2,2,2-trifluoroethoxy) phosphazene] (PBFP) membranes for the separation of benzene/cyclohexane by pervaporation. The repeat unit of PBFP was [-N=P(OCH_2CF_3)$_2$-]. It had the inorganic main chain, -N=P-, and carried hydrophobic organic side groups of -OCH_2CF_3. A separation factor of 12 was achieved with benzene being enriched in the permeate.

Removal/extraction of organic molecules from their dilute aqueous solutions is another important research topic for pervaporation (Blume et al., 1990; Fleming and Slater, 1992; Rautenbach et al., 1992). It preferentially transfers the minority component(s) through polymeric membranes from the liquid phase (feed) to the vapor phase (permeate). Potential applications are to the environmental and biotechnology industries, since both need removal or recovery of organic compounds from dilute solutions (Böddeker and Bengtson, 1991; National Research Council, 1987).

Separation of organics from water by pervaporation requires elastomeric (rubbery) polymers, such as silicone rubber (polydimethysiloxane, PDMS) and copolymers thereof, copolymers of styrene and styrene derivatives, polyurethane and polyether block amide (PEBA). A survey on various membranes and mixtures investigated is

presented in Table 4. Further, some pertinent fundamentals are pinpointed using the following illustrations.

Fritsch et al. (1993) reported that for pervaporation of trace organics (1,2-dichloroethane/water), polymers were effective by reducing water permeability in this order: PDMS < PDMS derivative < PDMS derivative/cellulose triacetate blends. At higher organic feed concentration (1-butanol/water), the PDMS derivative showed highest selectivity. In organic/organic separation, PDMS-related polymers swelled excessively. Suitable membrane polymers were poly (maleimide-*alt*-vinyl ether) copolymers, which were readily tailored by side-chain modification.

Bengtson and Böddeker (1988) reported the preparation of PEBA membranes. It comprised a polyether-block-polyamide (PEBA), a commercially available plastic, trade-named Pebax (Atochem), combining the properties of elastomers and thermoplasts. Pervaporation of low volatile organics (boiling points 110-249°C), including phenol, from aqueous solution was conducted. Enrichment factors were observed from 20 (benzoic acid) to above 700 (styrene), flux in the range of 0.4 to 8.4 g/(m^2h).

Bai et al. (1993) attempted separation of acetic acid/water mixture by pervaporation using silicone rubber-coated polyetherimide membranes. They found that the

Table 4 Extraction of organics from aqueous solutions by pervaporation

Material	Organics extracted				Reference
	alcohol	hydrocarbon	chlorinated solvent	ethers, ketones, or as specified	
Natural & synthetic rubber	x	x	x	x	Brun ('85b) [a]
	x		x	x	Kaschemekat ('89)
	x				Nijhuis ('89)
	x		x	x	Nguyen ('87)
Silicone & silicone rubber	x		x	x	Blume('87)
	x				Zhu ('87)
	x				Suematsu ('87)
	x				Tanigaki ('87)
	x				Hennepe ('87a,b)
	x	x	x	x	Eustache ('81)
P.E.B.A.[b]				phenols	Böddeker ('87)
	x	x	x	phenols	Bengtson ('88)
Plasma from silicon compounds	x				Masuoka ('87,'89)
	x				Kashiwagi ('88)
Perfluoro-tetrafluoro copolymers	x				Nakamura ('88)
	x				Okabe ('87)
PVF_2 [c]	x				Lee ('87)
Styrene-acrylate copolymer	x				Ishihara ('87)
	x				Yoshikawa ('87)
Porous glass	x				Lee ('88)
polyolefines				x	Featherstone ('71)
	x				Ohya ('86a,b)
polyvinyl-acetate			x		Zhu ('83)
Copolymers of hydrophilic-hydrophobic units	x				Nakagawa ('87)
Ion-exchange membranes				phenols	Böddeker ('87)

[a] '85 = 1985.
[b] P.E.B.A. = poly-[ether-block-amides]
[c] PVF_2 = polyvinylidene fluoride

composite membrane could become either water selective or acetic acid selective, depending on the pore size of the support membrane and the condition of the silicone rubber coating. Thus, the overall performance of the composite membrane can be governed either by the top coated layer or by the bottom support layer.

Effect of lamination of polydimethylsiloxane (PDMS)/aromatic polyamide (PA) membranes was examined for the same mixture (Deng et al., 1994). When two membranes were laminated, both component membranes contributed to the overall selectivity of the bilayer membrane. When a hydrophobic homogeneous membrane (PDMS) and an asymmetric hydrophilic membrane (PA) were laminated, with the former membrane contacting the feed liquid, the water selectivity of the latter one was intensified. This was because the densest and least porous section of the asymmetric membrane was kept dry and dominated the overall selectivity.

Technical and economic viability were examined, too. Wijmans et al. (1990) tested MTR-100 and MTR-200 composite membranes in spiral-wound modules. Systems tested included (1) 1000 ppm benzene in water, (2) 2% ethyl acetate in water, and (3) 2.0% dioxane, 0.6% acetone, and 0.1% methanol in water. These three mixtures represented three categories of applications, namely, pollution control of dilute solutions of hydrophobic solvents, solvent recovery from process waste waters, and volume reduction of mixed-solvent hazardous waste streams. The cost of the

pervaporation process compared favorably with other waste treatment methods.

Lipski and Côté (1990) studied a case in which the objective was 99% removal of 10 mg/L of trichloroethylene (TCE) from water at a feed flow rate of 10 m^3/h with a silicone rubber hollow fiber module. Cost of pervaporation was US\$0.56/m^3, compared with US\$0.80/m^3 for air stripping and/or granular activated carbon, on the aqueous or off-gas streams. Technical and economical viability were demonstrated.

To summarize, removal/extraction of organics from aqueous streams by pervaporation is a fast developing, attractive process, while organic/organic separation by pervaporation is still in its early development stage. It seems that pervaporation is evolving through three stages, judging from the availability of the various membranes for pervaporation process: dehydration of organics (developed)
--> extraction of minor organic compounds from water (developing) --> separation of organic/organic liquid mixtures (under development).

1.3.3 Applications of Surface Modifying Macromolecules

A surface modifying macromolecule (SMM) refers to a macromolecular species that is active at the interface between two phases. The dominant feature of an SMM is its ability to migrate preferentially toward a polymer-air interface. SMMs were used in

this work to modify the performance of pervaporation membranes. More details are presented in Theory and Methodology. Since use of an SMM in membrane formation has not yet been reported, this survey highlights applications of SMMs in fields other than membrane formation.

Hu and Sung (1979) showed that, resulting from their preferential migration, low surface energy oligomers were more abundant on the air-facing surface, as compared with the bulk composition. This trend was observed not only in the first 100 Å, but also into a depth as much as 1 μ.

Ward et al. (1984) reported the use of a proprietary tripolymer, containing a low surface energy block, in the development of a new biomedical polyurethaneurea. Their results showed that platelet adsorption was reduced 1000 fold for the polyurethane modified with less than 1% of the SMM.

Ratner et al. (1987) discussed a blend of surface active additive containing fluorine with a conventional polyurethane to increase the hydrocarbon content on the surface. They found that when a polyurethane was mixed with poly (dimethyl siloxane) (PDMS), silicone migrated to the surface, and the surface was almost entirely covered by a pure layer of PDMS. Ratner and Paynter (1984) examined the

importance of molecular weight distribution, bulk chemistry and casting conditions on polyurethane surfaces in medical usage.

Yu et al. (1990) further confirmed that addition of fluoro polyether glycol oligomers to polyurethanes would cause the low surface energy fluoro segment to be enriched at the surface in both air and water environments. They indicated that the morphology of the polymer surface appeared to be controlled by the polymer's bulk morphology and the polarity of the testing environment.

Kober and Wesslén (1992) prepared surface modifying additives from methylene diphenylene diisocyanate, poly (ethylene glycol) (PEG), and a fatty acid mono-glyceride as a chain extender. The additive itself had an advancing and receding contact angle of ~120° and ~5° respectively. The blend made of polyurethanes and 5% additive showed advancing and receding contact angles of 111° and 14° respectively. The low receding contact angle was attributed to the rearrangement and partial accumulation of the hydrophilic PEG blocks at the surface. A surface saturation effect was observed at 5% added polymer additive. The polymer additive was not extracted from the blends for a 10-week exposure to water.

Kasemura et al. (1993) blended fluorine-containing copolymers with an epoxy resin

to improve oil and water repellency. The fluorine content, determined by angular dependent X-ray photoelectron spectroscopy (XPS) in modified resin surfaces, increased with the shallowing of the sampling depths. It decreased rapidly under a mild argon ion-etching process and disappeared after 4 minutes. It was concluded that the fluorine-containing modifiers were concentrated in the outermost extremely thin layer of resin surface.

Park et al. (1994) studied the surface properties of polymer mixtures made of poly (perfluoroalkylethyl methacrylate) (PFMA) / poly (*n*-alkyl methacrylate)s. From contact angle and XPS data, they found that the fluoro polymer, PFMA, was preferentially arranged and concentrated at the polymer mixture-air interface. The fluorine atomic percentage for the take-off angle of 5° was about 24% for a PFMA / poly (methyl methacrylate) mixture containing 0.01 wt % of PFMA. The calculated surface free energy from contact angle data showed that the addition of the fluoro polymer significantly decreased the surface energy for the mixtures. For example, addition of 0.1 wt % of PFMA into poly (methyl methacrylate) lowered the surface free energy from 40 to 14 dynes/cm.

It can be well concluded from the above cited studies that the low surface energy component, which is an SMM, whether containing fluorine or not, will be enriched at the surface when it is added to another polymer system.

2. Theory and Methodology

This section contains three subsections. The first subsection presents a new concept on which a novel method to prepare composite membranes is based. The second one describes a new approach to determine preferential sorption of membrane materials by liquid chromatography. The last one outlines the transport equations used in this study.

2.1 A New Approach to Form Composite Membranes Using Surface Modifying Macromolecules (SMM)

Composite membranes generally comprise two distinctive layers made of two different materials as shown in Figure 2 (Strathmann, 1990). The top layer may be called the surface layer, while the bottom layer may be called the substrate. The surface layer acts as a selective barrier, while the substrate is a porous support. The advantage of a composite membrane is that both the surface layer and the substrate can be adjusted separately to provide improved membrane performance. Composite membranes successfully developed by North Star Research Institute, Minneapolis, Minnesota (Cadotte, 1981), Monsanto Company, St. Louis, Missouri (Henis and Tripodi, 1980) and Gesellschaft für Trenntechnik mbH, Neunkirchen-Heinitz, Germany (Brüschke, 1988), are the milestones in the advancement of membrane science and technology.

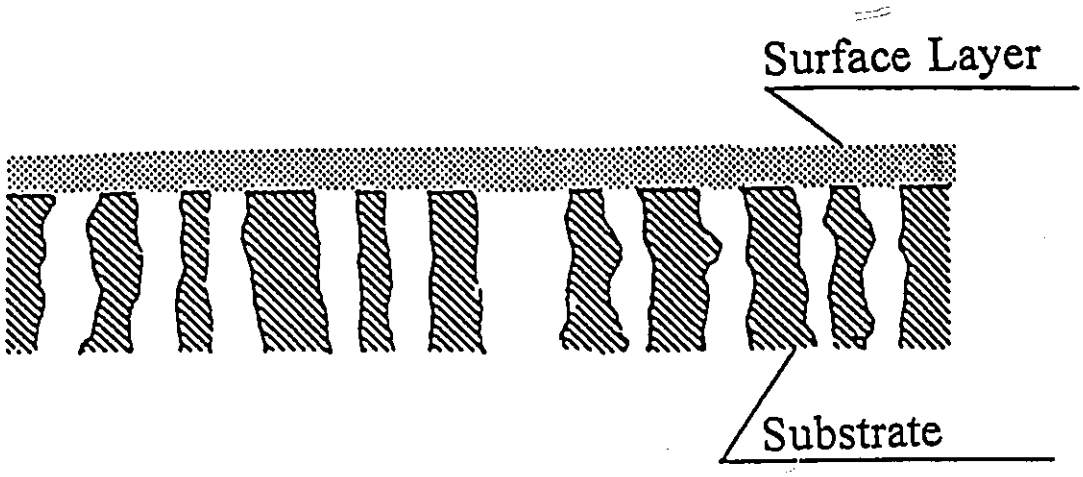

Figure 2 Schematic diagram of an asymmetric composite membrane (Strathmann, 1990).

Techniques used to form composite membranes may be grouped into four general types (Kesting, 1985):

(1) *Lamination* of a surface layer and a substrate;

(2) *Coating* the surface of a substrate with a polymer solution and drying;

(3) *Interfacial polymerization* of reactive monomers on the surface of a substrate;

(4) *Gas-phase deposition* of the surface layer on a substrate from a glow discharge plasma.

2.1.1 A New One-Step Method to Prepare Composite Membranes

As shown above, the fabrication of composite membranes usually involves two separate steps: formation of a substrate, and formation of a surface layer. To overcome the complexity of the two-step method, this study explores a new one-step method to prepare composite membranes, using a surface modifying macromolecule (SMM). The new method is described as follows.

Conceptually, thermodynamic principles stipulate that the formation of the lowest possible energy status is a universal tendency. The principal feature of a surface modifying macromolecule (SMM) is that it has a lower surface free energy than that of a base polymer. Thus, an SMM has the ability to migrate preferentially toward a polymer-air interface as shown in Figure 3. When an SMM is blended with a membrane casting solution made of a base polymer, an SMM/base polymer system is formed. When the solution is cast into a membrane in the air, the SMM with lower surface free energy tends to spontaneously migrate towards the membrane-air interface to minimize surface free energy. Migration of SMMs forms spontaneously a distinct surface layer dominated by the segregated SMMs, and a substrate made from a base polymer. Hence, a composite membrane, composed of two discrete layers of two different materials, can be constructed in a single step.

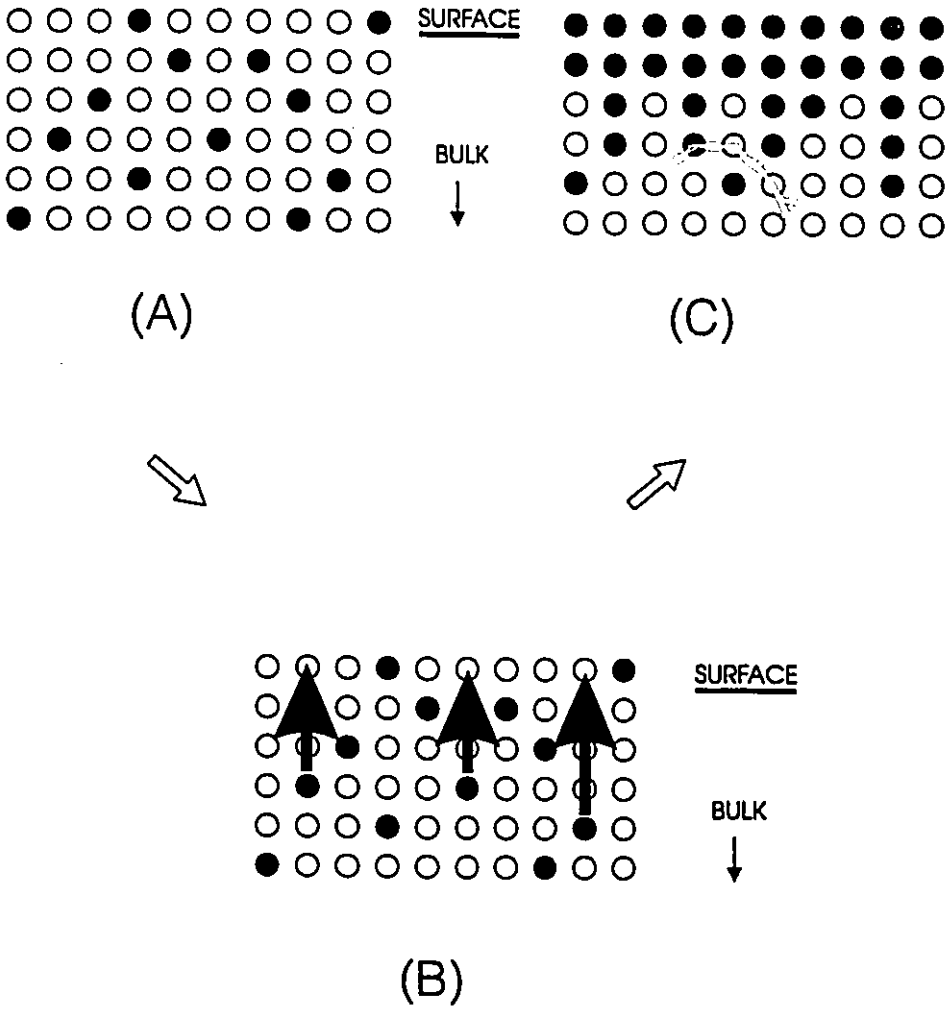

Figure 3 A schematic diagram illustrating the component with lower surface free energy migrating to the membrane surface. ●, SMM molecule which has lower surface free energy; O, base polymer and solvent. Case A: time zero; case B: time in between; case C: time infinite.

Experimentally, fluorochemicals become a natural choice as SMMs because of their extremely low surface free energy (Bajzer and Kim, 1994). In this work, a fluorine-containing SMM is blended with polyethersulfone (PES) in a membrane casting solution. Here PES is the base polymer. A membrane is cast on a glass plate. The solvent is then partially evaporated in the air. Afterwards, the membrane is gelled in water. Because the SMM is expected to migrate to the membrane surface and it has a fluorine-containing hydrophobic component, a hydrophobic membrane surface can be formed. The membrane surface is characterized by X-ray photoelectron spectroscopy (XPS) and contact angle measurement. Full details are described in the experimental section.

According to the resistance-in-series model (Côté and Lipski, 1988), the selectivity of a composite membrane is governed by the layer of the greatest resistance to the mass flow. If the resistance of the SMM layer is high enough, the overall selectivity of the membrane will be dominated by the SMM layer. In this case, the preferential transport of organic compounds is expected, since a hydrophobic membrane surface tends to favor the extraction of organics from their aqueous solutions (Brüschke, 1991; Böddeker and Bengtson, 1991). On the other hand, if the top hydrophobic surface layer is too thin and its resistance is too low to contribute to the overall selectivity of the membrane, the bulk PES rich layer will control the overall selectivity of the membrane. This will lead to the preferential

permeation of water since a PES membrane is known to be preferentially permeable to water. The membranes are evaluated in pervaporation separation of chloroform/water mixtures.

To summarize, the concept of an SMM's migration towards the membrane surface forms the basis of the new approach. This approach is to be demonstrated experimentally with the application of an SMM to the formation of composite pervaporation membranes.

2.1.2 Estimation of the Amount of SMM Needed to Cover a Membrane Surface

It is an interesting subject to determine the minimum amount of an SMM required to cover a membrane surface completely. Although a rigorous modelling is not the objective of this work, a very simple, quantitative analysis is herewith included (Ward et al., 1984). The analysis will allow us to calculate the amount of an SMM required to fully cover the surface, at least in an order of magnitude accuracy. The assumption involved in the analysis is that, prior to surface saturation, all SMMs present in the base polymer solution will migrate to the surface, forming its monolayer. Under this assumption, the SMM surface composition may be related to the SMM bulk composition by

$$H = F \cdot Y \cdot G \quad (1)$$

where H = (original) bulk volume fraction of an SMM (m^3/m^3)

F = area fraction of SMM additive in surface (m^2/m^2)

Y = the ratio of the area formed to the bulk volume (m^2/m^3)

G = SMM monolayer thickness (m).

When the surface is fully covered by SMMs, $F=1$. Thus, the bulk SMM volume fraction H corresponding to the full monolayer coverage can be estimated from the numerical values of Y and G. It will be demonstrated in the Results and Discussion that only a very small amount, not more than a few percent of SMM, is required to cover the surface completely.

2.2 A New Approach to Determine Preferential Sorption of Membrane Materials by Liquid Chromatography

This section explains why a liquid chromatography (LC) method is used and how it is applied to this study. First, the similarity between an LC system and a membrane separation process is described, followed by an outline of the conventional LC theory. Then, a new approach to the determination of preferential sorption, which is developed in this work, is presented.

2.2.1 Similarity between an LC System and a Membrane Separation Process

The liquid chromatography system consists of a carrier liquid (solvent), various components (solutes) dissolved in the liquid as well as a porous support (column). There is a distribution of components in the fluid between a mobile and a stationary phase due to the presence of the material packed in a column. This distribution results from the different adsorption potentials of the solute and solvent to the material packed in a column.

A direct relationship exists between the physico-chemical processes occurring in a liquid chromatography system and those at a membrane-solution interface (see Figure 4). Both are concerned with the behavior of a liquid layer influenced by the presence of an interface. This layer is known as the stationary phase in LC terms, while for a membrane process the term interfacial layer is used. The mobile phase in an LC system is analogous to the bulk solution of a membrane process. The

introduction of a solute in either system results in a concentration difference between the mobile (bulk) phase and stationary (interfacial) phase. In the case of an LC system, this concentration difference is reflected in the retention time of the solute. At a membrane-solution interface, it produces a positive or negative concentration gradient. Due to the similarities between the two systems, LC offers a means of studying the interactions between a solute and a membrane.

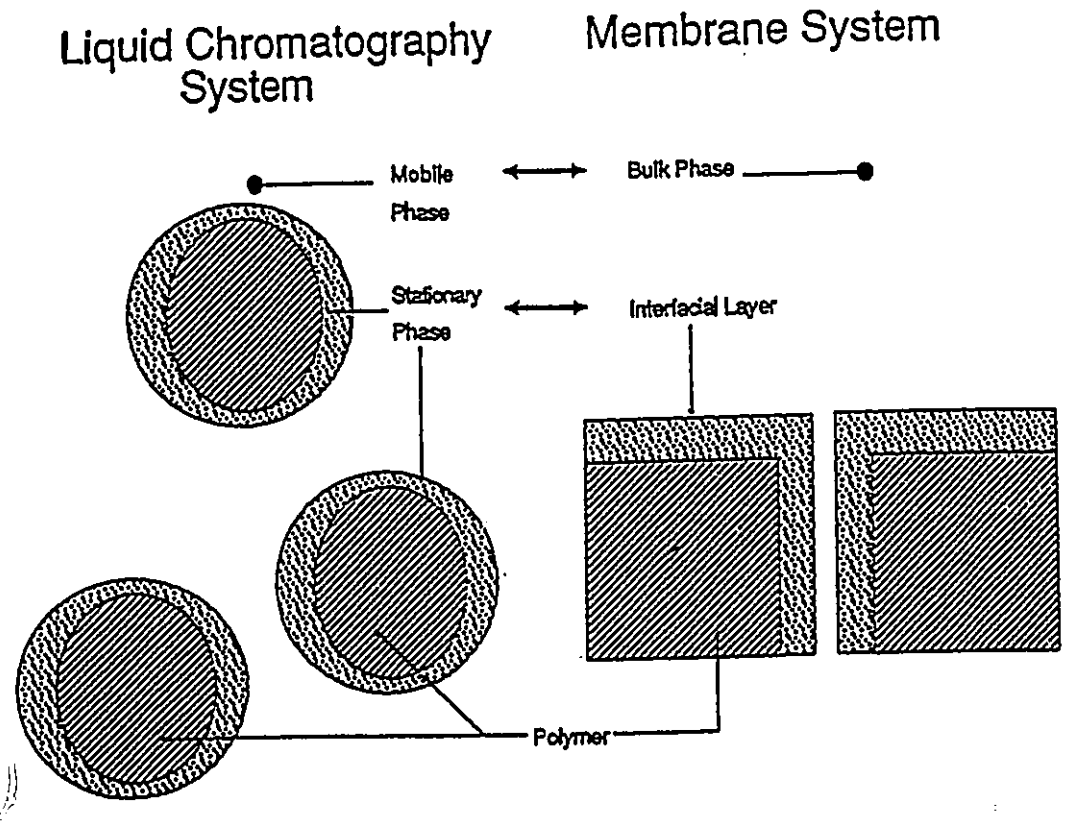

Figure 4 Relationship between a liquid chromatography system and a membrane system (Tam, 1989).

2.2.2 Conventional Liquid Chromatography (LC) Theory

The basic parameters involved in the classic LC theory are retention time and retention volume. Retention volume may be expressed by (Hamilton and Sewell, 1978)

$$V_{R,I} = V_m + K V_s \tag{2}$$

where $V_{R,I}$ is the retention volume of component i, V_m is the volume of the mobile phase, V_s is the volume of the stationary phase, and K is the equilibrium distribution coefficient. In adsorption chromatography the volume of the stationary phase V_s is replaced by the surface area of the adsorbent S so that

$$V_{R,I} = V_m + KS \tag{3}$$

Parallel to the above equation, Riedo and Kováts (1982) proposed a similar expression, which the new approach is based on,

$$V_{R,I} = V_\mu + S v_\mu^0 \chi_I \tag{4}$$

where

$$\chi_I = \left(\frac{\partial \Gamma_I}{\partial X_{\mu,I}}\right)_{x_\mu^0} \tag{5}$$

and

$$V_\mu = \sum_{I=a}^{m} X_{\mu,I}^0 V_{R,I^*} \tag{6}$$

The subscript μ referrs to the mobile phase. The superscript ^{o} means the initial state, i.e., the mobile phase before sample injection which is considered as perturbation to the mobile phase composition. v_μ^o is the mean molar volume of the mobile phase. Γ_I is surface excess of component i. $X_{\mu,I}$ and X_μ^o are the mole fraction of component i and the initial mole fraction of the mobile phase, respectively. i^* is an imaginary

solute (also termed a "labelled solute"), which is in every respect identical with component *i* in the mobile phase, with the exception of one property permitting its detection.

When one compares Equation (3) with (4), it is interesting to notice the similarity between the two. The coefficient $v_\mu^0 \chi_i$ in Equation (4) is analogous to the equilibrium distribution coefficient K in Equation (3).

2.2.3 Development of A New Approach to Analyze Liquid Chromatography Experimental Data

This section presents the development of a new approach to analyze liquid chromatography experimental data.

Combining Equation (4) and (5),

$$V_{R,I} = V_\mu + S\, v_\mu^0 \left(\frac{\partial \Gamma_I}{\partial X_{\mu,I}}\right)_{x_\mu^0} \tag{7}$$

Rearranging Equation (7),

$$\left(\frac{\partial \Gamma_I}{\partial X_{\mu,I}}\right)_{x_\mu^0} = \frac{V_{R,I} - V_\mu}{S v_\mu^0} \tag{8}$$

For a binary liquid mixture of A and B, Equations (8) and (6) reduce to

$$\left(\frac{d\Gamma_A}{dX_{\mu,A}}\right)_{x_{\mu,A}^0} = \frac{V_{R,A} - V_\mu}{S v_\mu^0} \tag{9}$$

$$V_{\mu}=X^{0}_{\mu,A}V_{R,A^{\bullet}}+X^{0}_{\mu,B}V_{R,B^{\bullet}} \quad (10)$$

$X_{\mu,A}^{o}$ and $X_{\mu,B}^{o}$ are initial mole fractions of component A and B in the mobile phase, respectively, which are known. It is assumed that S can be calculated as

$$S=X^{0}_{\mu,A}S_{A}+X^{0}_{\mu,B}S_{B} \quad (11)$$

S_A and S_B are the surface area determined by BET equation for the pure component A and B, respectively. Labelled solutes can be best approximated by compounds containing radioactive carbon (Knox and Kaliszan, 1985) or by deuterated compounds (Karch et al., 1976; McCormick and Karger, 1980a,b). Therefore, $V_{R,A^{\bullet}}$ and $V_{R,B^{\bullet}}$ may be approximated with the retention volumes corresponding to deuterated solutes A and B, respectively. Let $V_{R,A}$ and $V_{R,B}$ be the retention volumes of solutes A and B, respectively. In the case of p-xylene (A) and n-heptane (B), experimental data showed that the value of $V_{R,A^{\bullet}}$ was very close to that of $V_{R,A}$, with the difference being less than 4.3%. Thus, $V_{R,A}$ is considered a good approximation of $V_{R,A^{\bullet}}$. Similarly, $V_{R,B}$ is a good approximation of $V_{R,B^{\bullet}}$. This conclusion is considered to be applicable to other binary organic liquid mixtures as well. Then, Equation (10) becomes

$$V_{\mu}=X^{0}_{\mu,A}V_{R,A}+X^{0}_{\mu,B}V_{R,B} \quad (12)$$

2.2.4 Procedures to Determine Surface Excess and Adsorption Curve

Based on the above theoretical development, procedures to generate surface excess and adsorption curve by liquid chromatography are given as follows.

Step 1 Pure component A and B are injected into the mobile phase of known composition, $X_{\mu,A}^{o}$. The retention volumes, $V_{R,A}$ and $V_{R,B}$, corresponding to the injection of pure component A and B, are recorded. Noting $X_{\mu,B}^{o}=1-X_{\mu,A}^{o}$, Equation (12) is used to calculate V_{μ}. Then, $(d\Gamma_A/dX_{\mu,A})$ is generated from Equation (9) and plotted vs. $X_{\mu,A}^{o}$. Inside Equation (9), S comes from Equation (11), and, v_{μ}^{o} , the mean molar volume of the mobile phase (m^3/mol) can be related to the total molar concentration of the mobile phase C_t (mol/m^3) by $v_{\mu}^{o}=1/C_t$. Numerical values for C_t for the ethyl alcohol/n-heptane mixture studied in this work are available in the literature (Van Ness et al., 1967).

Step 2 A graphical integration is performed to obtain Γ_A corresponding to an initial mobile phase composition $X_{\mu,A}^{o}$

$$(\Gamma_A)_{X_{\mu,A}^{0}} = \int_{0}^{X_{\mu,A}^{o}} \left(\frac{V_{R,A}-V_{\mu}}{SV_{\mu}^{0}}\right) dX_{\mu,A} \qquad (13)$$

Step 3 Sorption layer thickness t_l is determined by

$$t_l = \frac{V_{sorbed}}{S} \qquad (14)$$

where V_{sorbed} , the volume of the sorbed phase corresponding to $X_{\mu,A}^{o}$, is experimentally determined by conventional sorption measurement of the CAB films which are under study in this work. CAB films are placed in an ethyl alcohol/n-heptane mixture. The weight and composition of the mixture sorbed by the CAB films are determined as described in the experimental section. V_{sorbed} is obtained by dividing the weight of sorbed liquid by the density of the sorbed liquid. $X_{k,A}$, the mole fraction of component A in the sorbed phase, is calculated by (Sourirajan and Matsuura, 1985)

$$X_{K,A} = X^{o}_{\mu,A} + \frac{\Gamma_A}{C_t\, t_i}$$

$$or \quad X_{K,A} = X^{o}_{\mu,A} + \frac{\Gamma_A v^0_\mu}{t_i} \qquad (note\ v^0_\mu = \frac{1}{C_t}) \tag{15}$$

Thus, t_i and $X_{k,A}$ can be obtained from Equations (14) and (15). Hence, the sorption curve can be built up based on the relationship between $X_{k,A}$ and $X_{\mu,A}{}^{o}$.

2.2.5 Determination of Surface Area by the BET Equation

The specific surface area of the polymer was determined using the BET equation, which may be written as (Brunauer et al., 1938)

$$\frac{p/p_0}{N_a(1-p/p_0)} = \frac{1}{N_{am}C} + \frac{C-1}{N_{am}C}(p/p_0) \tag{16}$$

where p and p_0 are the partial vapor pressure and saturation vapor pressure of the adsorbate vapor, and N_a is the amount of vapor adsorbed on the surface of the polymer packed in the column per unit weight of the polymer. N_{am} is the number of molecules required for a monolayer coverage of the surface of a unit weight of polymer. The constant C is related to the heat of adsorption. The quantities C and N_{am} can be determined from the slope and the intercept of the straight line obtained when $(p/p_0)/[N_a(1-p/p_0)]$ is plotted against p/p_0. The area A_m that each adsorbate molecule covers must be known. This area can be calculated by the following equation using cm·g·s units (Mohlin and Gray, 1974)

$$A_m = 1.091 \times (\frac{M}{\rho \cdot N_0})^{2/3} \tag{17}$$

where M and ρ are molecular weight and density of the adsorbate molecule, respectively, and N_0 is Avogadro number. Then, the surface area of the polymer, S_{sp}, can be calculated as $S_{sp} = N_0 \cdot N_{am} \cdot A_m$.

The method of generating N_a versus p is based on the gas chromatography method described by Mohlin and Gray (1974), Matsuura et al. (1983), Long et al. (1988) and Bao et al. (1989). According to the method N_a is given by

$$N_a = \frac{S_{locus} \cdot N}{m \cdot S_p} \tag{18}$$

where N, m, and S_p are the amount of adsorbate gas injected into the column, the amount of the polymer packed in the column, and the area of the adsorbate peak on the chromatogram corresponding to N mole injection, respectively; and S_{locus} is a quantity defined as

$$S_{locus} = \int_0^h (d_a - d_u)\, dh \tag{19}$$

which means the area bounded by the common curve along the height maxima, the gas hold-up distance, and a given record response (see Figure 5).

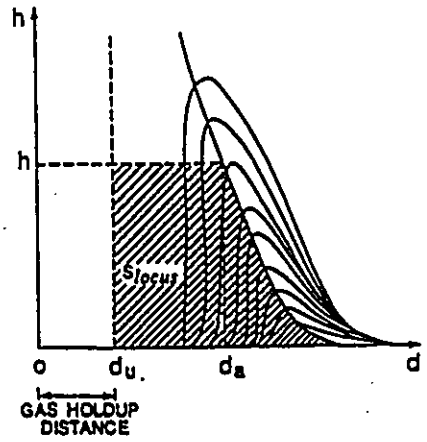

Figure 5 Superimposed chromatographic peaks for the calculation of area, S_{locus} (Matsuura et al., 1983).

Inside Equation (19), d_u is the gas hold-up distance and d_a is the distance on the chart corresponding to recorder response h. Partial vapor pressure p is given by

$$p = \frac{NRT}{\gamma S_P} h \tag{20}$$

where γ is the ratio of the volumetric flow rate of the carrier gas to the recorder chart speed. Since the hold-up distance d_u is the distance on the chart corresponding to retention time (or volume) of the unadsorbed gas, the retention volume of the unadsorbed gas, $(V_R')_u$, is related to d_u by

$$(V_R')_u = \frac{Q}{q} d_u \tag{21}$$

where Q and q are the carrier gas flow rate and the recorder chart speed, respectively. $(V_R')_u$ equals the sum of (i) dead spaces originating from the injector, the detector and the connecting tubes (referred to as dead space I), and (ii) the space in the column which is unoccupied by polymer powder (referred to as dead space II). To determine dead space I, the retention volume of nitrogen gas was determined when the column was replaced by an empty tube of known inside diameter and length. The dead space I is equal to the retention volume determined above minus the space in the empty tube. For dead space II, since the weight and density of the dry polymer powder in the column are known, the volume of the dry powder in the column is calculated. The volume of the unpacked column minus the volume of the dry polymer powder is the dead space II. $(V_R')_u$ is equal to the sum of dead space I and dead space II.

2.3 Transport Equations for Reverse Osmosis

The typical transport models for reverse osmosis are the solution-diffusion model (Lonsdale, 1965; Barrer and Ueberreiter, 1968), the irreversible thermodynamic model (Kedem and Katchalsky, 1958; Spiegler and Kedem, 1966) and the pore model (Merten, 1966; Jonsson and Boesen, 1975; Matsuura and Sourirajan, 1981; Mehdizadeh and Dickson, 1989, 1993). The pore model is chosen in this study because, out of the three models above stated, it is the only one which describes the influence of the interaction force between solute, solvent, and membrane material on the mass transport through open capillaries. Following is an outline of the Surface Force-Pore Flow Model, a quantitative expression of the pore model.

2.3.1 Fundamentals of the Surface Force-Pore Flow Model

Since the pores are similar to the molecules in size, the flow is not a continuum. However, properties such as pressure, concentration, etc. can be considered to be time-averaged quantities. In this model, the pores on the membrane surface are assumed equivalent to circular cylindrical pores, and the solute-membrane material interactions relative to solvent are expressed in terms of electrostatic or Lennard-Jones-type surface potential functions. The transport of solute and solvent through the membrane pores is governed by such surface forces, together with friction forces and solution velocity profiles within the pores. Based on the above model, appropriate transport equations are derived from a series of force, momentum, and mass balances, on a solute molecule flowing through an individual cylindrical pore of radius R and effective pore length δ. The foregoing analysis results in general expressions for solute separation and fluid flux which are valid whether the solute is negatively or positively adsorbed at the membrane-solution interface. Using the cylindrical coordinate system shown in Figure 6, the

concentration and velocity profile of the solution inside the membrane pore are analyzed in differential segments as a function of (r,z) covering the entire pore region, under the steady state. The detailed derivation can be found in the literature (Zhou et al., 1991). A summary of the analysis follows.

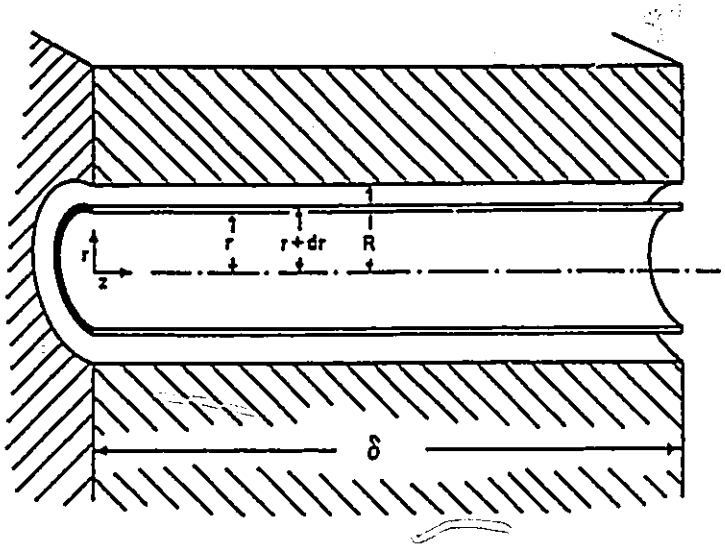

Figure 6 Cylindrical coordinates (r,z) in a membrane pore (Sourirajan and Matsuura 1985).

2.3.2 Necessary Refinement to the Definition of Pore Radius

Because the size of the molecules involved is generally comparable to that of the membrane pore, a distinction is made between the radius of the membrane pore and the radius of the channel for fluid flow. For purpose of analysis, the location of a molecule is defined as the location of its center (assuming a spherical shape for the molecules); this means that in the region of the pore where the center of the molecule cannot exist, the molecule as an entity does not exist. Thus, denoting D_A as the radius of the component having smaller radius (i.e., $D_A<D_B$), and R_b as the radius of the membrane pore, the effective radius of the membrane pore available for fluid flow is given by R_a , where

$$R_a = R_b - D_A \tag{22}$$

Let r represent the radial distance of the molecules from the center of the pore and $\underline{d}$ be the distance of the molecule from the pore wall as shown in Figure 7, then

$$\underline{d} = R_b - r \tag{23}$$

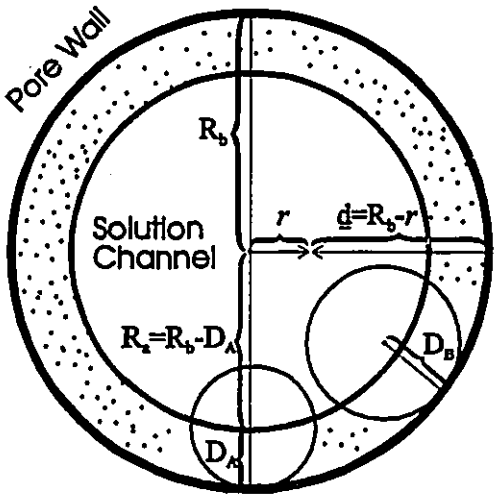

Figure 7 Relation of R_a and R_b, r and $\underline{d}$ (Based on Matsuura and Sourirajan, 1981 and 1985; Zhou et al., 1991).

2.3.3 Transport Equations Based on the Surface Force-Pore Flow Model

Based on the detailed analysis (Matsuura and Sourirajan, 1981 and 1985; Zhou et al., 1991), the following expressions are used in this work. In all expressions, Subscripts A and B refer to component A and B, respectively. Subscripts 2 and 3 denote the concentrated boundary solution on the high pressure side of the membrane (outside the pore) and the membrane permeated production solution on the atmospheric pressure side of the membrane (outside the pore).

The effective driving pressure for fluid flow through the membrane pore is:

$$P_2-P_3=(P_i-P_o)-\overline{C_A}\,\overline{V_A}(\pi_{B,2}-\pi_{B,3})-\overline{C_B}\,\overline{V_B}(\pi_{A,2}-\pi_{A,3}) \quad (24)$$

where P_2-P_3 is the effective driving pressure, P_i and P_o are the operating pressure applied at the pore inlet and the operating pressure at the pore outlet, respectively. $\overline{C}_A$ and $\overline{C}_B$ are the average concentrations of component A and B in the pore, respectively. Assumed that the average solution composition in the membrane pore is close to that of the permeate solution, C_{A3} and C_{B3}. Then, $\overline{C}_A$ and $\overline{C}_B$ can be represented by C_{A3} and C_{B3} , respectively. $\overline{V}_A$ and $\overline{V}_B$ are average molar volume of component A and B, respectively. $\pi_{A,2}$ and $\pi_{B,2}$ are the osmotic pressure of component A and that of component B at the pore inlet (outside the pore), respectively. $\pi_{A,3}$ and $\pi_{B,3}$ are the osmotic pressure of component A and that of component B at the pore outlet (outside the pore), respectively. Osmotic pressures π_A and π_B can be expressed by $\pi_A=(-RT/\overline{V}_B)\ln a_B$ and $\pi_B=(-RT/\overline{V}_A)\ln a_A$, where a_A and a_B are the activity of component A and B, respectively. An assumption is made that the concentration at the boundary layer is equal to the concentration in the bulk solution.

The radial velocity profile for the solution in the membrane pore is:

$$\frac{d^2u(r)}{dr^2}+\frac{1}{r}\frac{du(r)}{dr}+\frac{(P_2-P_3)}{\eta\delta}=0 \quad (25)$$

where u is the radial velocity as a function of radial distance r, η is the solution viscosity and δ is the length of the cylindrical pore.

The boundary conditions for Equation (25) are

$$At\ r=0,\ \frac{du(r)}{dr}=0 \tag{26}$$

$$At\ r=R_a,\ u(r)=0 \tag{27}$$

where R_a is the radius of the solution channel defined by Equation (22).

The concentration profile is expressed by

$$-RT\frac{\partial \ln a_A(r,z)}{\partial z} - (\chi_{AB}+\chi_{AM})\,u(r)\frac{C_{A3}(r)}{C_A(r,z)} + \chi_{AB}\,u(r)\frac{C_{B3}(r)}{C_B(r,z)}=0 \tag{28}$$

where R is the gas constant; T, temperature; a_A, activity of component A; χ_{AB} , proportionality constant defined by RT/D_{AB} (D_{AB} , diffusivity of component A in solvent B); χ_{AM}, friction constant defined by the following equation

$$b_A=\frac{\chi_{AB}+\chi_{AM}}{\chi_{AB}} \tag{29}$$

The friction constant b_A is given by

$$b_A=\begin{cases} [1-2.104\lambda_f+2.09\lambda_f^3-0.95\lambda_f^5]^{-1} & when\ \lambda_f\le 0.22 \\ 44.57-416.2\lambda_f+934.9\lambda_f^2+302.4\lambda_f^3 & when\ 0.22<\lambda_f<1 \end{cases} \tag{30}$$

where $\lambda_f=D_A/R_b$.

Boundary conditions for Equation (28) are obtained by applying the Maxwell-Boltzmann equation at both ends of the pore. They are given by

$$C_A(r,0)=C_{A2}e^{-\phi(C_{A2},r)/RT} \quad \textit{at the pore inlet} \tag{31}$$

$$C_A(r,\delta)=C_{A3}(r)e^{-\phi(C_{A3}(r),r)/RT} \quad \textit{at the pore outlet} \tag{32}$$

where $C_A(r,0)$ and C_{A2} are concentrations of component A at the pore inlet inside the pore and outside the pore, respectively (see Figure 8). Similarly, $C_A(r,\delta)$ and $C_{A3}(r)$ are concentrations of component A at the pore outlet inside the pore and outside the pore.

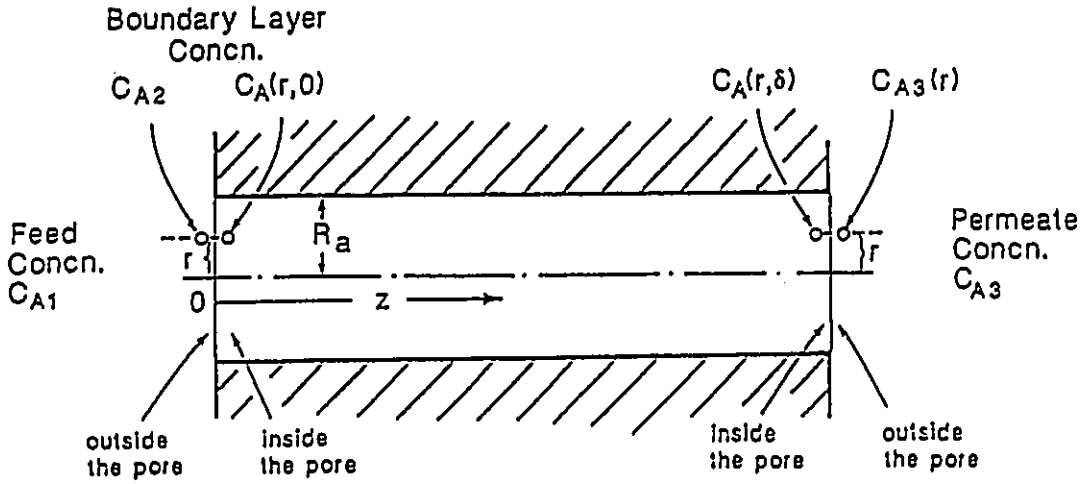

Figure 8 Relationship of concentrations inside and outside a cylindrical pore (Sourirajan and Matsuura, 1985).

Note that the concentration of the boundary layer, C_{A2} , does not depend on the radial distance r. On the other hand, the concentration at the pore outlet outside the pore $C_{A3}(r)$ is considered to depend on the radial distance r. Since the interfacial interaction force constant depends on the composition of the binary mixture, as will be explained later, the potential function ϕ depends on both the distance from the pore wall (or the distance from the center of the pore, r) and the concentration of component A outside the pore.

Differential equations (25) and (28) are used to solve functions u(r) and $C_A(r,z)$ under the boundary conditions (26), (27) and (31). The relationship between activity a_A and concentration C_A for the binary system ethyl alcohol/n-heptane, given by Van Ness et al. (1967), is used in the numerical solution. An appropriate $C_{A3}(r)$ should be chosen to satisfy both Equations (24) and (32) in this iteration process. Therefore, both u(r) and $C_{A3}(r)$ will be known after the calculation is completed. These u(r) and $C_{A3}(r)$ will be used in the following calculation.

The concentration of component A in the permeate solution C_{A3} is given by

$$C_{A3} = \int_0^{R_a} C_{A3}(r)\, 2\pi r\, u(r)\, dr \Big/ \int_0^{R_a} 2\pi r\, u(r)\, dr \qquad (33)$$

Furthermore, the relative permeation rate as expressed by $[PR]/[PSP]_B$ is calculated as

$$\frac{[PR]}{[PSP]_B} = \frac{\left(\int_0^{R_a} u(r)\, 2\pi r dr\right) \times \dfrac{(C_{A3}M_A + C_{B3}M_B)\overline{V}_B}{M_B}}{[\pi R_a^4 (P_2 - P_3)/(8\eta_B \delta)]} \qquad (34)$$

where [PR] and $[PSP]_B$ are membrane permeated product permeation rate and pure solvent (of component B) permeation rate, respectively, for a given area of membrane surface; M_A and M_B are the molecular weight of component A and B, respectively; and η_B is the viscosity of the pure liquid component B .

As for the potential function, ϕ, special considerations have to be given when the radius of component A molecule, designated as D_A, is smaller than that of

component B molecule, designated as D_B. A molecule is considered to be spherical in this model and its position is represented by that of the molecular center. Then, in the vicinity of the polymer-solution interface there is a space which is unoccupied by the center of component B molecules but can be occupied by that of component A molecules (a shadowed region near the interface as shown in Figure 9). Considering the existence of such a region, the concentration profile of component A molecule at the polymer-solution interface becomes such as illustrated in Figure 10. The potential function which represents the above concentration profile should then be such as given in Figure 11, which can be expressed by

$$\phi = \begin{cases} \infty & \text{when } d \le D_A \\ -\ln\dfrac{C_{A,pure}}{C_{A,b}} RT & \text{when } D_A < d \le D_B \\ -\dfrac{B_A RT}{d^3} & \text{when } d > D_B \end{cases} \qquad (35)$$

where $C_{A,b}$ is the concentration of component A in the bulk solution, and $C_{A,pure}$ is the concentration of the pure liquid component A. The molar concentration of an individual component is related to its mole fraction by the relation $C_{A,b}=X_{A,b} \times C_t$, where $X_{A,b}$ and C_t are the mole fraction of component A and the total molar concentration of the bulk solution, respectively. $\underline{B}_A$ is an interfacial interaction force constant depending on the chemical nature of the solute, the solvent, the membrane material and their mutual interactions. $\underline{B}_A$ is a measure of the resultant short range van der Waals force between the feed molecule and the solid membrane.

The following equation has been developed to relate specific surface excess to the interfacial potential function (Sourirajan and Matsuura, 1985)

$$\frac{\Gamma_A}{C_{A,b}} = \int_{D_A}^{\infty} \{\exp[-\phi(d)/RT] - 1\}\, d(d) \qquad (36)$$

When ϕ is determined from Equation (36) by using Γ_A obtained from Equation (13), the interaction parameter $\underline{B}_A$ is generated from Equation (35) for known D_A and D_B. ϕ is used in Equation (28).

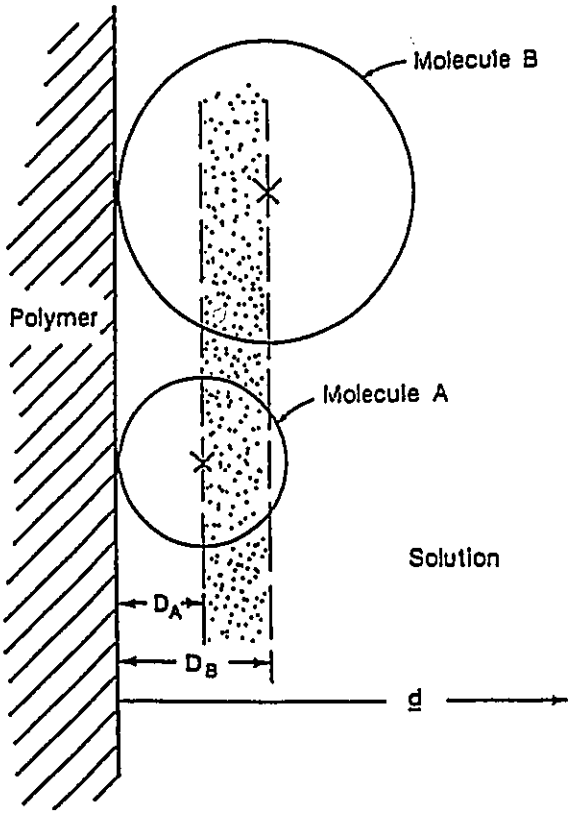

Figure 9 A shadowed region which is unoccupied by the center of the component B molecule but occupied by that of component A molecule.

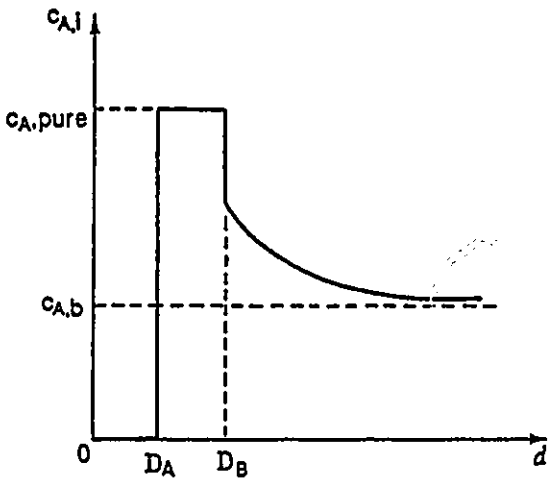

Figure 10 The concentration profile of component A at the polymer-solution interface in the case of the preferential sorption of component A.

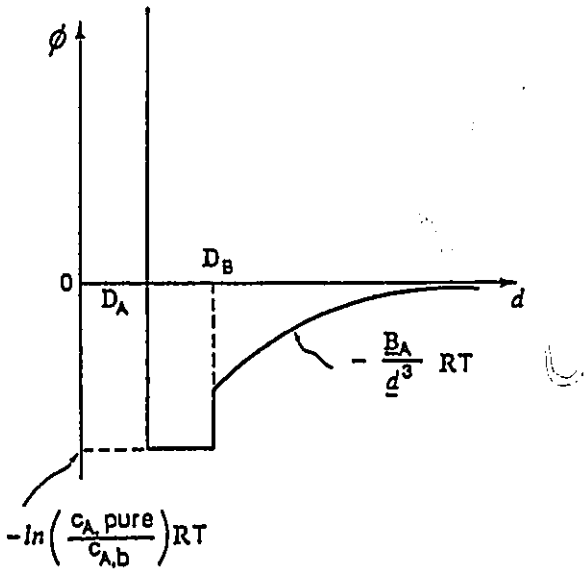

Figure 11 The potential profile of component A at the polymer-solution interface in the case of the preferential sorption of component A.

3. Experimental Methods

3.1 Materials

Chemicals used were of analytical grade and they were usually used without further treatment , unless otherwise stated. Other information such as the name of the supplier, the supplier's location and specifications are included in Appendix A.

3.2 Membrane Preparation Details

3.2.1 Cellulose Acetate Butyrate (CAB) Membranes

The film casting solution had the following composition (weight %):

cellulose acetate butyrate:	14.0
acetone:	74.0
water:	9.0
magnesium perchlorate:	3.0

Water was first added to a bottle equipped with a magnetic stirrer. Magnesium perchlorate was then added and fully dissolved in water. Then, acetone was added and mixed in the bottle. A colorless, transparent solution was formed. Cellulose acetate butyrate (CAB), whose structure is shown in Figure 12, was further added

into this solution while stirring was continued. It took about 24 hours for all the CAB powder to be fully dissolved. Thus, a transparent casting solution was obtained.

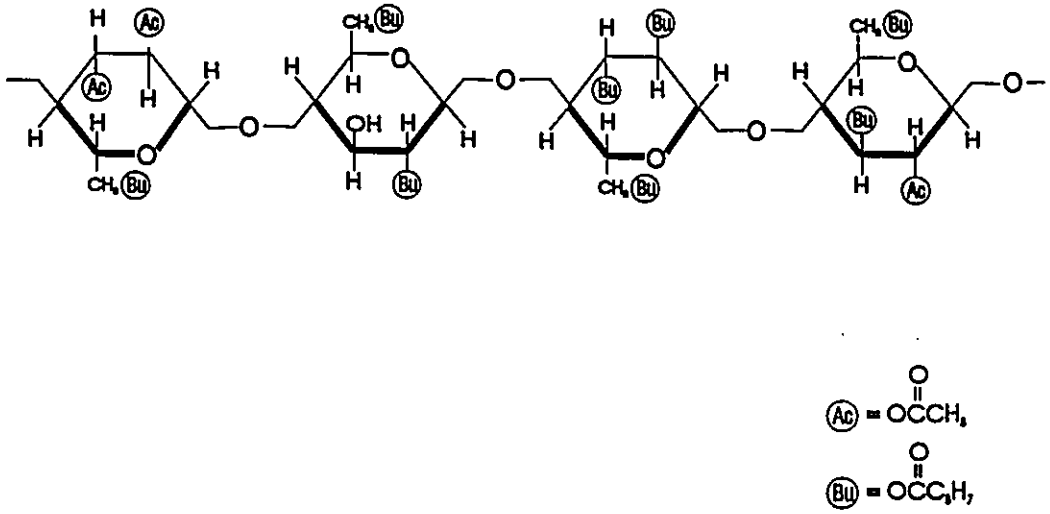

Figure 12 Chemical structure of cellulose acetate butyrate.

The above polymer solution was cast on a glass plate with 0.025 cm (0.01 inch) side runners to give this thickness to the as-cast film. Uniformity of film thickness was assured by passing a thick glass rod across the top of the plate. The glass rod was resting on the side runners only. Acetone was then allowed to evaporate at room temperature, 23-25°C, from the surface of the film on the glass plate for one

minute. The partially hardened film, together with the glass plate, was then carefully immersed into ice-cold water in a tray, where it was left overnight at that temperature. While standing in ice-cold water overnight, the film peeled itself off, or it could be removed by hand easily, from the surface of the glass plate. Then, the membrane was cut into coupons by punching a round knife on its surface. Membrane coupons were dried by a solvent-exchange procedure described in Section 3.2.5.

3.2.2 Aromatic Polyamide (PA) Membranes

The chemical structure of aromatic polyamide (PA) is shown in Figure 13. PA polymer was obtained from the Division of Chemistry, National Research Council of Canada (Nguyen et al., 1987). Its number averaged molecular weight = 31300. The polyamide material was dried under vacuum at 50°C for 48 hours. The film casting solution had the following composition (weight %):

aromatic polyamide:	16.91
lithium nitrate:	6.93
dimethyl acetamide (DMAc):	76.16

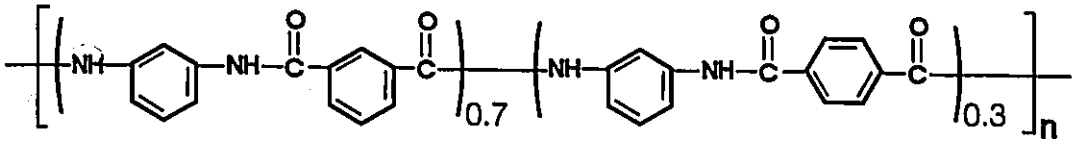

Figure 13 The chemical structure of the aromatic polyamide.

Aromatic polyamide (PA) membranes used in the experiments were prepared according to the following procedure. The polymer was added to a glass container containing lithium nitrate and the solvent dimethylacetamide. The polymer was fully dissolved within three days. The polymer solution so prepared was light yellow, semitransparent and viscous. This casting solution was filtered using a Millipore filter with a 5 μm Millipore polyvinylidene fluoride membrane. It was left overnight at room temperature, without stirring, to remove air bubbles trapped in the polymer solution.

The polymer solution was cast on a Pyrex™ glass plate using a casting blade to a thickness of 0.025 cm (0.01 inch). Then, the cast film was transferred into a convection oven preheated at 95°C, where it was kept for 10 minutes. The partially hardened film was then carefully immersed, together with the glass plate, into ice-cold water in a tray where it was left overnight. While standing in ice-cold water overnight, the film peeled itself off, or it could be removed by hand easily, from

the surface of the glass plate. The membrane was cut into small coupons. The coupons were dried by the solvent exchange procedure described in Section 3.2.5.

Another type of aromatic polyamide was also used for comparison. It was a composite membrane, FT-30 membrane obtained from Dow Chemical Company, Midland, Michigan.The membrane was made from cross-linked aromatic polyamide for seawater desalination and its commercial code was FT-30-SW30-8040.

3.2.3 Polyethersulfone (PES) Membrane Without and With Surface Modifying Macromolecules (SMM)

Polyethersulfone (PES) membranes without and with surface modifying macromolecules (SMM) were prepared. The chemical structure of PES is shown in Figure 14.

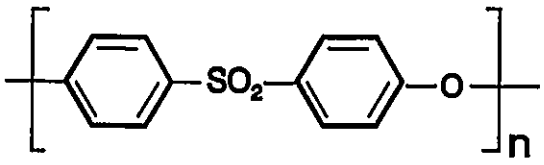

Figure 14 The chemical structure of polyethersulfone (PES).

SMMs were prepared by Pham (1995) by reacting methylene bis-phenyl diisocyanate (MDI) with polypropylene diol (PPO) to form a prepolymer. Then, the SMM was prepared by reacting the prepolymer with the fluorotelomer, Zonyl BA-L™ supplied by DuPont (BA-L). The fluorotelomers used in the synthesis were prepared as follows. The fluorotelomers were received as a mixture of fluorotelomers, whose structure is $F\text{-}(CF_2)_m\text{-}(CH_2)_2\text{-}OH$. The variable number ($m$) of ($CF_2$) repeat units ranges from 4 to 12. The mixture was distilled at 0.025 mmHg to yield three major fractions. Descriptions of each fraction are listed in Table 5. Fraction Low and High were used in this work. The chemical structures of MDI, PPO and BA-L, and the steps of the SMM synthesis are given in Appendix B. The general structure of the SMM is shown in Figure 15. Two different kinds of SMMs were used in the formation of PES membranes. The amount of each component used in the synthesis of SMMs is listed in Table 6 for different SMMs.

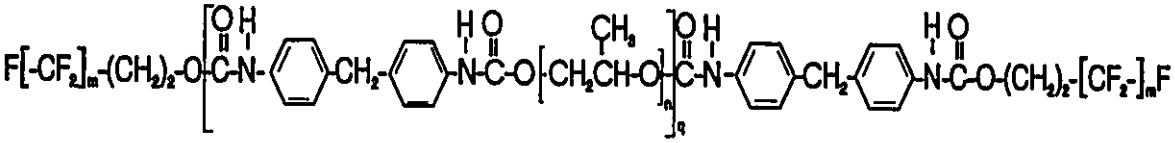

Figure 15 The chemical structure of the surface modifying macromolecule (SMM).

Table 5 Physicochemical properties pertinent to fluorotelomers (DuPont's Zonyl BA-L™)

BA-L fraction	m*	Vapor temperature range at 0.025 mmHg (°C)	Average molecular weight	Physical state
Low	4-8	50-55	443	colorless liquid
Medium	8-10	60-65	490	soft,white solid
High	≥10	70-90	589	white solid

* approximate number of (CF_2) unit based on DuPont's literature.

Table 6 The two different surface modifying macromolecules (SMM)

SMM	Reactant amount (millimoles in 50 mL of dimethylacetamide)			
No.	MDI	PPO	BA-L	BA-L fraction
41	22.5	15	15	Low
44	20	10	20	Low

The compositions of the different casting solutions were as follows. The concentration of SMM in the casting solution was changed from 0 to 3.5 wt % while polyethersulfone (PES) and polyvinylpyrrolidone (PVP) concentrations were maintained at 25 wt % and 6 wt % respectively, unless otherwise stated. The balance was dimethylacetamide (DMAc) solvent. The PES and PVP powder were dried at 150°C and 60°C respectively, in a convection oven for four hours before use. PVP of molecular weight 10,000 was used as a nonsolvent additive. Membranes were cast on a glass plate to a nominal thickness of 2.5×10^{-4} m. Immediately after the casting, the films were transferred into a convection oven preheated at 95°C where they were kept 2 to 16 minutes; this was referred as the evaporation period. The cast films were then gelled by immersing the glass plate into ice-cold water. The membranes were kept in the gelation medium overnight. Specific conditions for membrane preparation are provided in Table 7. PES membranes and PES/SMM membranes were dried by the same solvent exchange technique described in Section 3.2.5, unless otherwise stated.

3.2.4 Silicone Rubber Membranes

The silicone rubber membranes used in this work were MEM-100 membranes commercially obtained from General Electric Co. with a thickness of 7.5×10^{-5} m.

Table 7 Conditions of polyethersulfone membrane preparation

Variable	Condition
Casting temperature	room temperature, 23-25°C
Thickness	2.5×10^{-4} m
Evaporation in air	as short as possible, < 1 second
Evaporation in oven	95°C, various time ranging from 2 to 16 minutes
Gelation media	ice-cold water, overnight
Drying method	first solvent exchanged with ethyl alcohol, then, air dried

3.2.5 Solvent-Exchange Procedure

Membranes used in this work were dried by a solvent exchange technique, unless otherwise stated. In this technique, the water in the membranes after the gelation process was replaced by ethyl alcohol with successive immersions in ethyl alcohol/water solutions (overnight for each immersion). This process was repeated with solutions of different ethyl alcohol content using the following order, 25, 50, 75, 100 vol %. Then, ethyl alcohol was subsequently air evaporated at room temperature for 24 hours to yield the final dry membranes.

3.3 Description of Reverse Osmosis Experiments

The static reverse osmosis cell, which was used in the experiments, is a stainless steel pressure chamber consisting of two detachable parts (see Figure 16). The membrane is mounted on a stainless steel porous plate embedded in the lower part of the cell through which the membrane permeated liquid is withdrawn at atmospheric pressure. The upper part of the cell contains the feed solution under pressure which is in contact with the membrane. The two parts of the cell are clamped and sealed tight using rubber O-rings. Compressed nitrogen gas was used to pressurize the system. About 250 g of feed solution was used each time. The feed solution was kept stirred during the experiment by means of a magnetic stirrer fitted in the cell about one quarter of an inch above the membrane surface.

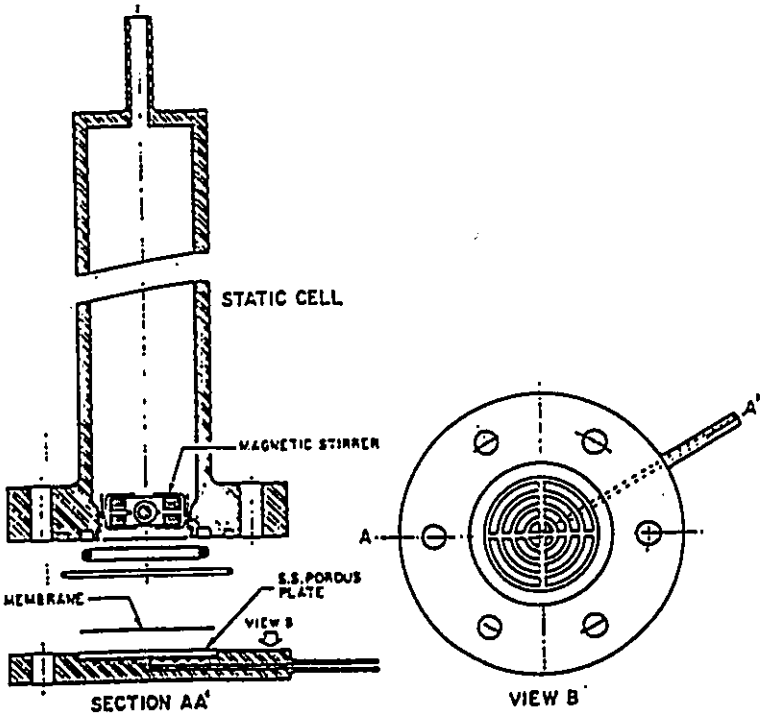

Figure 16 Static testing cell (Sourirajan and Matsuura, 1985).

After membranes were installed in static cells and pressurized at 500 psig for two hours, the first 5 mL of membrane permeated solution, which was referred to as permeant, was discarded and the next 5 mL of permeant was collected as a sample in a weighed dry glass bottle. The time required to accumulate 5 mL of product was recorded. The permeation rate was calculated by dividing the weight of the permeate by the time required for the collection of the sample. In all cases, the permeation rates were reported in units of g/h for 9.6 cm^2 effective membrane surface area at 500 psig. All reverse osmosis experiments were carried out at the laboratory temperature (23-25°C).

3.4 Description of Pervaporation Experiments

The cells used for the pervaporation experiments were the same as those static cells which were used in reverse osmosis experiments. The effective area of the membrane was 9.6 cm^2. About 250 g of feed liquid was loaded in the cell and the vacuum was applied at the downstream side of the membrane. The permeant sample was condensed and collected in a cold trap cooled with liquid nitrogen. The first two hours' permeate was discarded. The amount of the sample removed by membrane permeation was kept below 2% of the initial feed volume. The permeation rate was determined by measuring the weight of the sample collected

during a predetermined period. The composition of the sample was determined either by a refractometer or by a purge-and-trap gas chromatograph. All pervaporation experiments were carried out at the laboratory room temperature (23-25°C). The downstream pressure was controlled within 3±1 mmHg, unless otherwise stated. A detailed description of the pressure control system is attached in Appendix D.

3.5 Analytical Methods

Vinyl acetate/hexane mixtures were analyzed by refractometry. A carrier solvent continuously flowed through the optical cell of the refractometer. A 10-μL sample was injected into the carrier solvent. The difference of the refractive index between the sample cell and reference cell was detected and recorded. The calibration curve was generated by plotting the refractometer response (expressed in terms of area) against the known composition of the corresponding mixture injected. The calibration curve was a straight line. A Waters Differential Refractometer R401 equipped with a Waters 745 Integrator was used. HPLC grade hexane was used as a carrier solvent. The flow rate of the carrier solvent was set at 2.0 mL/min. A column with 0.757 g cellulose was connected between the injector and the refractometer detector to generate a smooth, reproducible response signal from the refractometer.

Ethyl alcohol/n-heptane mixtures were also analyzed by refractometry. HPLC grade ethyl alcohol was used as a carrier solvent. The calibration curve was generated by plotting the refractometer response (expressed in terms of area) against the known composition of the corresponding mixture injected. The shape of the calibration curve was close to a straight line. The flow rate of the carrier solvent was set at 1.0 mL/min. A column with 0.8893 g cellulose acetate was connected between the injector and the refractometer detector to generate a smooth, reproducible response signal from the refractometer.

The chloroform concentration in water mixture was analyzed by a purge-and-trap gas chromatography method. It comprised a purge and trap unit, Tekmar liquid sample concentrator LSC-2 for the concentration of compounds, a Supelco Volatile Purge and Trap Method 624 trap, a Varian Vista Series 6000 gas chromatograph, a Supelco packed column (Carbopack B 60/80 Mesh, 1% SP-1000, 8 feet by 1/8 inch SS), a flame ionization detector, and a Waters 820 chromatography data station for peak analysis. The settings for each of these units were in accordance with the manufacturers' recommendations. They are given in Table 8.

Table 8 Setting for the purge-and-trap gas chromatograph

Purge-and-trap settings	**Gas chromatograph settings**
Time (min.)	*Column temperature program*
Purge: 11	45°C for 3 minutes
Desorb: 4	8°C/min up to 220°C
Bake: 7	220°C for 12 minutes
Temperature (°C)	
Purge ready: 40	*Gas flow rates (mL/min)*
GC oven: 50	Nitrogen: 40
Desorb preheat: 115	Helium: 31
Desorb: 180	Hydrogen: 391
Bake: 210	

The calibration curve was prepared by making a stock solution first. A stock solution was made using 2 L of deionized milliQ™ water in a 2 L volumetric flask, with a stirring magnet and a Parafilm™ seal. A predetermined amount (30-80 mg) of chloroform was injected into the flask by a gastight syringe. Standard solutions were made using 100 mL volumetric flasks, a weighed amount of deionized milliQ™ water, a stirring magnet, and particular volumes of stock solution measured by disposable borosilicate serological pipets. The standards were transferred, immediately after stirring, to 60 mL hypovials which were sealed with Teflon™ lined septa and an aluminum crimped lid, then stored for no more than 24 hours in a refrigerator at about 5°C. The sample size of all injections to the

LSC-2 was 5000 μL out of a 10,000 μL syringe. The calibration covered a range from 10 ppb to 40 ppm chloroform and all permeate was diluted to fall within this range. The calibration curve is given in Appendix E.

3.6 Chromatography Experiments

Column Packing

Cellulose acetate butyrate and polyethersulfone polymers were packed in two separate columns. For both columns, stainless steel tubing with a length of 0.6096 meters (2 feet) and an inside diameter of 0.001575 meters (0.062 inches) was used. The procedure to fill the column was as follows. The stainless steel tubing was cut to the required length. The tubing was washed consecutively with soap solution, water, methanol, acetone, and again with water to remove any dirt or oil from the internal tube surface. This was followed by a 4-hour drying in an oven at 260°C. Cellulose acetate butyrate (Eastman CAB-171-40) powder was dried at 60°C overnight. Then, the powder was subjected to sieving, to collect a fraction with a size range of 38-53 μm. The polymer powder was packed dry from one end of the tube while vacuum was applied at the other end. The amount of CAB powder in the column was known to be 0.0005120 kg by weighing the column before and after packing of polymer powder. The column was washed with pure ethyl alcohol

continuously overnight before it was used for chromatography experiments. The same procedure, including sieving, was followed to pack polyethersulfone powder into stainless steel tubing. The weight of the packed polyethersulfone was 0.001689 kg.

3.6.1 Liquid and Gas Chromatography Experiments with the CAB Column

Liquid Chromatography Experiments with the CAB Column

The liquid chromatography system is schematically given in Figure 17. A Waters Associate Liquid Chromatograph (Model 501) fitted with an R401 refractometer was used in this work. The refractometer signal was fed to a Waters 745 integrator. The time taken for the appearance of the maximum recorded response after each injection was defined as the retention time. The retention volume was obtained by multiplying the retention time by the flow rate of the mobile phase.

To conduct the liquid chromatography experiment, a mixture of ethyl alcohol (A) and n-heptane (B) of known composition was pumped into the column as a chromatography solvent (the mobile phase). Then, 10 μL of pure A and 10 μL of pure B were manually injected from a 50 μL Hamilton syringe into the solvent stream as chromatography samples and their retention times were recorded corresponding to the given mixture composition, $X_{\mu,A}^{o}$. The mobile phase flow rate

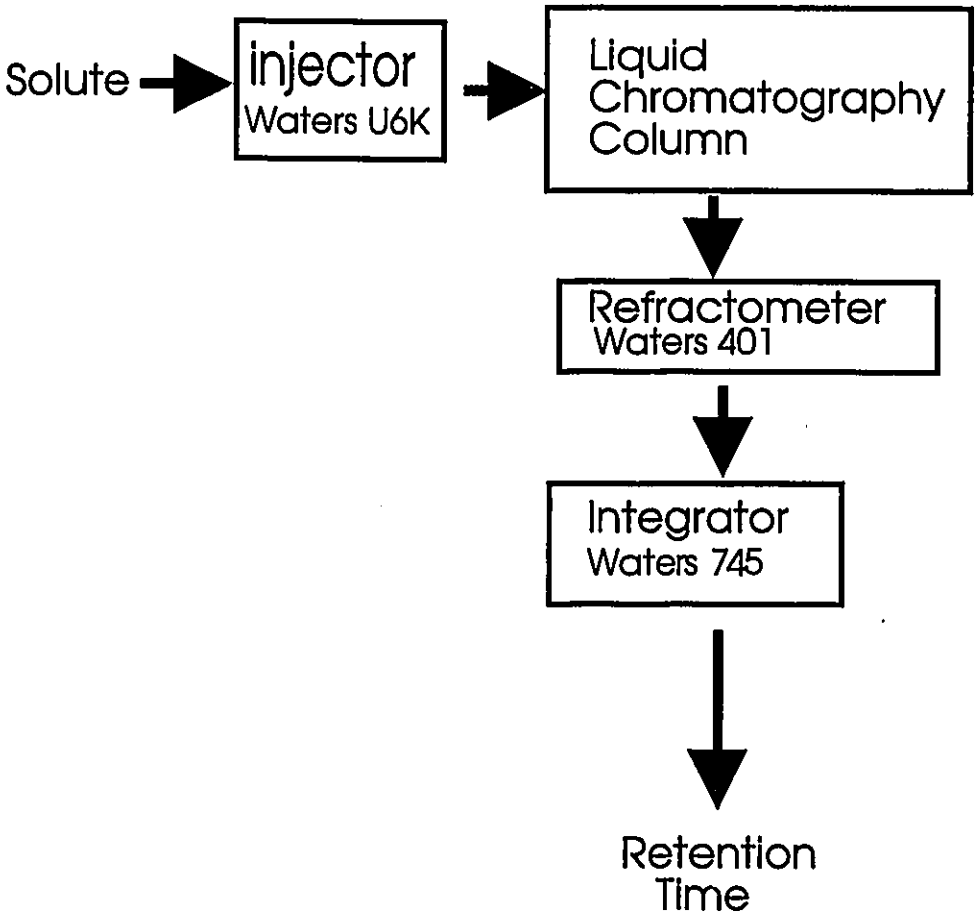

Figure 17 Liquid chromatography system set-up.

was set at 0.3 mL/min and the column pressure drop was below 300 psi. A 15-micron filter was placed in between the column outlet and the detector inlet to prevent any leakage of packed material from the column. This filter was kept in a 50 wt % nitric acid aqueous solution after use every day. The retention volume was obtained by multiplying the retention time and the flow rate. The surface excess value, Γ_A , was calculated using the experimental retention time data from Equations 11 to 13. When the given mixture (mobile phase) composition, $X_{\mu,A}^{o}$, changed, so did the retention time. Thus, the surface excess was obtained in the entire composition range of the binary mixture.

Surface Area Determination by Gas Chromatography

In order to obtain the interfacial properties of the polymer by liquid chromatography, the total surface area of the cellulose acetate butyrate (CAB) powder in the chromatography column was required. The method chosen was a vapor-liquid saturation method as outline by Huber and Gerritse (1971), Mohlin and Gray (1974) and Matsuura et at. (1981). The same CAB column used in the liquid chromatography experiment was loaded into a gas chromatograph. The experiment was carried out with helium as the carrier gas at a flow rate of 33.3 cm^3/min and at an oven temperature of 76.4°C. The column was kept at 76.4°C and

flushed with dry helium gas for at least 12 hours before chromatographic experiments. The helium gas was dried by passing through a glass tube containing Drierite™ (the drying particle from Anachemia Inc., Montreal, Canada). Solvent (either ethyl alcohol or n-heptane) was injected into the column in amounts that varied from 0.1 μL to volumes that caused saturation (in excess of 40 μL). For each of these injections, the retention time, the peak height and the peak area were recorded. The gas chromatographic experiment was performed using a Varian 1400 Model equipped with a thermal conductivity detector.

3.6.2 Gas Chromatography and Liquid Experiments with the PES Column

Gas chromatography and liquid chromatography experiments were performed to determine the sorption properties of water and chloroform in vaporous and liquid phases for the polyethersulfone (PES) material.

Gas Chromatography Experiments

The column containing polyethersulfone was flushed with helium gas overnight before testing. A Varian Series 1400 gas chromatograph equipped with a thermal conductivity detector was used. The column temperature was kept at 100.5°C. One μL of pure water or chloroform was injected into the carrier gas stream. The carrier gas was helium flowing at the rate of 31.0 cm^3/min.

Liquid Chromatography Experiments

The same column as in the gas chromatography experiment was used in the liquid chromatography experiment. The column was washed with distilled water overnight before testing. A Waters liquid chromatograph Model 501 fitted with a R401 refractometer was used. A 10-μL sample of pure chloroform or deuterium oxide in lieu of distilled water was injected into the stream of the mobile phase. Distilled water was used as the mobile phase and its flow rate was set at 5.0×10^{-9} m^3/s (0.3 mL/min). The pressure drop across the column was less than 2.07×10^6 Pa (300 psi).

3.7 Sorption Measurement of CAB Material

Sorption measurements of cellulose acetate butyrate (CAB) material were conducted for both CAB films and CAB powder. The experimental procedure was as follows.

For sorption measurement of CAB films, homogeneous CAB films were prepared by dissolving 14 wt % of CAB in acetone (86 wt %). The CAB solution was cast on a glass plate placed in a fume hood. Acetone was evaporated by leaving the cast film in the air at room temperature for 24 hours. The membrane sheet was easily

peeled off the glass plate and was cut into membrane coupons. These membrane samples were placed in a desiccator and vacuum was applied. Constant weights of dry samples were reached in about 48 hours. These dry membrane samples were immersed in a liquid mixture of ethyl alcohol/n-heptane, whose composition was known, for 48 hours at room temperature. The samples were removed from the mixture, blotted free of surface liquid, weighed and placed in a dry container. The container was connected to a vacuum line and the liquid in the films was transferred into a nitrogen cold trap by applying vacuum for 6 hours. The amount and composition of the liquid collected in the cold trap was determined by weighing and by gas chromatography, respectively.

For sorption measurement of CAB powder, the column made of CAB powder for liquid chromatography experiments was used. It was dried in an oven at 60°C for 24 hours and then vacuum-dried for 4 hours. A mixture of ethyl alcohol (*A*)/n-heptane (*B*) of known composition was circulated through the column for 48 hours using a Waters 501 HPLC solvent delivery system. Then, the column was detached from the circulating system and the liquid inside the column was transferred into a cold trap by applying vacuum. The amount and composition of the liquid collected in the cold trap were determined by weighing and by gas chromatography, respectively. The liquid collected in the cold trap was considered

to be the mixture of the bulk liquid filling the void space inside the column and the liquid sorbed by the CAB powder inside the column. Since the total weight and composition of the above binary mixture were known, the total number of moles of each component, $n_{A,total}$ and $n_{B,total}$, could be determined. The weight of the bulk liquid filling the void space was calculated by subtracting the weight of the sorbed liquid, which could be obtained from the film sorption data, from the total weight of the mixture. An assumption was made that the bulk liquid had the same composition as the feed liquid mixture. Then, since the weight and composition of the bulk liquid were known, the number of moles of *A* and *B* in the bulk portion, $n_{A,bulk}$ and $n_{B,bulk}$, could be determined. Thus, the number of moles of *A* and *B* sorbed by the CAB powder was determined as $n_{A,sorbed}= (n_{A,total} - n_{A,bulk})$ and $n_{B,sorbed}= (n_{B,total} - n_{B,bulk})$, respectively. The mole faction of *A* in the liquid mixture sorbed in CAB powder was calculated using $n_{A,sorbed}$ and $n_{B,sorbed}$. The same procedure was repeated for the ethyl alcohol/n-heptane mixtures of different feed compositions. The ethyl alcohol mole fraction of the sorbed portion was plotted against that of the feed.

3.8 Other Measurements

Other measurements were performed to characterize the membranes. Samples for

the following measurements were prepared in the same way as the PES/SMM membranes were prepared, unless otherwise stated.

Contact angles of water on PES and PES/SMM membranes were measured at the Ottawa Civic Hospital of University of Ottawa. Films for contact angle measurements were prepared by casting the membrane casting solutions on clean glass slides. Then, they were transferred into an oven preheated at 95°C and heated for 10 minutes, followed by drying in a convection oven at room temperature for 24 hours and vacuum-drying at 50°C for 24 hours. A Ramé-Hart Model A-100 goniometer was used. Distilled water was purified using a Barnstead NANOpure II unit, and initial water drops (2.0×10^{-4} mL for each) were deposited on the film surface with a Ramé-Hart, Model 100-10 μL gas tight syringe. The volume of the drop was increased by adding slowly more water using the same microsyringe. The advancing and receding contact angles were determined when the profile of the drop no longer changed with the addition and subtraction of water, respectively.

Elemental analysis was performed at Guelph Chemical Laboratory, Guelph, Ontario, to determine the bulk elemental compositions of the SMM. The fluorine content of SMM was reported as a weight percent. X-ray photoelectron spectroscopy (XPS) and scanning electron microscopy (SEM) were done at the Center for Biomaterials at the University of Toronto and the Department of

Chemistry at the University of Ottawa, respectively.

Gel permeation chromatography (GPC) was used to determine the average molecular weights (relative to polystyrene standards) of SMM and PES. Three Waters Ultrastyragel columns (10^3, 10^4 and 10^5 Å pore sizes), a high pressure solvent delivery system (Waters 510) and a differential refractive index detector (Waters 410) were used. The solvent phase was HPLC grade dimethylformamide containing 0.05 M LiBr. The flow rate was 1 mL/min and the column temperature was 80°C. The sample size was 200 μL and the polymer concentration was 0.2 g/100 mL.

Information on the precision of the measurements is indicated by error bars.

4. Results and Discussion

The following sections are results and discussion, which focus on the characterization of the membrane materials and the evaluation of the membranes. First, the results related to pervaporation (Section 4.1) and then, the results related to reverse osmosis (Section 4.2) will be presented. Finally, comparison is made between the results of reverse osmosis and those of pervaporation (Section 4.3).

4.1 Results and Discussion Related to Pervaporation Studies

4.1.1 Chromatography Results

Gas chromatography and liquid chromatography experiments were performed to determine the sorption properties of water and chloroform in vaporous and liquid phases. They were conducted using a polyethersulfone (PES) column.

Gas chromatography experiments showed the retention volume of water and chloroform to be 4.79×10^{-5} and 2.20×10^{-4} m^3, respectively. Liquid chromatography experiments gave the retention volume of deuterium oxide (in lieu of water) and chloroform to be 1.82×10^{-6} m^3 and 1.88×10^{-6} m^3, respectively. The peak shape was narrow for water, whereas broad peaks were observed for chloroform both in gas and liquid chromatography. Peak shape and retention volume are indicators of the sorption strength (Hamilton and Sewell, 1978). Both wider peak shape and larger retention volume reflect stronger adsorption. The difference in the peak shape and retention volume data between chloroform and water/deuterium oxide demonstrates that chloroform is preferentially adsorbed to the polyethersulfone material in the vapor phase, although it is only slightly preferentially adsorbed in the liquid phase.

4.1.2 Effect of Solvent Evaporation Period on PES Membrane

As mentioned in the experimental part, the preparation of the membranes involved solvent evaporation. During this step, membranes were kept in a preheated oven for various periods, to evaporate the solvent partially. To examine the effect of solvent evaporation period, two casting solutions were prepared, one without SMM and the other with SMM (0.5 wt %). Their respective compositions are given in Table 9. The membranes were used without drying.

Table 9 The composition of two casting solutions both of which have 1-, 3-, and 5-minutes evaporation periods

Compound	Composition, wt %	
	Solution without SMM	Solution with SMM
SMM†	0	0.5
Polyethersulfone	25	25
Polyvinylpyrrolidone	6	6
Dimethylacetamide	69	68.5

† The type of SMM used was SMM41.

The effect of the solvent evaporation period on the performance of PES membrane without SMM is shown in Figure 18. Note that the feed chloroform concentration was 1000 ppm. Figure 18a shows that the chloroform concentration in the permeate was lower than that in the feed, indicating that PES membrane was water selective.

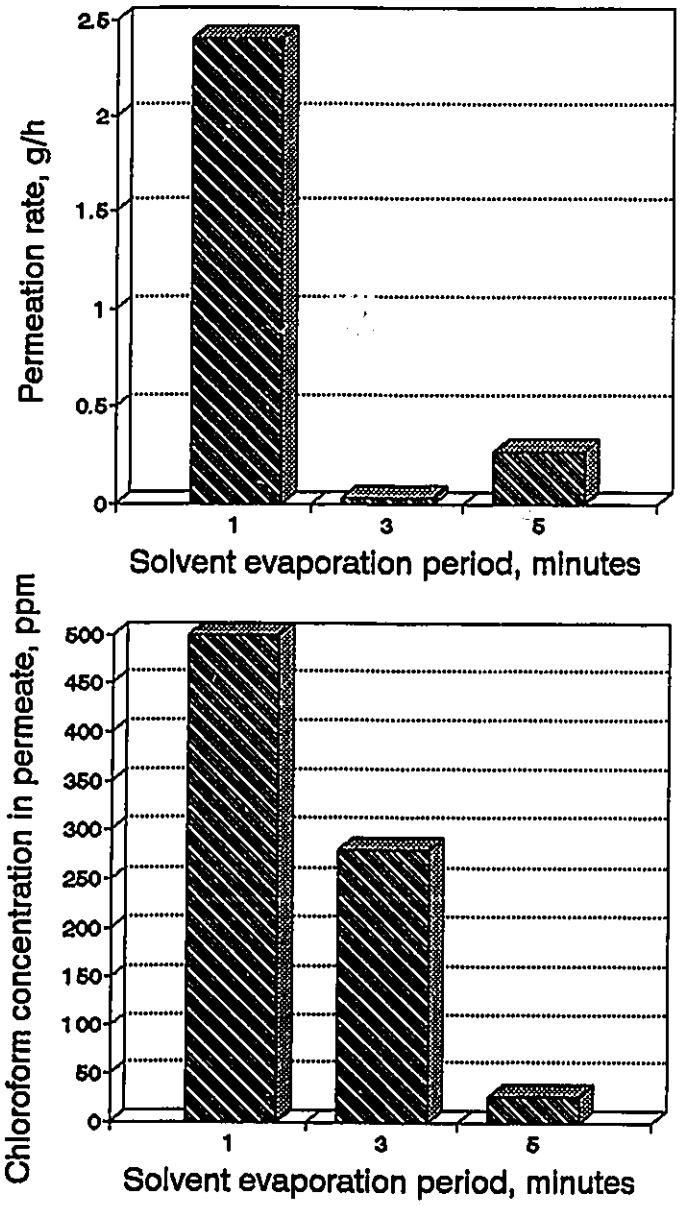

Figure 18 Effect of evaporation period on pervaporation performance of polyethersulfone membrane without SMM additive for the chloroform/water mixture. Temperature: 23°C. Downstream pressure: 3 mmHg (400 Pa). Effective membrane area: 9.6×10^{-4} m^2. Feed chloroform concentration: 1000 ppm.

The chloroform concentration in the permeate decreased as the evaporation period became longer. Figure 18b shows that the permeation rate for the membrane with 3- and 5-minute evaporation period was significantly lower than that for the membrane with 1-minute evaporation period.

The separation mechanism may help to explain the water selectivity exhibited by the PES membrane. In general, separation is controlled by two factors, namely, the thermodynamic factor and the kinetic factor (Sourirajan and Matsuura, 1985). The former is caused by the sorption equilibrium of the minor component, while the latter is the reflection of the relative mobility of the minor and major components in the membrane. These two factors may work together to enhance the preferential permeation of the minor component or they may compete with each other. In the pervaporation system discussed here, chloroform is the minor component and water is the major component. Based on the results of the chromatographic experiments, it is known that the minor component (chloroform) is preferentially adsorbed to the membrane material in both liquid and vapor phase. Therefore, the thermodynamic factor favors the preferential permeation of chloroform.

Comparing the relative size of water and chloroform, the molar volume of water is 18.016×10^{-6} m^3/mole, while that of chloroform is 80.181×10^{-6} m^3/mole. Since the friction against the movement of the permeant molecule in a pore increases with an increase in the size of the permeant molecule relative to that of the pore (Sourirajan and Matsuura, 1985), the friction on the water molecule would be less than that on the chloroform molecule. In other words, the kinetic factor favors the preferential permeation of the water molecule. Therefore, in this particular system the equilibrium and the kinetic factors are competing with each other.

The data in Figure 18a indicate that the kinetic factor dominated the separation, resulting in the preferential permeation of water. The PES membrane with various evaporation periods all showed selectivity towards water.

The data in Figure 18 also indicate that longer solvent evaporation period leads to a higher separation. It is common knowledge that ultrafiltration membranes are porous (Sourirajan and Matsuura, 1985). Since the polyethersulfone ma.erial and the conditions of membrane preparation used in this study are similar to those for ultrafiltration membranes, the fabricated membranes are believed to be porous. In the case of ultrafiltration membranes, an increase in evaporation period will decrease the average pore size on the membrane surface (Sourirajan and Matsuura, 1985). Smaller pore size makes it more difficult for chloroform to go through the membrane pore due to its larger molecular size compared with water. Hence, the water selectivity is enhanced due to the smaller pore size resulting from a longer evaporation period.

The substantial decrease in the permeation rate accompanied by evaporation period longer than 3 minutes corresponds to the expected decrease in the pore size associated with an increase in evaporation period.

The effect of evaporation period on the performance of a PES membrane with SMM was also examined using a PES casting solution containing 0.5 wt % SMM when other preparation conditions remained the same. The experimental results are shown in Figure 19. A similar pattern prevails when the results are compared with those in Figure 18. The notable difference is the steeper decline in chloroform concentration in the permeate with the presence of SMM when Figure 19 is compared with Figure 18. The effect of SMM concentration on the membrane performance will be discussed separately in Section 4.1.6.

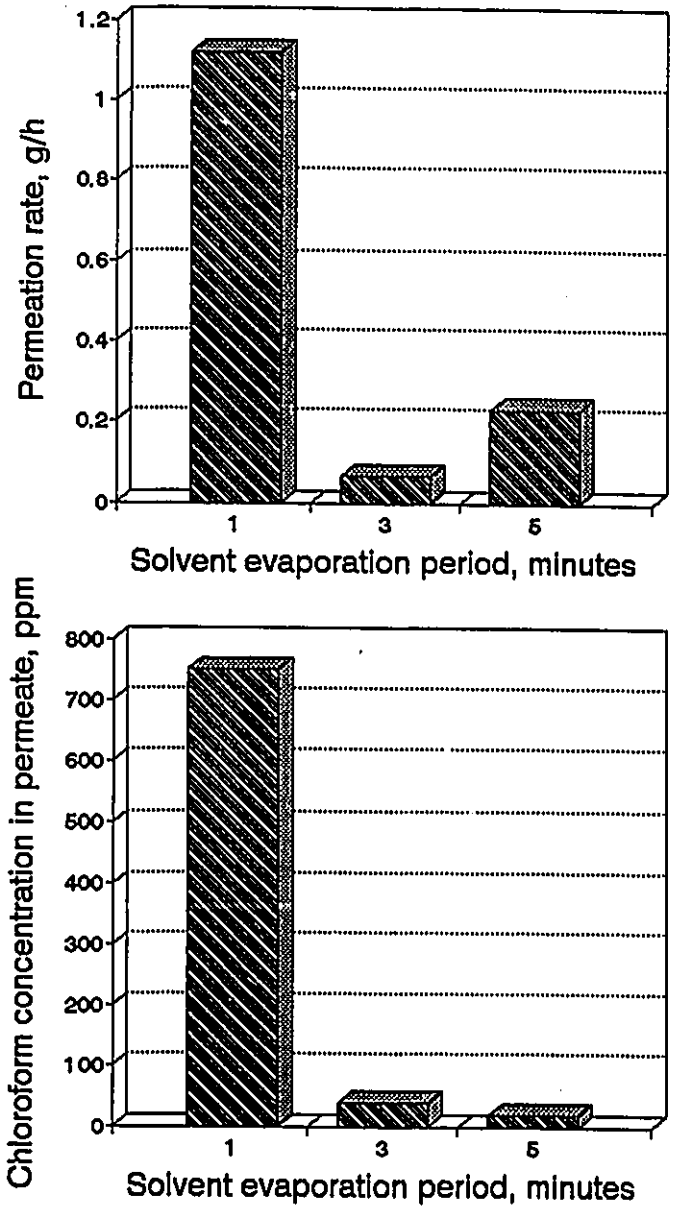

Figure 19 Effect of evaporation period on pervaporation performance of polyethersulfone membrane with 0.5 wt % SMM additive for the chloroform/water mixture. Temperature: 23°C. Downstream pressure: 3 mmHg (400 Pa). Effective membrane area: 9.6×10^{-4} m^2. Feed chloroform concentration: 1000 ppm.

4.1.3 Membrane Morphology Study by Scanning Electron Microscopy

Polyethersulfone membranes containing 1 wt % SMM were prepared using the method described in the experimental sections. The membrane casting solution contained 25 wt % polyethersulfone, 1 wt % SMM (SMM41), 6 wt % polyvinyl-pyrrolidone and the remaining solvent dimethylacetamide. The cast membranes went through partial solvent evaporation. The evaporation period ranged from 2 to 10 minutes in an oven at 95°C. The cross-sections of the membranes were examined using scanning electron microscopy and the micrographs taken are shown in Figures 20 and 21.

The membrane with a 2-minute evaporation period shown in Photograph (a) in Figure 20 features a thin dense skin layer and a finger-like porous substrate. This is more evident from Photograph (b) in Figure 20, showing the microscopic picture taken near the skin layer. The finger-like pores occupy a large part of the porous substrate but they do not penetrate the entire cross-section. The pores increase in diameter from the top to the bottom side.

Photograph (a) in Figure 21 shows that the membrane with a 5-minute evaporation period has a structure similar to the membrane with a 2-minute evaporation period. Photograph (b) in Figure 21 shows the cross-section of the membrane with a 7-minute evaporation period. The membrane shows a sponge-like structure with a dense skin at the surface and a porous structure underneath with a relatively uniform pore size distribution over the entire cross-section. Photograph (c) in Figure 21 shows the cross-section of the membrane with 10-minute evaporation period. Unlike the membranes that are structurally asymmetric as shown in Photographs (a) and (b), no visible pores are observed in the cross-section of the membrane at the resolution level of the electron microscope.

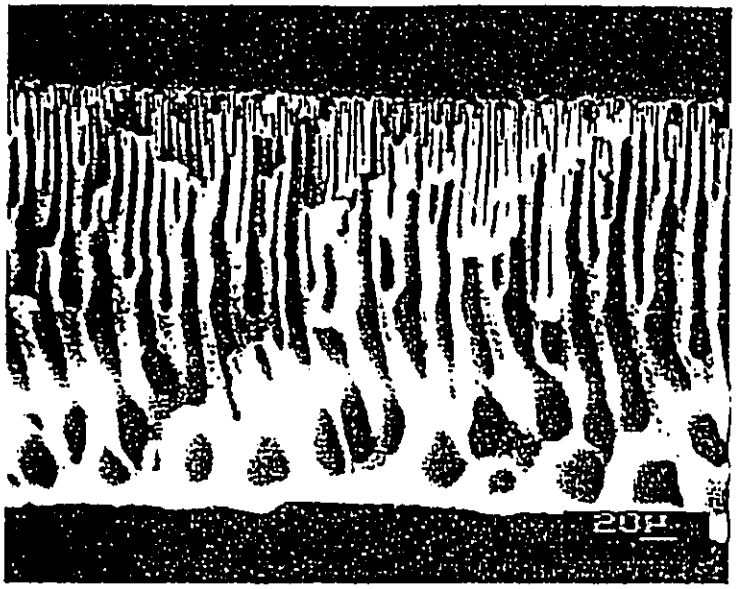

(a)

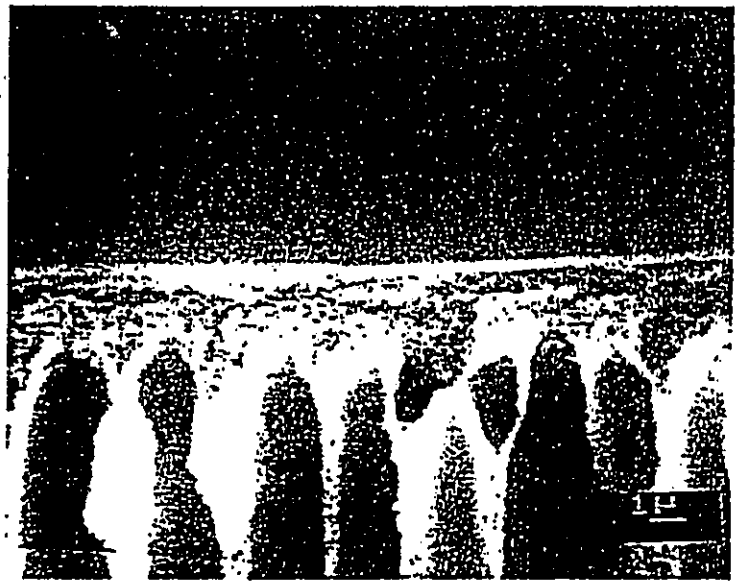

(b)

Figure 20 The scanning electron micrographs of membrane cross-section for membrane with 2-minute evaporation period. (a) lower magnification, (b) higher magnification near skin side.

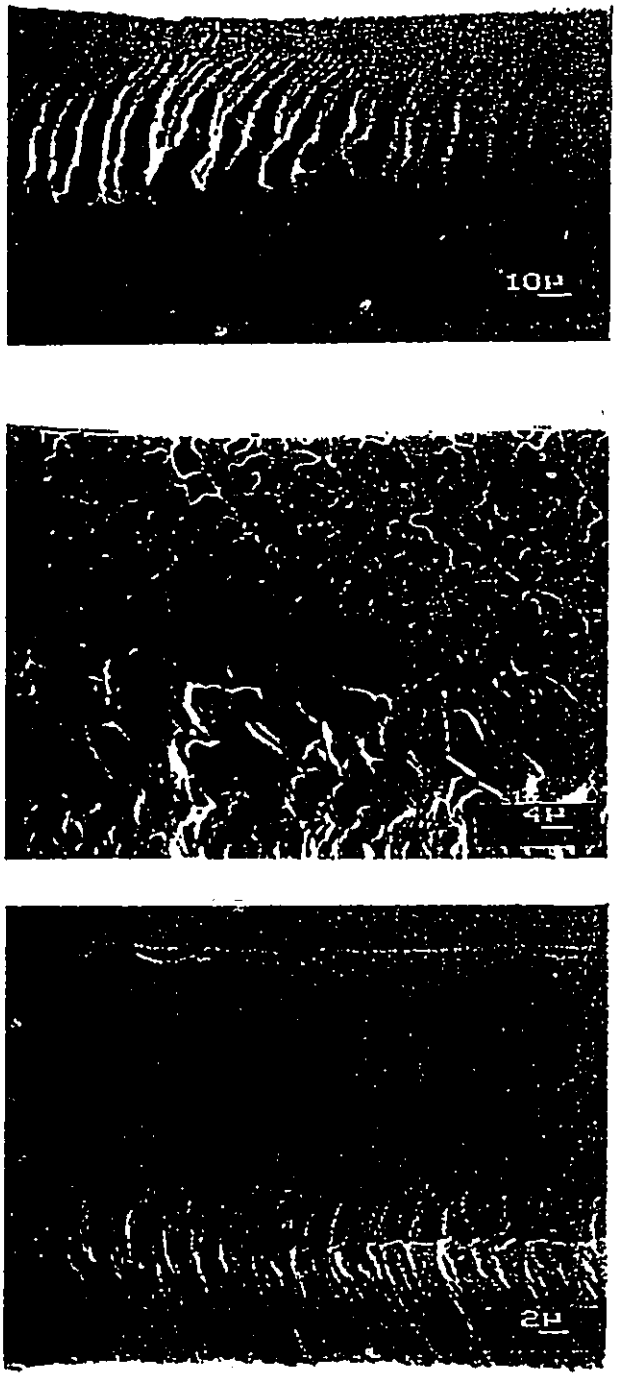

(a)

(b)

(c)

Figure 21 The scanning electron micrographs of membrane cross-section for membranes with various evaporation period. (a) 5 minutes, (b) 7 minutes, and (c) 10 minutes.

Note that the only difference in the preparation conditions for the above mentioned four membranes is in the solvent evaporation period prior to gelation. During the solvent evaporation period, the local concentration of polymer on the surface of the cast polymer film increases due to the loss of solvent. On the other hand, the solvent evaporation period also influences the kinetic aspect of membrane formation. According to Strathmann (1990), fast precipitation of a polymer solution in a nonsolvent tends to produce a finger-like structure. When the solvent loss on the film surface cannot be compensated for by the solvent diffusion from the film interior to the surface, phase separation in the surface region takes place. As a result, the resistance to the solvent-nonsolvent exchange in the later gelation step increases, and the polymer precipitation slows down, leading to a sponge-like structure. This explains the structural difference in the membranes with different evaporation periods. Higher polymer concentration at the point of precipitation resulting from longer evaporation periods also tend to result in denser membranes that are believed to be responsible for the observed higher separation and lower permeation rate.

Clearly, the solvent evaporation step in membrane preparation procedure has a significant effect on the structure of the resulting membrane. Simply by varying the solvent evaporation conditions, membranes with significantly different structures can be produced from the same membrane casting solution. Most importantly, Figures 20 and 21 demonstrate that an asymmetric membrane can be prepared from the solution containing SMM.

An important clarification should be made regarding the possible migration of SMM towards the membrane-air interface. If SMM ever migrated towards the membrane-air interface, it would be in the outmost region within the skin layer. To put it into perspective, the entire thickness of the membrane is about 0.1 mm, while

the thickness of the active surface layer is only 30-100 nm (Matsuura 1994). As will be shown later (Figure 23) within the outmost 2 nm sampling range, the SMM concentration decreases significantly as the sampling depth increases. Although we cannot differentiate the SMM layer from the top skin layer in Figures 20 and 21, it should be pointed out that it is the outmost surface region that SMM migrates to and accumulates there, if migration of SMM ever happens.

4.1.4 Results of Contact Angle and XPS Measurements for PES/SMM Membranes

Films for contact angle measurement were prepared according to the description in Section 3.8. For XPS measurements, polyethersulfone (PES) membranes containing different amounts of SMM were prepared according to the phase inversion method described in Section 3.2.3. In the casting solutions, PES and PVP contents were maintained at 25 wt % and 6 wt %, respectively. The amount of SMM varied from 0 to 3.5 wt % in the casting solutions. The remaining was the solvent dimethylacetamide. These PES/SMM membranes were dried by the solvent exchange technique described in Section 3.2.5. The type of SMM used was SMM44 (cf. Table 6 on p. 52 for details).

The surface of PES/SMM membranes was characterized by contact angle and X-ray photoelectron spectroscopy (XPS) measurements. The background and theory relevant to these two complementary analytical methods are discussed elsewhere (Mohr et al., 1991). Generally, contact angle measurement yields information on the uppermost surface, to a depth of ~ 10 Å, while XPS probes the immediate subsurface region to a depth of ~ 60-90 Å in polymers (Le Roux et al., 1994).

The results of the contact angle measurement for PES/SMM membranes are shown in Figure 22. It shows that both the advancing and the receding contact angle increase significantly with an increase in the SMM concentration in the casting

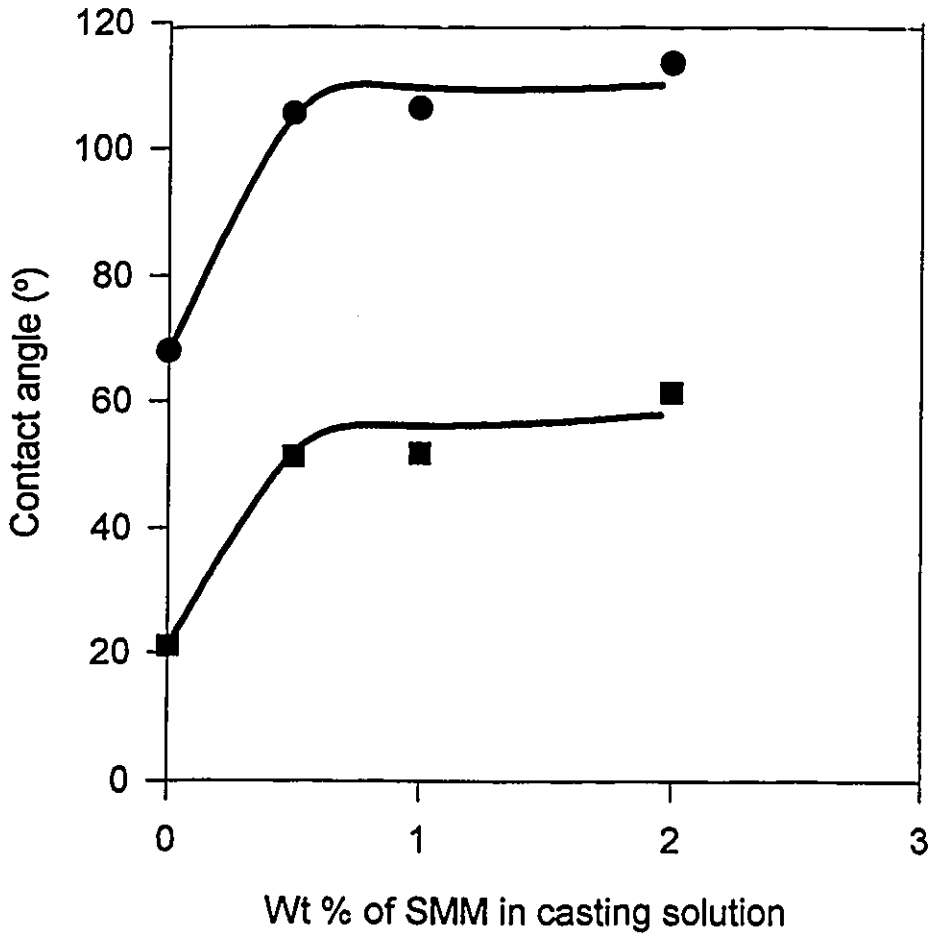

Figure 22 Effect of the SMM concentration on contact angles of water on the surface of polyethersulfone/SMM membranes. ●, advancing contact angle; ■, receding contact angle.

solutions when the SMM concentration is less than 0.5 wt %, and level off at higher SMM concentrations. For instance, the advancing contact angle increases from 68° to 105° with an increase of SMM from 0 to 0.5 wt %. This could be due to the existence of SMMs containing fluorine tails on the membrane surface. This will be further discussed below in conjunction with the XPS results. The contact angle results indicate that the addition of the SMM increases notably the contact angles of the PES/SMM membrane. The significant increase in contact angle suggests that the PES/SMM membrane has a more hydrophobic surface than the PES membrane.

The XPS sampling was performed at different angles in a range between 15° and 90°. The data obtained at 15° represent the chemical composition of approximately the top 2 nm of the surface, whereas the information collected at 90° is associated with approximately the top 10 nm (Andrade, 1985). The element fluorine is associated with the SMMs while the element sulfur is only found in PES. The ratio of atomic fluorine to atomic carbon, F/C, is indicative of the SMM's polyfluoro-segment, whereas the ratio S/C is indicative of PES. The high resolution data from XPS provide information such as the ratios of $-CF_2-$/C-C, $-CF_3$/C-C, both from SMM's polyfluoro-segment, and $-CF_3/-CF_2-$, indicating a degree of orientation of the polyfluoro-segment.

The XPS results for the PES/SMM membranes are shown in Figure 23. The fluorine concentration at the membrane surface, expressed as the ratio F/C, is given at different XPS take-off angles. Changing the take-off angle effectively varies the probing depth between a maximum of ~ 10 nm below the sample surface at a take-off angle of 90° and a depth of ~ 2 nm at an angle of 15° (Andrade, 1985). Note that the SMM is the only source of fluorine. Figure 23 indicates the existence of

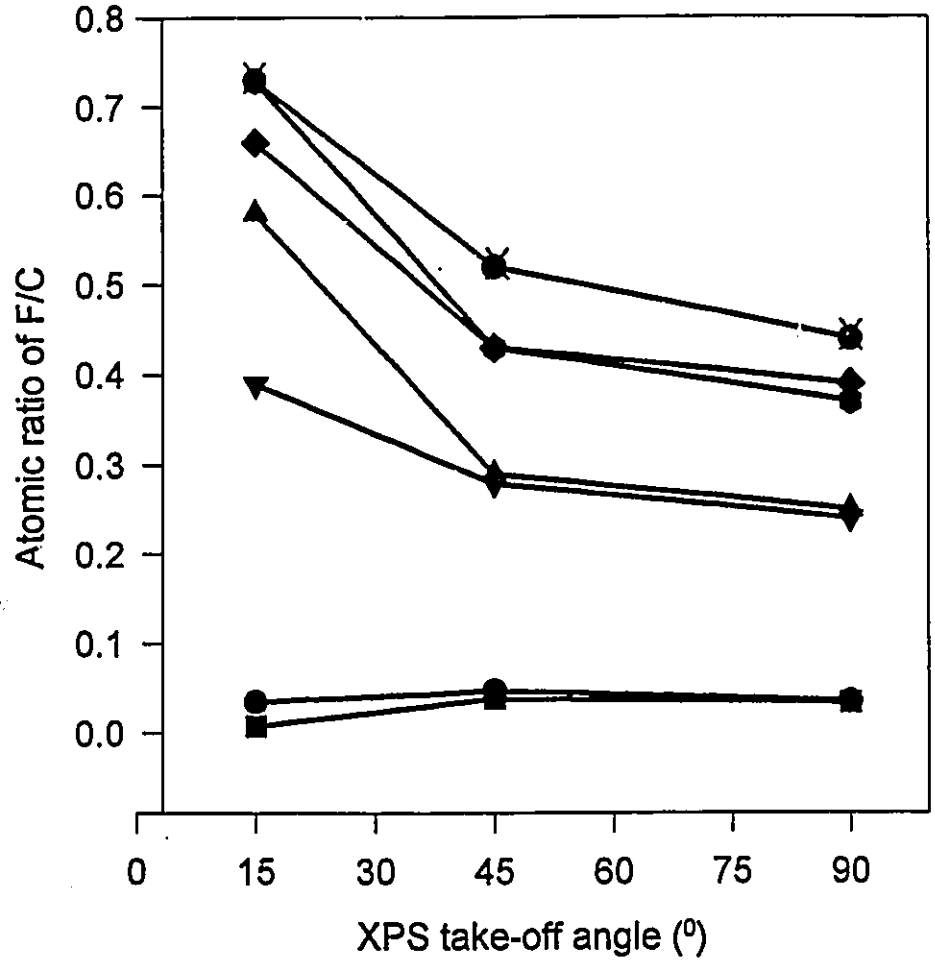

Figure 23 XPS composition of atomic fluorine with respect to atomic carbon for the polyethersulfone/SMM membranes. SMM wt % in the casting solution:

●, 0.5 %; ■, 1.0 %; ▲, 1.5 %; ▼, 2.0 %; ◆, 2.5 %; ⬢, 3.0 %; ✖, 3.5 %.

fluorine concentration gradients (i) between the surface and the bulk, and (ii) within the probing depth. Based on the results of elemental analysis and the composition of the casting solution, addition of 1.5 wt % of SMM to the membrane casting solution corresponds to the ratio F/C = 0.01 in the bulk of the dry membrane (see Appendix F). The data in Figure 23 indicate that the fluorine concentration is much higher at the membrane surface than in the bulk. This is strong evidence that fluorine-containing SMM migrates to and accumulates at the membrane surface.

The SMM used has a molecular weight of 1.3×10^4 which is smaller than PES's molecular weight of 1.0×10^5. SMM also contains a surface active segment involving fluorine. It is hypothesized (Fang et al., 1994) that these two features lead to the migration of SMM to the surface when mixed with PES.

Further, the data in Figure 23 also show that the fluorine concentration gradient exists within the probing depth. For example, when 1.5 wt % of SMM is added to the membrane casting solution, the ratio F/C increases from 0.25 to 0.58 with a change of the take-off angle from 90° to 15°. Elemental analysis shows that pure SMM44 has an F/C ratio of 0.23 (see Appendix G). Since the fluorine content at the outermost surface layer of the membrane is much greater than that of the SMM, it can be concluded that the entire membrane surface is covered by the SMM and the fluorine tail of the SMM molecule is oriented upwards at the membrane surface.

This also helps to explain the contact angle data in Figure 22. The addition of SMM to the PES membrane leads to the formation of an SMM layer at outmost membrane surface. Like many other fluoro compounds, the fluorine tail of the SMM is of hydrophobic nature. This increased hydrophobicity of the membrane

surface is reflected in the significant increase in contact angle.

The increase in the fluorine content towards the surfaces is accompanied by a decrease in the sulfur content as shown in Figure 24. The sulfur content decreased from the 10 nm to the 2 nm layer, suggesting a decrease in PES presence at the surface. Moreover, the theoretical S/C ratio calculated based on the chemical structure of the PES repeating unit was 0.08. The measured values for both take-off angles were all below that.

The trend of increasing fluoro-segment content towards the membrane surface is further evidenced by the high resolution data shown in Figures 25 and 26. Figure 25 shows a higher $-CF_3$ content towards the surface. The $-CF_3$ group was not detected for 0.5 and 1.0 wt % of SMM in the casting solution. Figure 26 indicated higher $-CF_2-$ content towards the surface. The results in Figures 25 and 26 imply that the orientation of these polyfluoro-end is predominantly towards the membrane surface while the main chain of SMM is located relatively deeper away from it.

This is supported by the trend shown in Figure 27. It shows a relative increase in $-CF_3$ group at the upper surface as compared with $-CF_2-$ group. The observed orientation of the polyfluoro-segment rationalizes the observed atomic fluorine content, which is larger than these of the pure SMM itself. High resolution data demonstrate the orientation of the polyfluoro-ends towards the membrane surface.

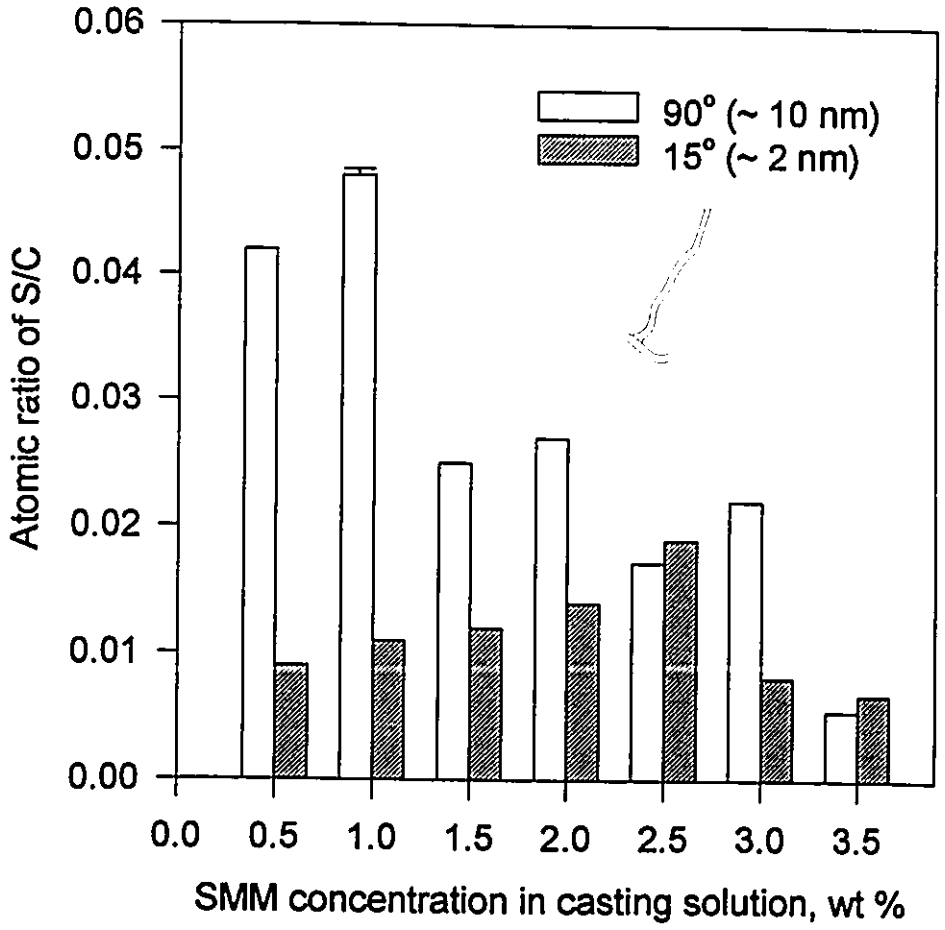

Figure 24 XPS composition of atomic sulfur with respect to atomic carbon for the PES/SMM membranes.

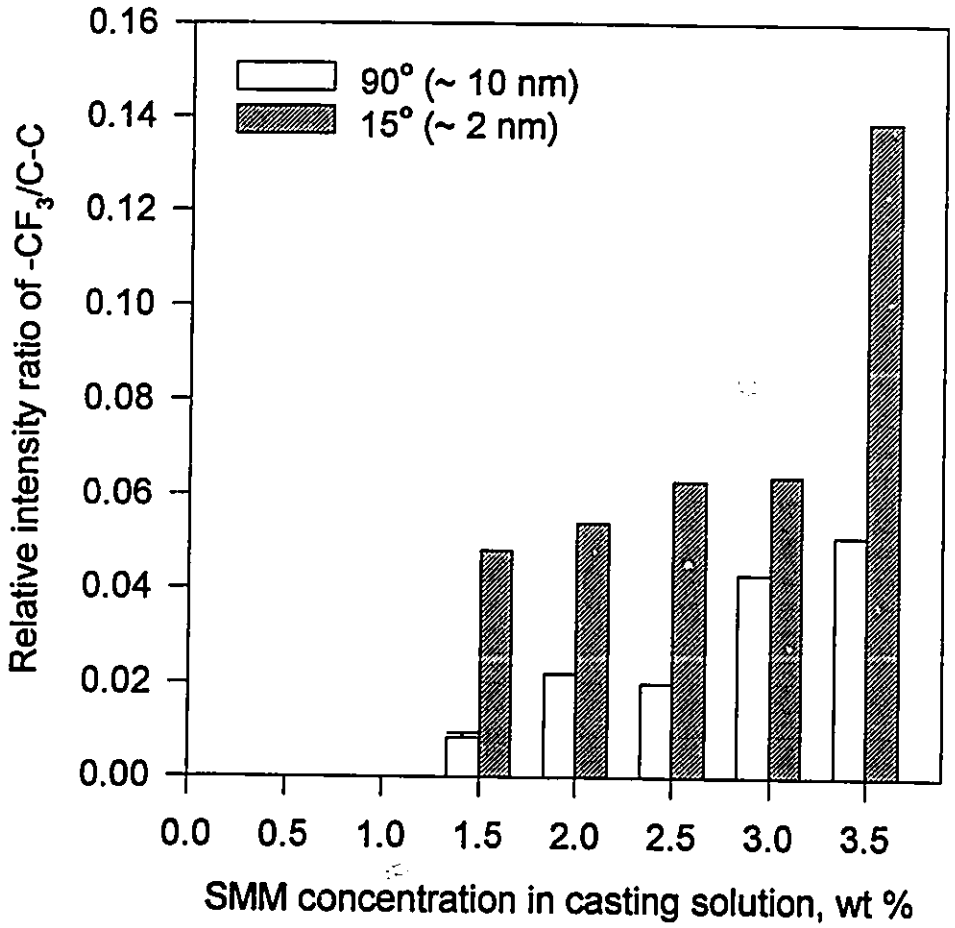

Figure 25 XPS composition of $-CF_3$ group with respect to C-C for the PES/SMM membranes.

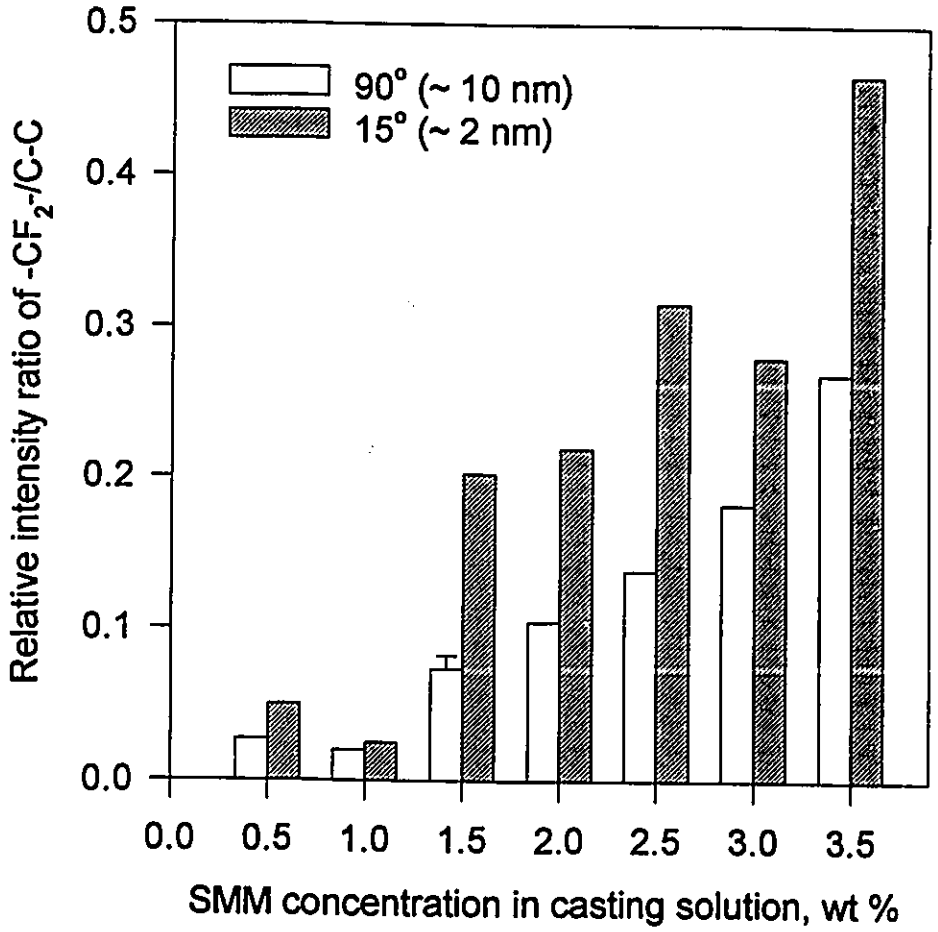

Figure 26 XPS composition of $-CF_2-$ group with respect to C-C for the PES/SMM membranes.

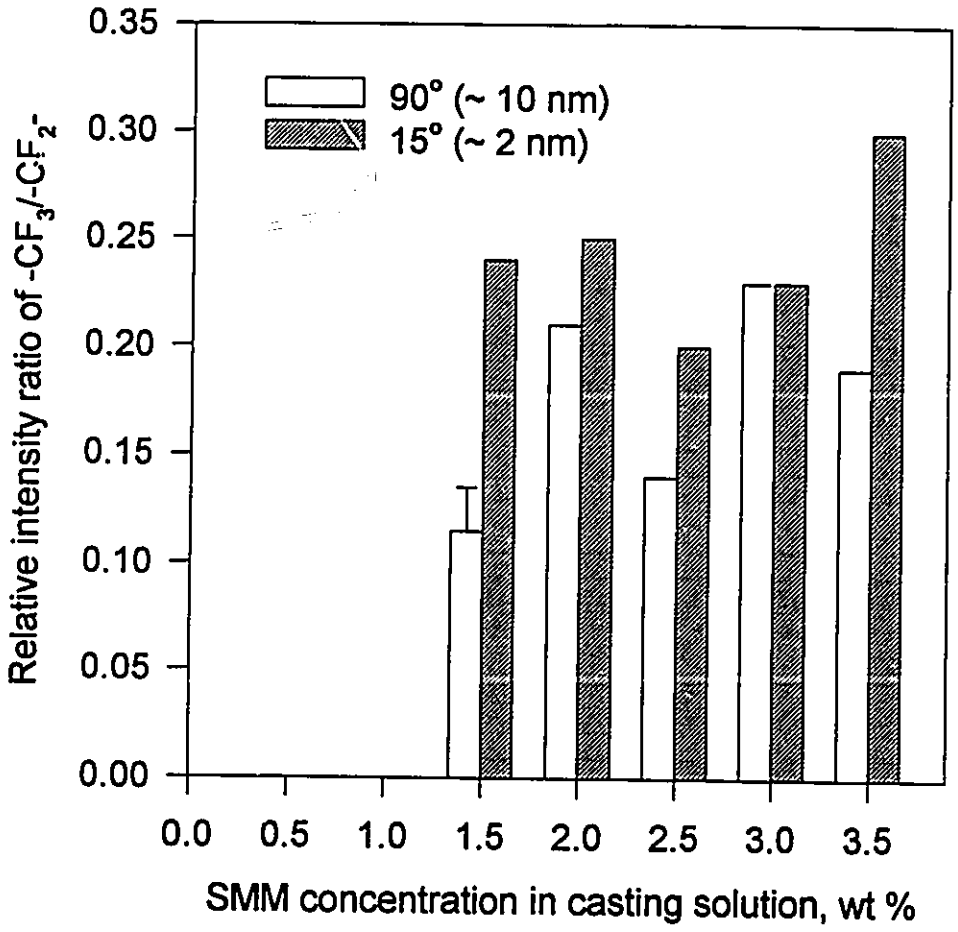

Figure 27 XPS composition of $-CF_3$ group with respect to $-CF_2-$ for the PES/SMM membranes.

The above XPS results were obtained from PES/SMM membranes with an evaporation period of 7 minutes. The observed trends were further supported by the XPS data obtained from membranes which had an evaporation period of 2 and 5 minutes. The casting solution was made of (in wt %) 25 % polyethersulfone, 6 % polyvinylpyrrolidone, 1 % SMM (SMM44) and 68 % dimethylacetamide. The XPS results are summarized in Table 10.

For the membrane with a 2- and 5-minute evaporation period, a higher fluorine content towards the membrane surface was observed in terms of a higher F/C ratio, higher $-CF_3$/C-C ratio, higher $-CF_2$-/C-C ratio and higher $-CF_3$/$-CF_2$- ratio. This certainly indicated the orientation of SMM's polyfluoro-segment towards the upper surface. The data in Table 10 further show that, when the evaporation period was increased from 2 to 5 minutes, the ratio F/C increased significantly which was accompanied by a drop in sulfur content. Possibly it indicates that some amount of time is required for the SMM to migrate to the membrane surface. The XPS data from the membranes with a 2- and 5-minute evaporation period are consistent with those obtained from the membrane with a 7-minute evaporation period. Together, these results clearly show that the SMM materials have successfully migrated to the membrane surface.

Table 10 XPS composition of PES/SMM membrane with 2- and 5-minute evaporation period†

Ratio	2-minute evaporation period		5-minute evaporation period	
	take-off angle		take-off angle	
	90°	15°	90°	15°
F/C	0.04	0.07	0.44	0.53
S/C	0.056	0.056	0.014	0.0068
$-CF_3/C-C$	N/D‡	N/D	0.03	0.10
$-CF_2-/C-C$	0.05	0.06	0.19	0.39
$-CF_3/-CF_2-$	——	——	0.14	0.25

† The composition of the casting solution in wt %: 25 % polyethersulfone, 6 % polyvinylpyrrolidone, 1 % SMM (SMM44) and 68 % dimethylacetamide. Evaporation temperature: 95°C.

‡ N/D means not detected.

To summarize, the addition of SMM to a membrane casting solution leads to SMM's migration towards the membrane-air interface and the formation of a layer of SMM. This is supported by both the contact angle and XPS data. Naturally, membrane separation performance will be affected, which will be discussed later.

4.1.5 Estimation of the Amount of SMM Needed to Cover a Membrane Surface

The amount of SMM needed to cover a membrane surface completely can be estimated using Equation (1) in Section 2.1.2, i.e., $H = F \cdot Y \cdot G$, where H is the bulk volume fraction of an SMM (m^3/m^3), F is the area fraction of SMM additive in surface (m^2/m^2), Y is the ratio of the area formed to the bulk volume (m^2/m^3), and G is the SMM monolayer thickness (m). When the surface is fully covered by SMM, $F = 1$. Thus, the above equation reduces to $H = Y \cdot G$. The variables are determined as follows. By definition,

Y= the area formed by SMMs / the bulk volume
= the area formed by SMMs / [(the area formed by SMMs)×(membrane thickness)]
= 1 / (membrane thickness)

The membrane thickness varied from 5.2×10^{-5} m to 11.6×10^{-5} m (cf. Table 11 in Section 4.1.9). Take the arithmetic average of the two as an estimate. Then, the membrane thickness = $(5.2 + 11.6) \times 10^{-5} / 2 = 8.4 \times 10^{-5}$ m.

"The monolayer thickness varies between about 4 to 50 Å depending on the chemistry/ conformation of the additive" (here the additive is SMM) (Ward et al., 1984). First we use 50 Å as the monolayer thickness. Substituting the numerical values into Equation (1), we have

$H = Y \cdot G$
= [1 / (membrane thickness)]·[monolayer thickness]
= $(1/ 8.4 \times 10^{-5}$ m)· $(50 \times 10^{-10}$ m)
= 60×10^{-6}
= 60 ppm

Similarly, when 4 Å is used as the monolayer thickness, $H = 4.8$ ppm. If multilayer accumulation of SMM on the membrane surface is allowed, a 100 Å thickness would give $H = 120$ ppm, which is still well below 1% (1% = 10,000 ppm). XPS results do show the existence of significant amount of SMM within 100 Å range from the surface. These results illustrate clearly that only a small amount of SMM is needed to cover the membrane surface completely .

4.1.6 Effect of SMM Concentration on Pervaporation Membrane Performance

Polyethersulfone (PES) membranes containing different amounts of SMM were prepared according to the phase inversion method described in Section 3.2.3. The casting solution was made of 25 % PES, 6 % PVP, 0 to 3 % SMM and the remaining solvent dimethylacetamide. These PES/SMM membranes were dried by the solvent exchange technique described in Section 3.2.5. The type of SMM used was SMM44 (cf. Table 6 on p. 52 for details). Figure 28 shows the effect of SMM concentration on the separation and the permeation rate of the pervaporation membrane. For the feed chloroform concentration of 1000 ppm, Figure 28a shows that the chloroform concentration in the permeate ranged from not detected to 58 ppm, indicating that the membrane was water selective. Without the addition of SMM, the chloroform concentration in the permeate was 58 ppm. When SMM was added, the chloroform concentration in the permeate was substantially lower. In the cases of adding 0.5 wt %, 1.5 wt % and 2.0 wt % of SMM, no chloroform was detected. In other words, water selectivity is enhanced by adding a small amount of SMM into the polyethersulfone membrane casting solution.

The preferential permeation of water for the PES/SMM membrane, illustrated in Figure 28a, was unexpected, particularly since the PES/SMM membrane surface

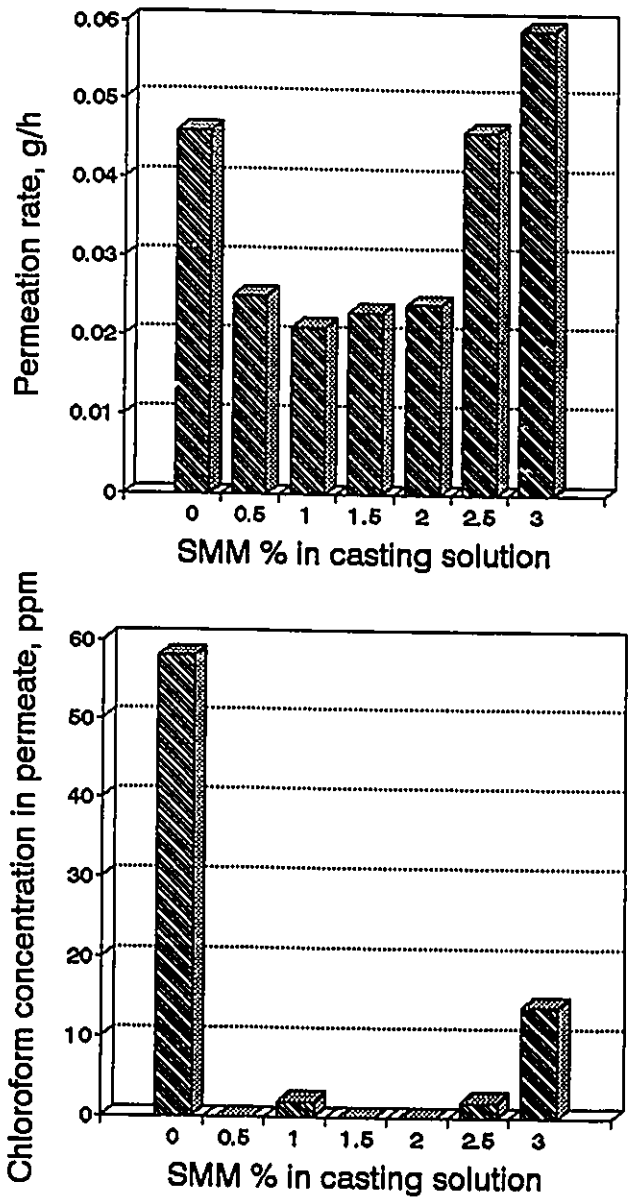

Figure 28 Effect of SMM concentration in the casting solution on pervaporation performance for the chloroform/water mixture. Temperature: 23°C. Feed chloroform concentration: 1000 ppm. Downstream pressure: 3 mmHg (400 Pa). Effective membrane area: 9.6×10^{-4} m^2. Evaporation period: 7 minutes.

showed significantly hydrophobic character (Section 4.1.4). While there may be other explanations for the phenomenon, it is suspected at the moment that the relatively thick bulk PES rich layer, which is known to be preferentially permeable to water, dominated the mass transport character over the thin surface layer of polyfluoro-tail. According to the resistance-in-series model (Côté and Lipski, 1988), the selectivity of a composite membrane is governed by the layer of the greatest resistance to the mass flow. The top hydrophobic surface layer was possibly too thin and its resistance was too low to contribute to the overall selectivity of the membrane. On the other hand, the top hydrophobic surface layer may have prevented the swelling of the bulk PES rich layer and hence enhanced its water selectivity over the larger chloroform molecules.

An alternative explanation is the possible reorientation of the hydrophilic segment of SMM. The idea that unsymmetrical molecules will be oriented at an interface is well accepted nowadays (Adamson, 1990). The principle is that molecules will be oriented so that they adopt the lowest surface-energy configuration (Brady, 1994). Adamson (1990) points out further that for an interface between water and a polar-nonpolar material, the polar end of the organic molecule is oriented towards the water. Schmidt et al. (1994) also indicate that polar solvents such as water can effectively orient a polar-nonpolar material. As has been described earlier, SMM is composed of alternating blocks of polar (methylene bis-phenyl diisocyanate) and non-polar (polypropylene diol) segment units, with both ends being capped by a fluorotelomer ($F-(CF_2)_m-(CH_2)_2-OH$). When the SMM membrane is brought in contact with an aqueous feed solution, because water strongly interacts with SMM's polar segment, water alters the surface molecular structure by orienting the polar segment outwards towards the membrane surface. The polar segment is hydrophilic because it contains the functional group -NHCO-. When the extent of water-

induced molecular reorientation is large enough, the membrane becomes water selective. A partial reorientation may lead to organic selectivity. This is in part confirmed by the fact that the membrane preferentially permeates ethyl acetate for an aqueous feed solution containing 60 % ethyl acetate (Baig, 1996). In other words, the membrane can exhibit dual selectivity. It is believed the intensity of the reorientation of the polar group to be the primary determinant of whether the membrane is water selective or organic selective.

The above two mechanisms may contribute independently or synergically to the overall selectivity of the membrane. Further work will be required to validate the above hypothetical explanations.

The surface hydrophobicity is evidenced by the lower permeation rate of the PES/SMM membrane shown in Figure 28b. When the concentration of SMM increases, the permeation rate declines initially. When elevated amounts of SMM are added to the membrane casting solutions, more than 2.5 wt % in the present case, the SMM itself may cause perturbations in the surface morphology of the substrate PES membrane and subsequently lead to a decrease in separation and an increase in permeation rate.

To summarize, membranes with SMM have superior performance for pervaporation separation of chloroform/water. The membrane permeation rate declines initially and then increases as the SMM concentration in the casting solution increases.

4.1.7 Pervaporation Separation Performance versus Time

Pervaporation experiments were conducted to examine the effect of running time

on the pervaporation performance using the membrane containing 0, 0.5 and 1.0 wt % of SMM. The type of SMM used was SMM44. Details of membrane preparation were given in Section 4.1.6. The concentration profile versus running time is shown in Figure 29a. For the membrane containing 0.5 and 1.0 wt % of SMM, the chloroform concentration in the permeate changed very little against the running time. For the membrane containing no SMM, the chloroform concentration in the permeate increased, and then leveled off over time. This reflects the fact that a longer period is required to reach adsorption equilibrium for the polyethersulfone membrane. Since the PES membrane containing SMM can quite effectively block the passage of chloroform through the membrane, adsorption equilibrium can be reached in relatively shorter time. The permeation rate of the membrane is plotted against the running time in Figure 29b. A similar pattern prevails. The permeation rate of the membrane containing 0.5 and 1.0 wt % of SMM remained relatively stable, while that of the PES membrane stabilized after longer time.

4.1.8 Effect of Feed Concentration

Pervaporation results at different feed concentrations for PES membranes, one without SMM, the other with 0.5 wt % SMM, are shown in Figures 30 and 31, respectively. The membrane preparation conditions were already described in Section 4.1.2, except that the evaporation period was 7 minutes. For the PES membrane without SMM, Figure 30 shows that the chloroform concentration in the permeate increased from 11 to 58 ppm, and the permeation rate increased from 0.033 to 0.046 g/h when the chloroform concentration in the feed increased from 100 to 1000 ppm. A higher chloroform concentration in the feed tends to increase the swelling of the top surface layer, leaving the top surface layer swollen and loose. Therefore, a lower separation and a higher permeation rate were observed in Figure 30.

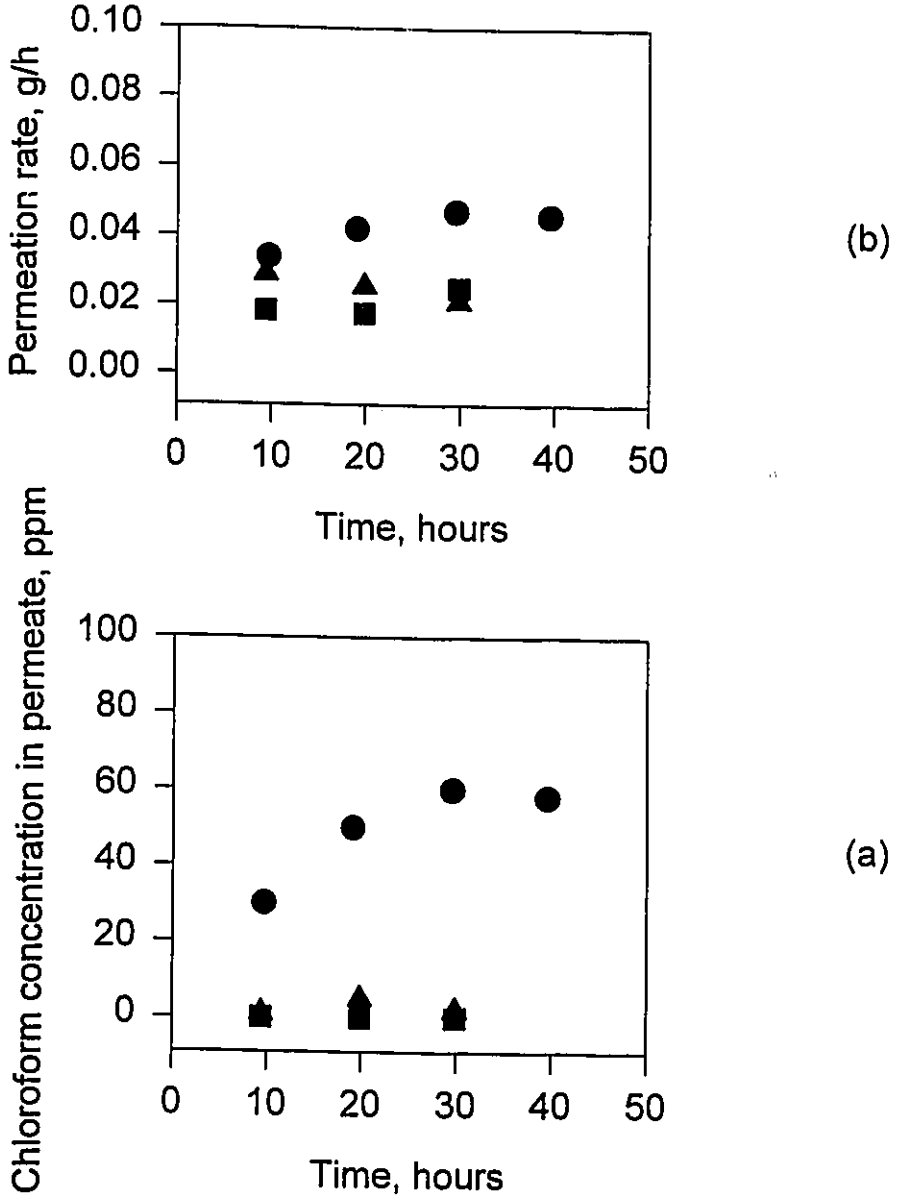

Figure 29 Effect of running time on the pervaporation of chloroform/water mixture. Temperature: 23°C. Feed concentration: 1000 ppm. Downstream pressure: 3 mmHg (400 Pa). Effective membrane area: 9.6×10^{-4} m^2. Evaporation period: 7 minutes. SMM wt %: ●, 0 %; ■, 0.5 %; ▲, 1.0 %.

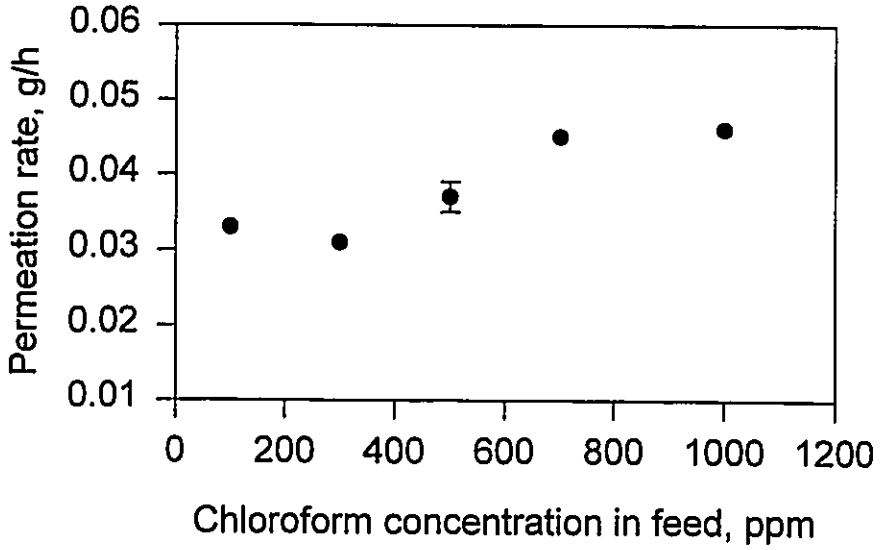

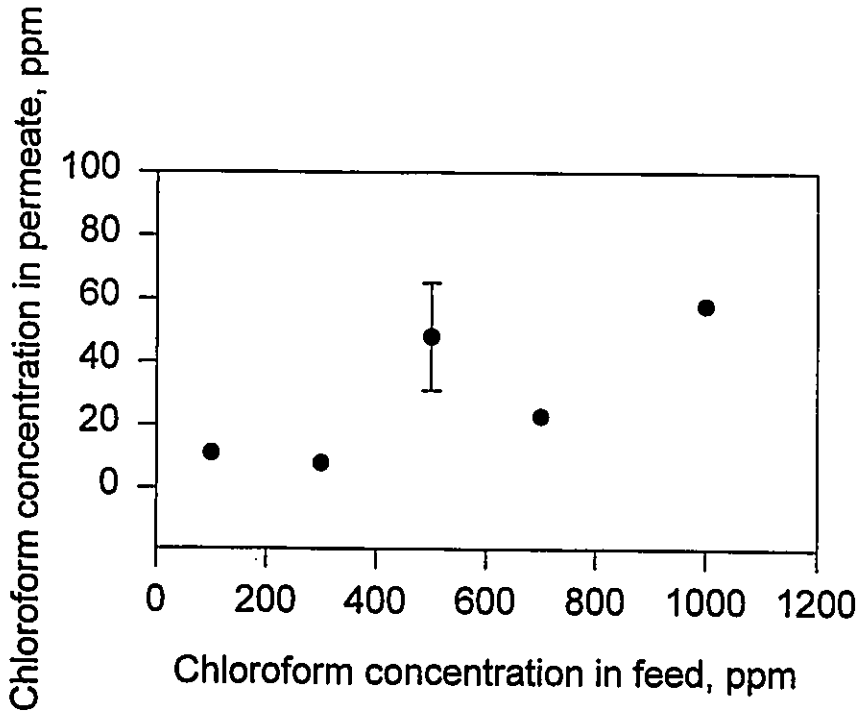

Figure 30 Effect of feed concentration on pervaporation performance using polyethersulfone membrane without SMM. Feed: chloroform/water mixtures. Temperature: 23°C. Downstream pressure: 3 mmHg (400 Pa). Effective membrane area: 9.6×10^{-4} m^2.

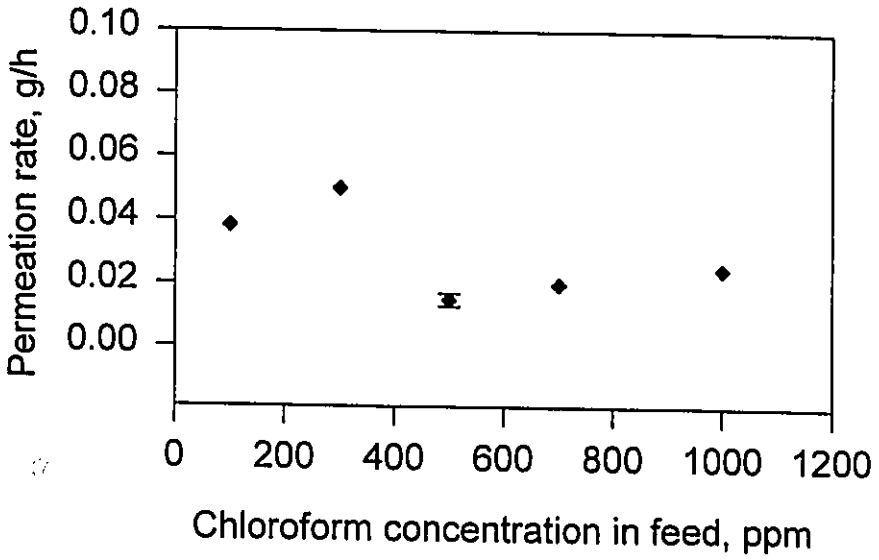

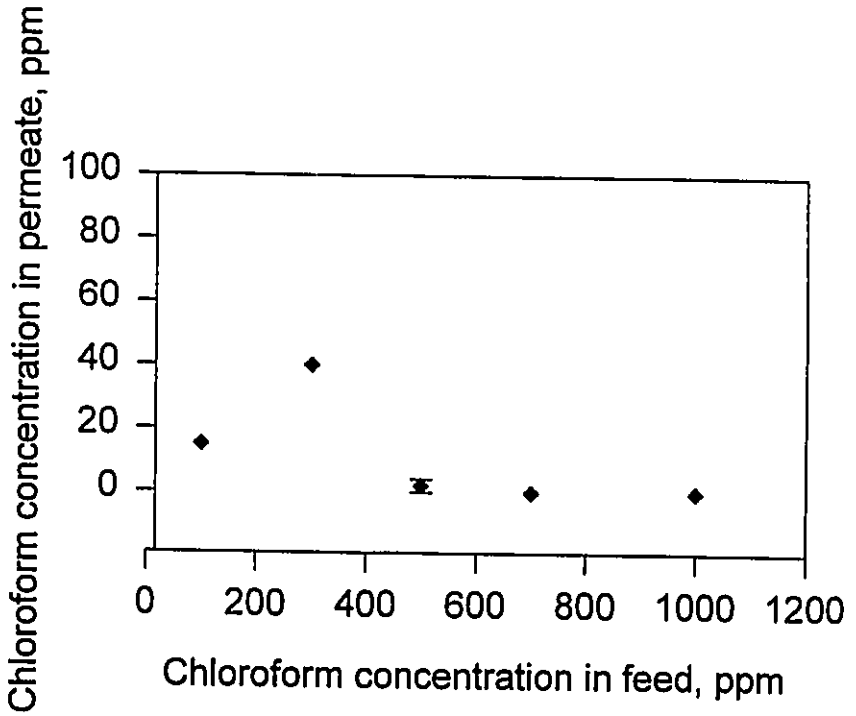

Figure 31 Effect of feed concentration on pervaporation performance using polyethersulfone membrane with 0.5 wt % SMM. Feed: chloroform/water mixtures. Temperature: 23°C. Downstream pressure: 3 mmHg (400 Pa). Effective membrane area: 9.6×10^{-4} m^2.

For the PES membrane with 0.5 wt % SMM, Figure 31 shows that the chloroform concentration in the permeate decreased as the feed concentration increased. As has been discussed in Section 4.1.6, for the PES/SMM membrane, the bulk PES rich layer largely determines the separation when the top surface layer is highly swollen. At a lower chloroform concentration in the feed, the extent of swelling could be less so that the SMM layer at the top surface also contributed to the separation. Accordingly the water selectivity of the PES/SMM membrane was weakened due to the strong hydrophobic character of the SMM. There was no clear-cut relationship between the permeation rate and the feed concentration.

4.1.9 Effect of PVP Concentration

When pervaporation membranes were prepared, 6 wt % of polyvinylpyrrolidone (PVP) was used to form the membrane casting solution. This section examines the effect of PVP concentration on membrane thickness, on pervaporation membrane performance and on the XPS results, in the aforementioned order.

First, let us discuss the effect of PVP concentration on membrane thickness. In a separate set of experiments, polyethersulfone (PES) membranes containing different amount of PVP were prepared according to the phase inversion method described in Section 3.2.3. These PES/SMM membranes were dried by the solvent exchange technique described in Section 3.2.5. To examine the effect of PVP concentration on membrane thickness, membranes were cast from the solution made of 25% PES, 1% SMM, and different amounts of PVP. The balance was dimethylacetamide which was used as a solvent. The evaporation period was 7 minutes at 95°C. Although membranes were cast with the same nominal thickness, the membranes that were obtained after drying had different thickness.

Table 11 lists the dry membrane thickness corresponding to different concentrations of PVP in the casting solution. The thickness of dry membrane increased steadily with an increase in the PVP concentration in the membrane casting solution. For example, when the PVP concentration increased from 0 to 8% in the casting solution, the thickness of the dry membranes increased from 4.2×10^{-5} m to 11.6×10^{5} m. PVP itself is a polymer with a molecular weight of 10,000 (the one used in the study). The addition of PVP polymer into the polyethersulfone solution is destined to increase the solution viscosity. In fact, visual observation confirmed

Table 11 Dry membrane thickness vs. PVP concentration in membrane casting solution†

PVP concentration in casting solution, wt %	Thickness of the dry membrane (× 10^{-5} m)
0	4.2
1	5.2
2	6.1
3	8.2
4	9.8
8	11.6

† Composition of the cast solution: 25% PES, 1% SMM (SMM41), different amount of PVP as indicated in the table. The balance was dimethylacetamide. Evaporation period: 7 minutes at 95°C.

that the higher the PVP concentration in the casting solution, the more viscous the solution became. When the solution was cast on a glass plate and placed in an oven at 95°C, the solvent dimethylacetamide (DMAc) started to evaporate. Less solvent evaporated from the more viscous solution. Hence, less shrinkage in membrane thickness occurred. Therefore, higher PVP concentrations in the casting solution lead to thicker membranes.

To evaluate the effect of PVP concentration on the pervaporation membrane performance, two sets of membranes were made, one without SMM and the other with 1 % of SMM. Their respective compositions are given in Table 12. The membranes had an evaporation period of 7 minutes at 95°C. The membranes were used without drying.

Table 12 The composition of casting solutions with various PVP concentrations[†]

Compound	Composition, wt %	
	Solution without SMM	Solution with SMM
SMM[‡]	0	1
Polyethersulfone	25	25
Polyvinylpyrrolidone	0, 1, 2, 3, 4 and 8	0, 1, 2, 3, 4 and 8
Dimethylacetamide	the balance	the balance

[†] Evaporation period: 7 minutes at 95°C.

[‡] The type of SMM used was SMM41.

Figure 32 shows the effect of PVP concentration on the pervaporation membrane performance without the presence of the SMM. It shows that chloroform concentration in the permeate became higher as the PVP % in the casting solution increased. In other words, the separation decreased in terms of the selectivity to water. On the other hand, the membrane permeation rate increased continuously with an increase in PVP content in the casting solution. PVP is known to yield increased ultrafiltration permeation rate of the resulting membrane for the polyethersulfone/N-methyl-2-pyrrolidone (NMP) system (Sourirajan and Matsuura, 1985). PVP is dissolved in a gelation bath, but a residual amount of PVP remains in the membrane (Miyano, et al., 1990). The hydrophilic nature of PVP is believed to contribute to a higher permeation rate. This may hold true for the present system, the polyethersulfone/dimethyl acetamide system as well. Hence, the higher permeation rate was observed for higher PVP concentration in the casting solution. Excessive amount of PVP may lead to markedly larger pore size of the resulting membrane. Accordingly, a lower separation and a higher permeation rate were observed.

Figure 33 shows the effect of PVP concentration on the pervaporation membrane performance with the presence of SMM. The permeation rate increased as the PVP concentration in the casting solution increased. As for the separation, the membrane was water selective at PVP concentration of 2 % or lower, while the membrane became chloroform selective when the PVP concentrations was 3 % or higher. The reason for PES/SMM to show water selectivity has been discussed earlier (Section 4.1.6). As for the selectivity towards chloroform, there are several possible explanations for this phenomenon.

The first explanation is related to the membrane thickness. Increasing the viscosity of the casting solution tends to induce a sponge-structured membrane and thus tends to increase

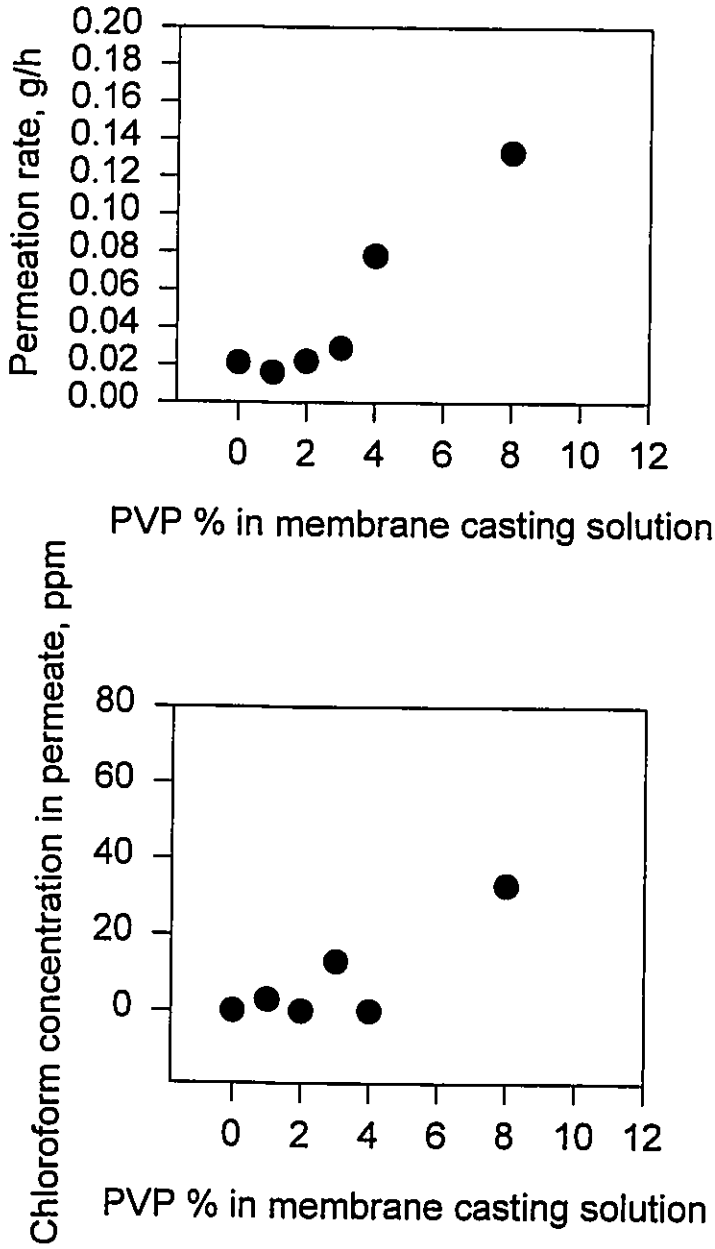

Figure 32 Effect of polyvinylpyrrolidone (PVP) concentration on the pervaporation performance of PES membranes without the presence of SMM. Feed chloroform concentration: 1000 ppm. Temperature: 23°C. Effective membrane area: 9.6×10^{-4} m^2. Downstream pressure: 3 mmHg (400 Pa). Evaporation period: 7 minutes.

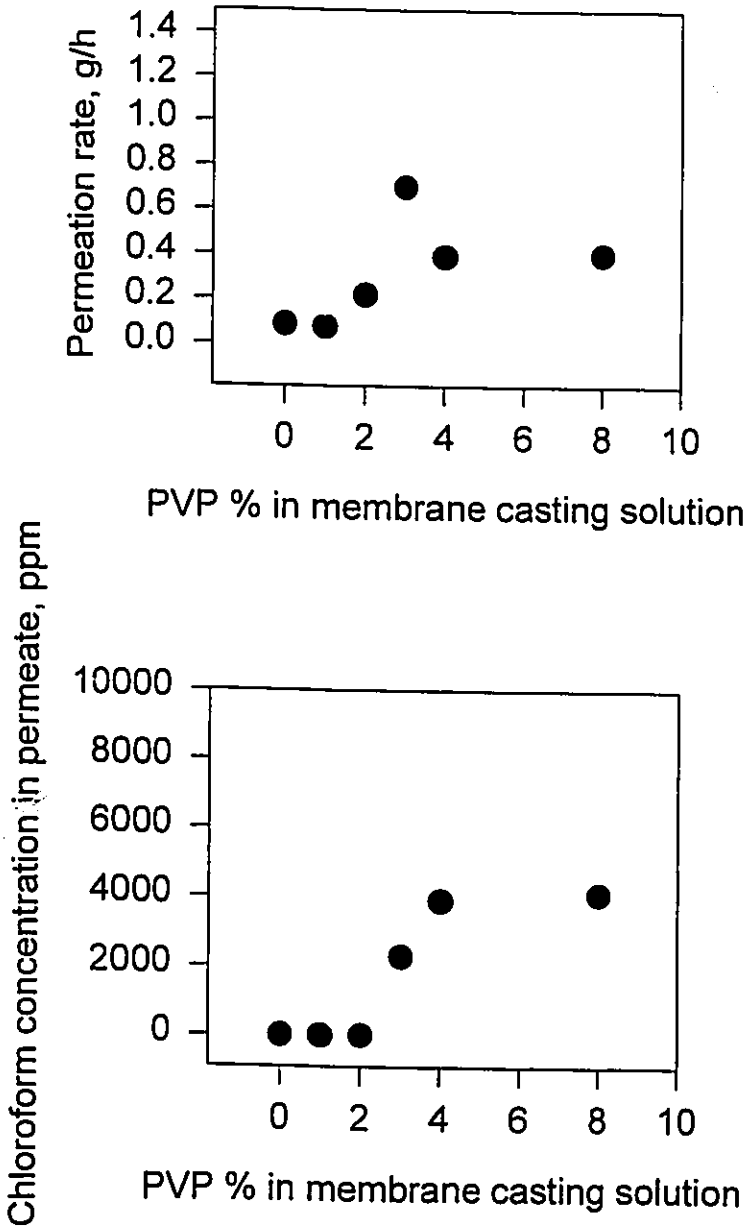

Figure 33 Effect of polyvinylpyrrolidone (PVP) concentration on the pervaporation performance of PES/SMM membranes. Feed chloroform concentration: 1000 ppm. Temperature: 23°C. Effective membrane area: 9.6×10^{-4} m^2. Downstream pressure: 3 mmHg (400 Pa). Evaporation period: 7 minutes.

the strength of the surface of polymer film first precipitated (Strathmann, 1990). Consequently, the higher viscosity of the casting solution associated with higher PVP concentration probably leads to increased thickness of the SMM layer on the surface of the PES/SMM membrane. According to the resistance-in-series model (Côté and Lipski, 1988), the selectivity of a composite membrane is governed by the layer of the highest resistance to the mass flow. The resulting top surface layer that was hydrophobic became possibly thick enough and its resistance was high enough to contribute significantly to the overall selectivity of the membrane. This explains the reversal of the membrane selectivity when the PVP concentration in the casting solution was higher.

The second explanation is associated with the property of the surface of the pore. The addition of significant amount of PVP can produce membranes with pores of larger sizes, both on the top surface layer and in the sublayer underneath. SMM can migrate to the surface of these pores and result in a hydrophobic internal surface as if the pores were surface coated with a layer of SMM. This can lead to the preferential permeation of chloroform.

The third explanation lies in the molecular interaction between PVP and SMM. Miyano et al. (1990) reported that PVP was retained inside the ultrafiltration membranes made of polysulfone material. It is believed that PVP is present in the PES/SMM membrane, too. The mutual interaction between PVP and SMM is possible because of their molecular structures. SMM is made of a hydrophilic block capped by fluoro alcohol at both ends, i.e., having the structure of [fluoro block]-[hydrophilic block]-[fluoro block]. The chemical structure of PVP is shown in Figure 34. PVP is readily soluble in water and has a great ability to associate, and to form 'complexes', with a wide variety of organic materials (Alger, 1989). Hence, the hydrophilic PVP may form a complex with the hydrophilic block in the SMM,

pulling the hydrophilic block downward from the membrane surface. This leads to the SMM being dispersed over a thicker layer from the surface. An increased PVP content in the casting solution can have greater capacity to associate with the SMM and thus results in an even thicker layer of SMM. Because of its hydrophobic nature, the resulting thicker layer of SMM favors the preferential permeation of chloroform. According to Peterson and Cadotte (1990), a composite membrane has a 20 to 200 nm thin dense polymer barrier over a thick microporous support membrane. The thickness of the SMM layer is believed to be in that range as well to contribute effectively to the overall separation.

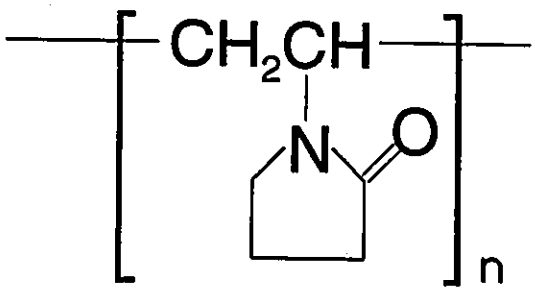

Figure 34 The chemical structure of polyvinylpyrrolidone (PVP).

The pertinent XPS data provide some support to the third explanation. Figure 35 shows the XPS results for the membranes that contained different amounts of PVP. Membrane preparation details were already given in Table 12 except the PVP concentrations used were 0, 0.5, 1 and 2.0 wt %. Figure 35 shows that the fluorine content at the surface decreased when PVP was added to in both the top 2 nm and the top 10 nm region of the membrane surface. For example, the ratio of F/C declined from 0.74 to 0.34, corresponding to an increase in PVP content from 0 to 2 %, in the top 2 nm region. The reduced ratio of F/C at the surface implies that SMM was dispersed across a broader depth, leading to a thicker layer of SMM.

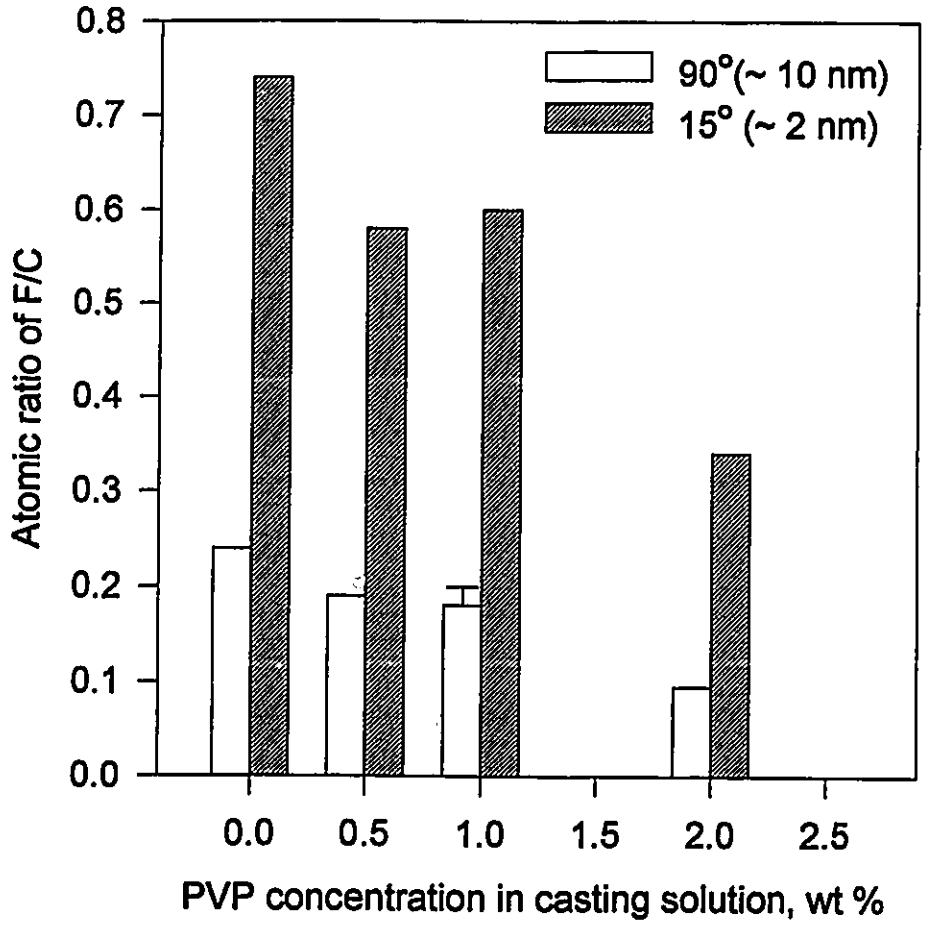

Figure 35 Effect of PVP concentration in the casting solution on the atomic ratio of fluorine over carbon.

4.1.10 PES and PES/SMM Membranes for the Separation of Ethyl Alcohol/n-Heptane Mixtures by Pervaporation

Pervaporation separation of ethyl alcohol/n-heptane mixtures was also attempted using PES and PES/SMM membranes. Table 13 lists the permeation rates of pure ethyl alcohol and pure n-heptane for both types of membranes. When 1% of SMM was added to the membrane casting solution, the permeation rate for pure ethyl alcohol decreased from 0.76 to 0.59 g/h, while that of pure n-heptane increased from 0.65 to 0.77 g/h. It has been confirmed by the contact angle and XPS measurements that the PES/SMM membrane has a much more hydrophobic surface than the PES membrane without SMM when both membranes were prepared from casting solutions containing the same amount of PES polymer. The membrane with an increased hydrophobicity tends to decrease the permeation of the hydrophilic component while enhancing the permeation of the hydrophobic component.

Table 13 Pervaporation permeation rates of pure ethyl alcohol and pure n-heptane for PES and PES/SMM membranes

Membrane	Permeation rate, g/h *	
	Pure ethyl alcohol	Pure n-heptane
PES †	0.76	0.65
PES/SMM ‡	0.59	0.77

* Effective membrane area: 9.6×10^{-4} m^2, tested at room temperature, downstream pressure: 3 mmHg (400 Pa).

† Composition of the PES membrane casting solution: 25% PES, 2% PVP, 73% DMAc. Solvent evaporation period: 90 seconds at 95°C.

‡ Composition of the PES/SMM membrane casting solution: 1% SMM (SMM41), 25% PES, 2% PVP, 72% DMAc. Other conditions were the same as the PES membrane.

Pervaporation results of ethyl alcohol/n-heptane mixtures are shown in Figure 36. Figure 36a demonstrates that the PES/SMM membrane increases the permeation rate of n-heptane, and lowers the permeation rate of ethyl alcohol. Figure 36b shows that the mole fraction of ethyl alcohol in the permeate for the PES/SMM membrane is lower than that for the PES membrane. This change in the permeation rate of individual component is also attributed to the increased hydrophobicity of the PES/SMM membrane. In the mixture of ethyl alcohol/n-heptane, ethyl alcohol is hydrophilic relatively to n-heptane, or n-heptane is more hydrophobic than ethyl alcohol. As a result of the increased hydrophobicity of PES/SMM membrane, the permeation rate of ethyl alcohol is reduced, and that of n-heptane is increased.

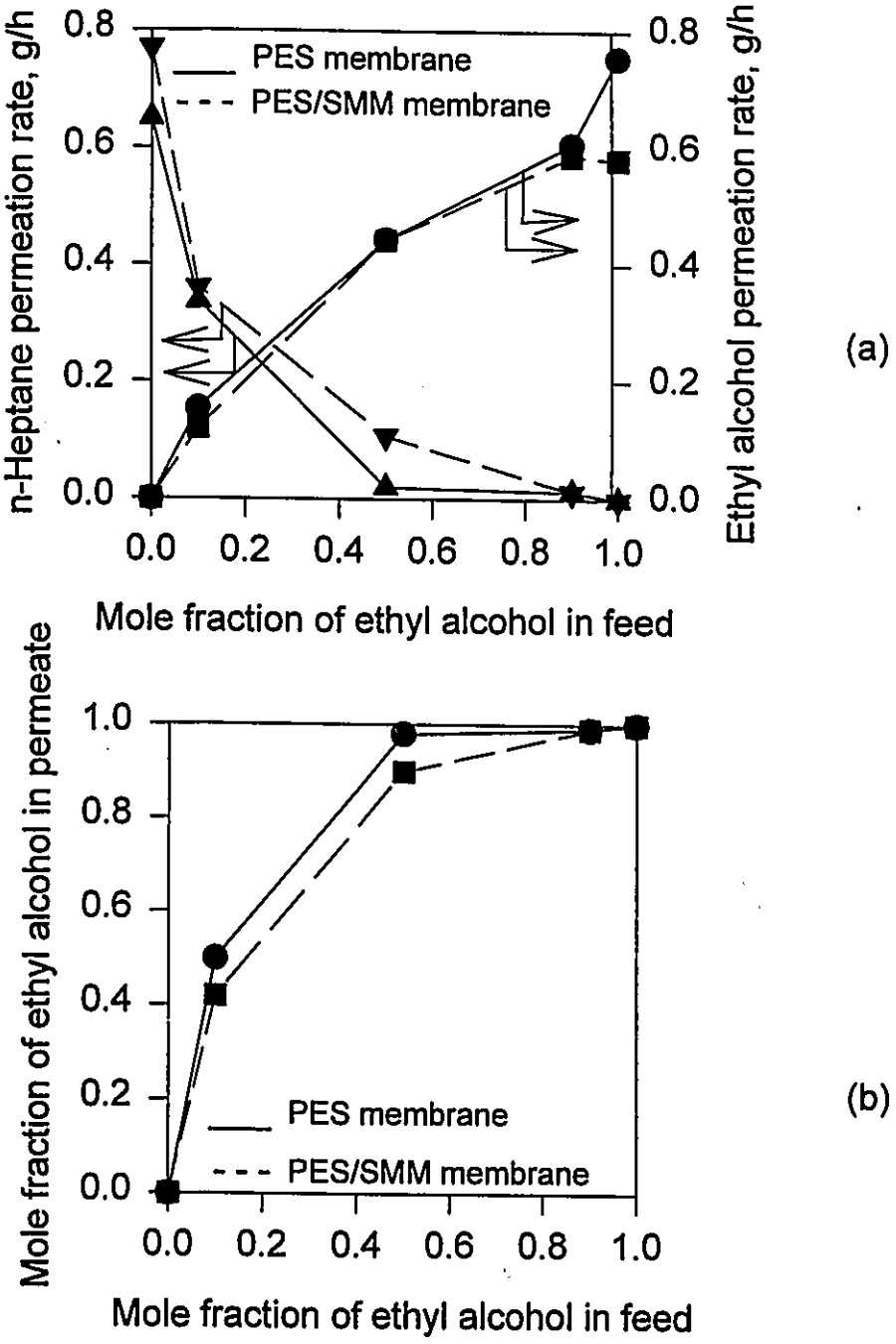

Figure 36 Effect of SMM on the pervaporation separation of ethyl alcohol/n-heptane mixtures. Temperature: 23°C. Solvent evaporation period: 90 seconds at 95°C. Effective membrane area: 9.6×10^{-4} m^2. Downstream pressure: 3 mmHg (400 Pa).

The following statements summarize the results and discussion related to pervaporation studies (Section 4.1).

1. Chloroform is strongly preferentially adsorbed, in comparison to water, to the PES material in the vapor phase and only slightly preferentially adsorbed in the liquid phase.

2. Polyethersulfone membrane is water selective in pervaporation separation of the chloroform/water mixture. A longer evaporation period leads to a higher separation and a lower permeation rate for the mixture.

3. The scanning electron microscopic study shows that asymmetric membranes can be prepared from polyethersulfone solutions containing SMM. Membranes with different structures can be obtained by varying the solvent evaporation period.

4. Contact angle data show that adding SMM in the casting solution significantly increases both the advancing and the receding contact angles of water on the surface of PES/SMM membranes. This suggests that the PES/SMM membrane has a more hydrophobic surface than the PES membrane.

5. The XPS results indicate that the fluorine concentration is much higher at the membrane surface than in the bulk. The membrane surface is covered by a layer of SMM and the fluorine tail of the SMM molecule is oriented upwards at the membrane surface.

6. The combination of Statements 4 and 5 confirms that adding SMM to a membrane casting solution leads to fluorine-containing SMM to migrate to and to accumulate at the membrane-air interface.

7. Only a small amount of SMM, typically less than 1 %, is needed to cover the membrane surface completely.

8. Polyethersulfone membranes containing SMM have a superior performance for pervaporation separation of chloroform/water.

9. It takes longer time for a PES membrane to reach a stable separation and a stable permeation rate for pervaporation separation of chloroform/water than for a PES/SMM membrane.

10. For a PES membrane, a higher chloroform concentration in the feed leads to a higher chloroform concentration in the permeate; while for a PES/SMM membrane, higher chloroform concentration in the feed leads to a lower chloroform concentration in the permeate for pervaporation separation of chloroform/water. As for permeation rate, it increases with an increase in feed chloroform concentrations with respect to a PES membrane. There is no particular trend found for a PES/SMM membrane.

11. For a PES membrane without SMM, a higher PVP concentration in the casting solution results in a lower separation and a higher permeation for pervaporation separation of chloroform/water. For a PES/SMM membrane, higher PVP concentration in the casting solution leads to a higher permeation rate and changes the membrane from water selective to chloroform selective.

12. When compared with a PES membrane, a PES/SMM membrane increases the permeation rate of n-heptane, and lowers the permeation rate of ethyl alcohol for pervaporation separation of ethyl alcohol/n-heptane mixtures.

4.2 Sorption Studies and Reverse Osmosis Separation for the Binary Mixtures of Ethyl Alcohol/n-Heptane

The mechanism of a membrane separation is controlled by 1) preferential sorption of one species to the membrane; 2) differing rates of transport through the membrane for different species. Sorption studies provide fundamental information such as which component is preferentially sorbed and how much is sorbed by the membrane or the membrane material. Therefore, in order to better understand the membrane separation mechanism, it is especially important to study the sorption properties of membranes and membrane materials. This section presents the results of the sorption studies as well as the results of the reverse osmosis separation of the binary mixtures of ethyl alcohol and n-heptane. Ethyl alcohol and n-heptane are defined as component A and B, respectively.

4.2.1 Determination of Sorption Properties for the Cellulose Acetate Butyrate Membrane/Ethyl Alcohol/n-Heptane System

In this work, the determination of preferential sorption for the cellulose acetate butyrate membrane/ethyl alcohol/n-heptane system is attempted both by the direct sorption measurement and by the liquid chromatographic method. The direct sorption measurement is conducted for cellulose acetate butyrate (CAB) powders, homogeneous CAB membranes and a membrane stack made of several asymmetric CAB membranes. The pertinent results are presented and discussed from Sections 4.2.1.1 to 4.2.1.3.

4.2.1.1 Results of Liquid Sorption Experiments

Cellulose acetate butyrate (CAB) powders and homogeneous CAB membranes were prepared as described in Sections 3.6 and 3.7 of Experimental Method, respectively. Direct liquid sorption measurement experiments were conducted for both the CAB powders and the homogeneous CAB membranes. The results of the liquid sorption experiments, one obtained from the CAB powders and the other obtained from the homogeneous CAB membranes, are presented in Figures 37 and 38, respectively.

Figure 37 shows the liquid sorption data obtained from the cellulose acetate butyrate powders for the binary mixtures of ethyl alcohol and n-heptane at 23°C. In this figure the mole fraction of ethyl alcohol in the bulk solution is plotted against the mole fraction of ethyl alcohol in the sorbed phase. One obvious feature of Figure 37 is that the concentration of ethyl alcohol in the sorbed phase is higher than that in the bulk solution. For example, when the mole fractions of ethyl alcohol in the bulk solution are 0.1 and 0.3, the corresponding mole fractions of ethyl alcohol in the sorbed phase are 0.57 and 0.79, respectively. From this figure, it is evident that cellulose acetate butyrate powders preferentially sorb ethyl alcohol from the binary mixtures of ethyl alcohol and n-heptane.

The preferential sorption of ethyl alcohol by the cellulose acetate butyrate material can be explained by the molecular interaction. As shown in Figure 12 already (see p. 47), the chemical structure of CAB contains -OH functional groups and numerous oxygen atoms, which means that CAB is a hydrophilic polymer. An ethyl alcohol molecule is also hydrophilic with an -OH functional group. On the other hand, n-heptane is known to be a hydrophobic aliphatic saturated hydrocarbon. Therefore, CAB polymer interacts more strongly with ethyl alcohol molecules than

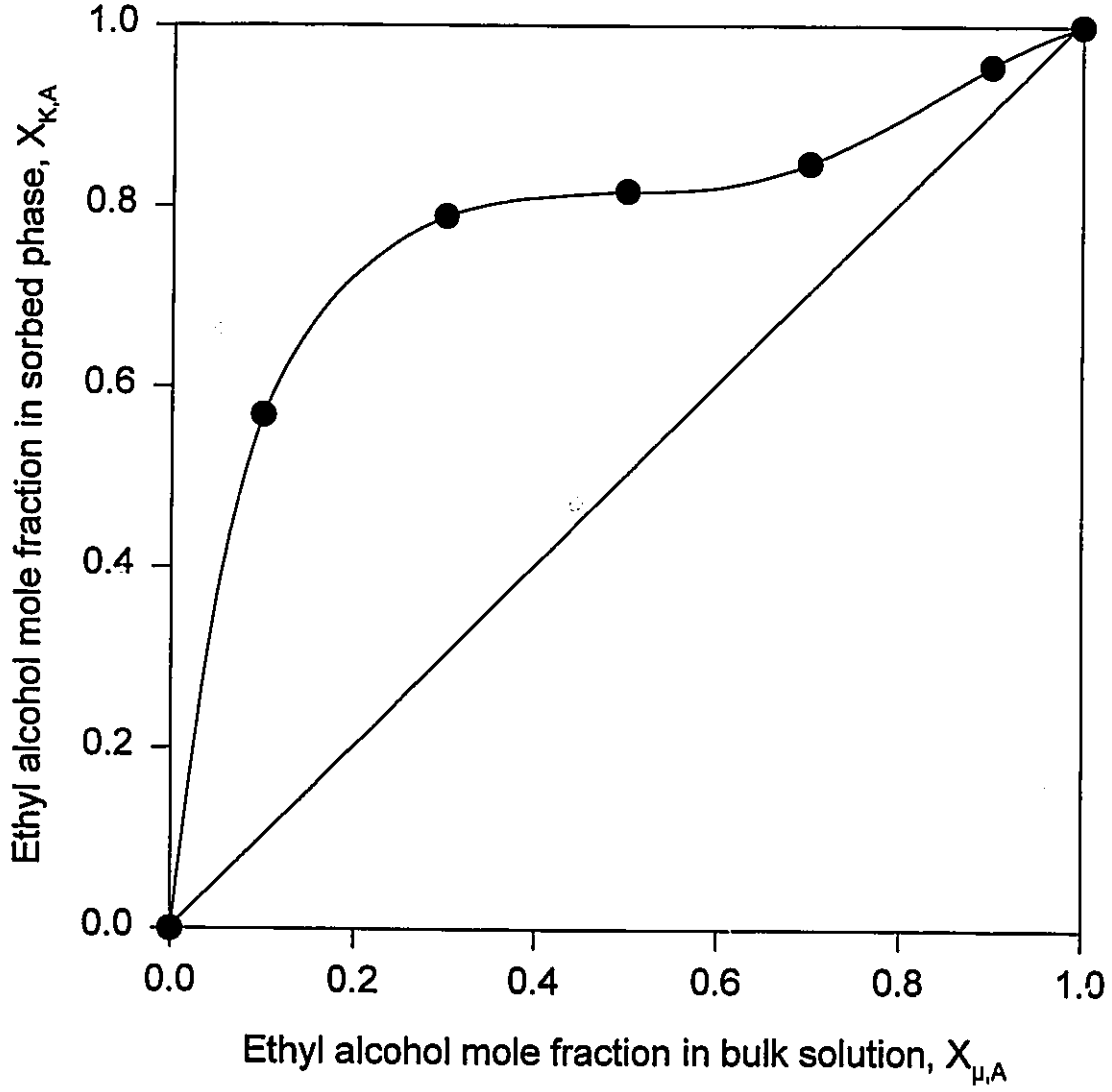

Figure 37 Liquid sorption data for ethyl alcohol/n-heptane system for the cellulose acetate butyrate powders (Eastman CAB-171-40) at 23 °C.

with n-heptane molecules, leading to preferential sorption of ethyl alcohol.

Another feature of Figure 37 is that the difference between the mole fraction of ethyl alcohol in the sorbed phase and that in the bulk solution decreases as the mole fraction of ethyl alcohol in the bulk solution increases, as indicated in Table 14. The difference decreases from 0.47 to 0.06 corresponding to an increase in the mole fraction of ethyl alcohol in the bulk solution from 0.1 to 0.9, respectively. The phenomenon indicates that the intensity of the preferential sorption is weakened as the ethyl alcohol concentration in the bulk solution increases.

Table 14 Liquid sorption data for cellulose acetate butyrate powders/ethyl alcohol/n-heptane system at 23°C

Mole fraction of ethyl alcohol in the bulk solution	The difference between the mole fraction of ethyl alcohol in the sorbed phase and that in the bulk solution
0.00	0.00
0.10	0.47
0.30	0.46
0.50	0.32
0.70	0.15
0.90	0.06
1.00	0.00

The liquid sorption experiments were conducted for the cellulose acetate butyrate homogeneous membranes using binary mixtures of ethyl alcohol and n-heptane at 23°C. The results are shown in Figure 38. In this figure the mole fraction of ethyl alcohol in the bulk solution is plotted against the mole fraction of ethyl alcohol in the sorbed phase as well as the total sorbed amount per unit weight of the homogeneous cellulose acetate butyrate membrane (kg/kg of homogeneous membrane). The figure shows that the mole fraction of ethyl alcohol in the sorbed phase is higher than that in the bulk solution. The amount of the sorbed liquid increases steadily when the mole fraction of ethyl alcohol in the bulk solution increases. The figure also shows that 0.05 and 0.11 kg of pure heptane and pure ethyl alcohol, respectively, is sorbed per kg of homogeneous membranes. This suggests that ethyl alcohol is more strongly sorbed than heptane.

4.2.1.2 Vapor Sorption Studies for the Cellulose Acetate Butyrate/Ethyl Alcohol/n-Heptane System

In addition to the liquid sorption measurements, vapor sorption studies were conducted for ethyl alcohol vapor and heptane vapor, using the cellulose acetate butyrate powders packed in a column which was fitted in a gas chromatograph. The details of the experiments were given in Section 3.6. The results of the vapor sorption studies using gas chromatography experiments are summarized in Figure 39. The figure is a correlation of N_a versus p/p_0, with respect to both ethyl alcohol and n-heptane, where N_a and p/p_0 are the amount of vapor sorbed on the surface of the polymer and the relative pressure, respectively. Unfortunately, the restrictions involved in the gas chromatographic experiments allowed us to obtain data below the relative vapor pressure of 0.33 for ethyl alcohol and 0.43 for n-heptane. Similar restrictions have been reported by Deng et al. (1990). Figure 39 shows that the

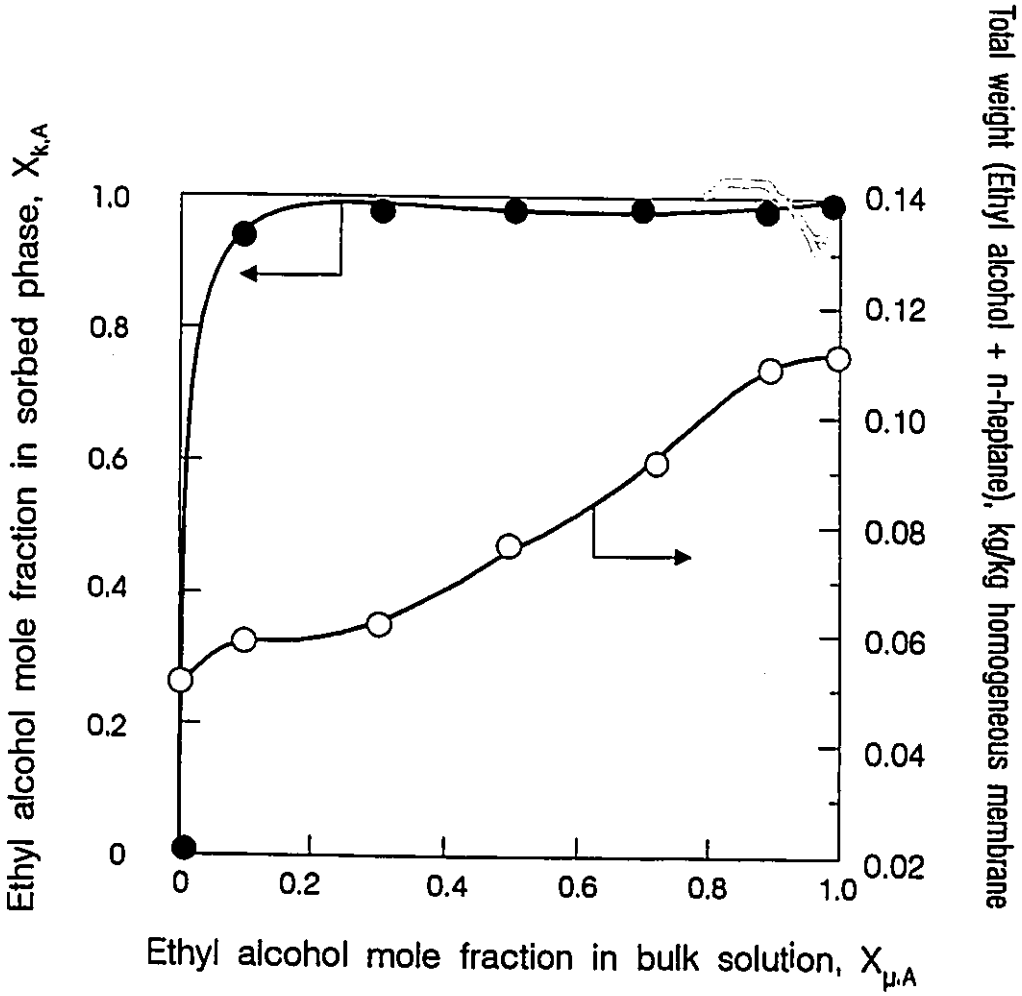

Figure 38 Liquid sorption data for ethyl alcohol/n-heptane system for the cellulose acetate butyrate (Eastman CAB-171-40) homogeneous membranes at 23 °C.

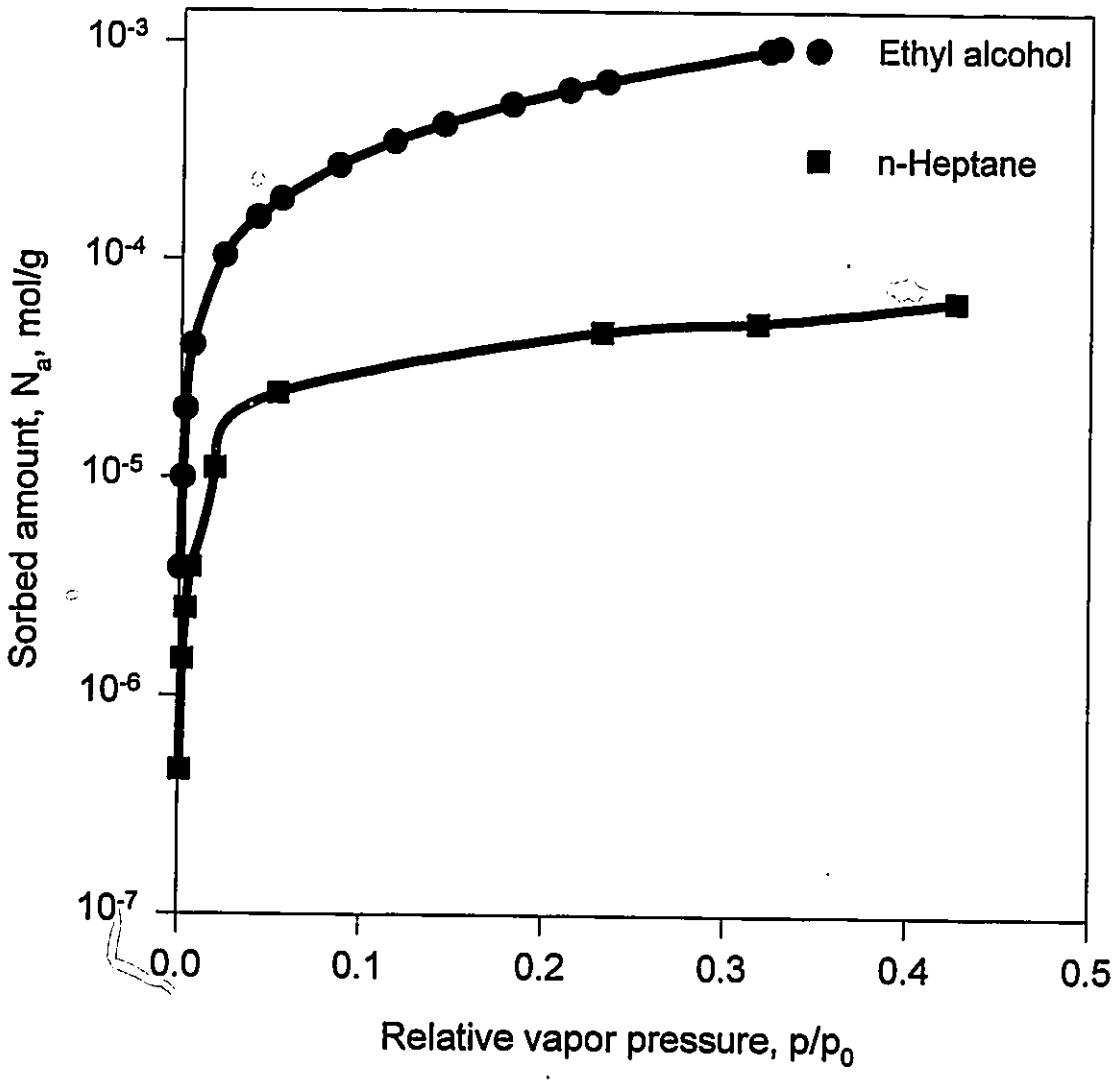

Figure 39 The amount of vaporous ethyl alcohol and n-heptane sorbed onto the cellulose acetate butyrate powders (Eastman CAB-171-40) versus relative pressure at 76.4°C.

cellulose acetate butyrate polymer sorbed more ethyl alcohol vapor than heptane vapor within the range of the relative vapor pressures studied.

The BET plots for both n-heptane and ethyl alcohol have given straight line relationships as shown in Figure 40. The surface areas of the cellulose acetate butyrate polymer particles were obtained by the method described in Theoretical and Methodology. The results were 10.74 and 145.95 m^2/g for n-heptane and ethyl alcohol, respectively. The much higher value of the surface area determined using ethyl alcohol indicates the stronger swelling of the cellulose acetate butyrate polymer by ethyl alcohol.

It is clear from the above results that ethyl alcohol is more strongly sorbed than n-heptane to the cellulose acetate butyrate material in vapor phase. These results are consistent with the results obtained from the liquid sorption study. In other words, both the liquid sorption and the vapor sorption studies indicate that the cellulose acetate butyrate material preferentially sorbs ethyl alcohol from the binary mixtures of ethyl alcohol and heptane.

4.2.1.3 Studies on the Penetrant Concentration inside Membranes

The word penetrant refers to the liquid inside the membranes which are used in the reverse osmosis experiments. The objective of this study is to examine directly the relationship between the composition of the bulk solution and the composition of the solution permeating inside the membranes, when a steady state is reached in the reverse osmosis experiment. For this purpose, asymmetric cellulose acetate butyrate membranes were prepared and reverse osmosis experiments were performed according to the experimental conditions described in Sections 3.2 and 3.3 of

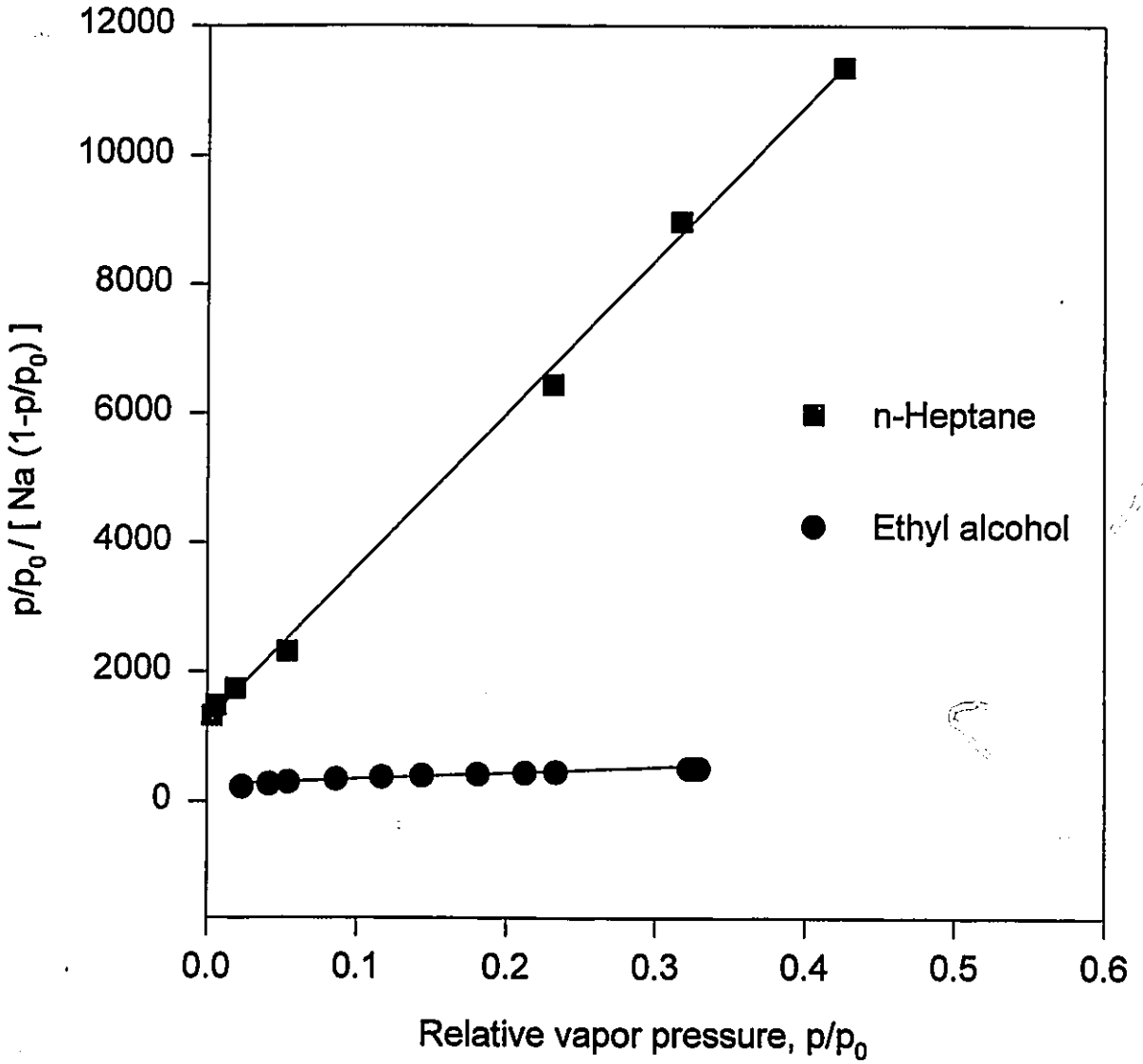

Figure 40 BET plots of ethyl alcohol and n-heptane sorption to the cellulose acetate butyrate powders (Eastman CAB-171-40) at 76.4°C.

Experimental Methods, respectively. The feed liquid was the binary mixture of ethyl alcohol and n-heptane.

To determine the penetrant concentration inside a membrane, membranes were stacked one on top of another. Skin layers of all membranes were directed to the feed side. For instance, a three-membrane stack comprised three membranes stacked in the aforementioned manner. Then, the membrane stack was placed in the reverse osmosis test cell and the reverse osmosis experiment was performed. When the reverse osmosis experiment was finished, the membrane stack was removed from the test cell, blotted free of surface liquid and placed in a moisture-free container. The container was connected to a vacuum line and the liquid in the membrane stack was transferred into a cold trap by applying vacuum for 6 hours. The composition of the liquid collected in the cold trap was determined by gas chromatography.

The results of the above experiments are given in Table 15. For both the three- and six-membrane stacks, the mole fraction of ethyl alcohol inside the membranes is higher than the mole fraction of ethyl alcohol in the feed. The results can be interpreted as a combined effect of the preferential sorption of ethyl alcohol to the cellulose acetate butyrate membranes and the higher mobility exhibited by an ethyl alcohol molecule relative to a n-heptane molecule due to the smaller molecular size of ethyl alcohol. It is natural to regard the detected penetrant concentration as the averaged result of the penetrant concentration within each individual membrane. When the number of membranes in a stack increases from three to six, there is little change in the penetrant concentration. The stack comprising nine membranes was also tested, but no permeate was detected within 12 hours. As for the permeation rate, an increase in the number of membranes in a stack reduces the

permeation rate.

Table 15 Penetrant concentration in the stacked cellulose acetate butyrate membranes under the reverse osmosis conditions†

Number of membranes in a stack	Mole fraction of ethyl alcohol in feed	Mole fraction of ethyl alcohol inside membranes	Permeation rate of the membrane stack‡, g/h
3	0.470	0.790	0.15
6	0.475	0.805	0.05

† The operating pressure for the reverse osmosis experiments: 500 psig. Duration of each experiment: 12 hours. System: asymmetric cellulose acetate butyrate membrane/ethyl alcohol/n-heptane.

‡ Effective membrane area: 9.6×10^{-4} m^2.

It helps to understand the results by examining the role which concentration polarization may play in a membrane separation process. The term concentration polarization is explained as follows. Because the membrane has the ability to transport one component in the feed mixture more readily than the other component, or in some cases completely retains molecules of the latter component, there will be an accumulation of retained molecules near the membrane surface. Unless the retained molecules diffuse back to the main body of the feed solution quickly, the concentration of the retained molecule in the vicinity of the membrane surface increases until a steady state is reached in which the diffusion rate, enhanced by the high concentration near the membrane surface, counterbalances the rate of the accumulation near the membrane surface. This phenomenon is called

concentration polarization (Mulder, 1991; Matsuura, 1994). The high concentration near the membrane surface increases the osmotic pressure of the feed solution, which reduces the effective pressure applied to achieve the separation. Therefore, the existence of concentration polarization reduces the driving force for a membrane separation process and results in a reduced separation and a lower permeation rate.

Concentration polarization may exist in three regions for a membrane stack as illustrated in Figure 41a. Region I is near the surface of the membrane at the top which faces the feed solution. A magnetic stirrer is mounted right above the membrane surface in the reverse osmosis cell and the stirrer provides good mixing. Also, the permeation rate of the membrane stack is relatively low. Thus, concentration polarization in this region is considered insignificant. Region II is the space between two membranes. Under the operating pressure of 500 psig, the membranes are tightly stacked so that little space remains. Thus, almost no permeating liquid can exist in this region. Hence, concentration polarization in region II is not considered, either. Region III is the void space in the porous sublayer inside the bottom side of a membrane. This void space results from the asymmetric structure of an asymmetric membrane as illustrated in Figure 41a. An asymmetric membrane comprises a skin layer and a porous sublayer. Preferential permeation of one component in Region III can lead to concentration polarization inside the membrane.

To examine the possibility of concentration polarization in Region III, let us take the stack containing three membranes as an example. Assume that the porous sublayer acts only as a mechanical support and the separation and permeation rate are largely determined by the skin layer. Further assume that stacked membranes

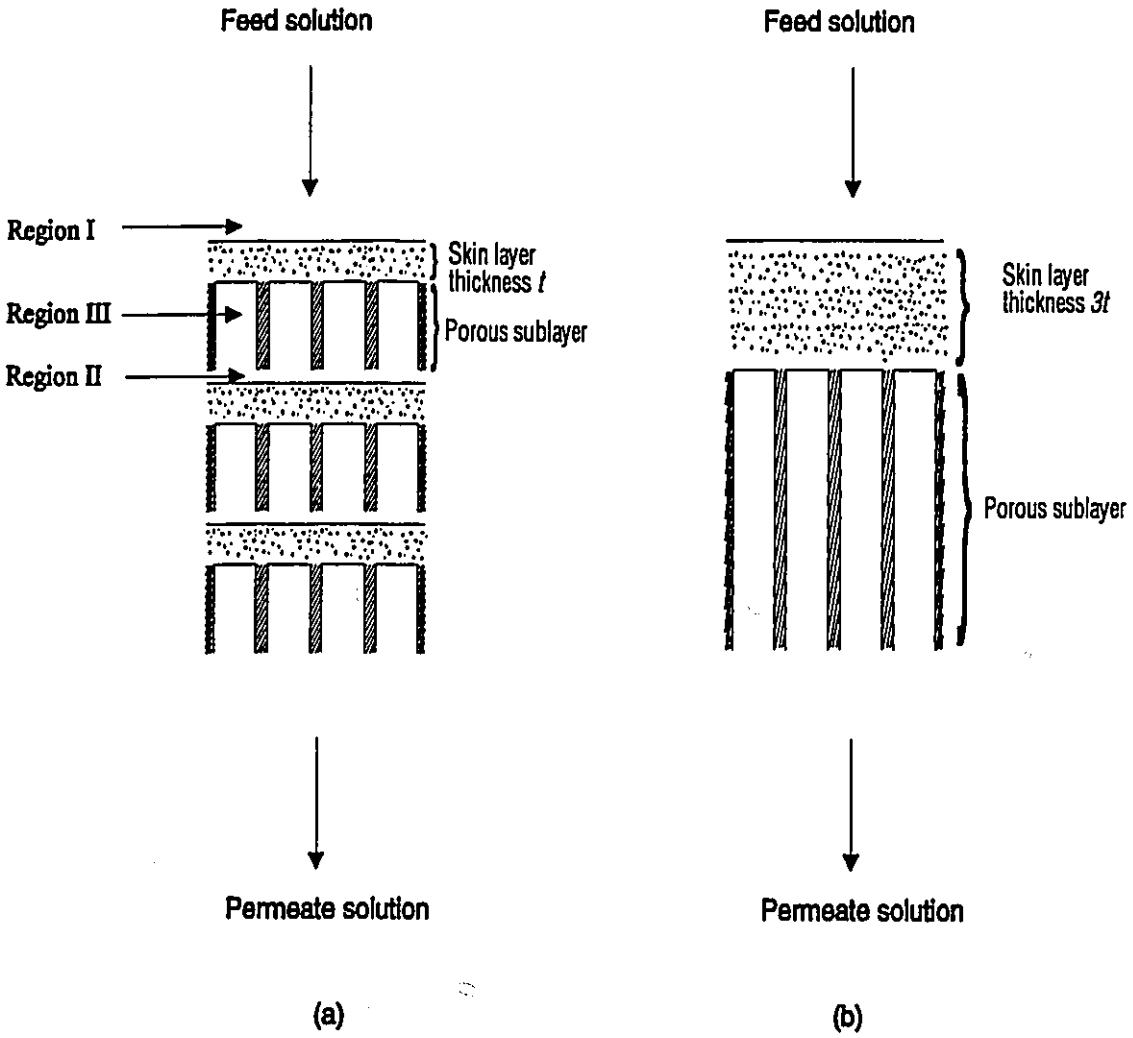

Figure 41 Schematic diagram of stacked, asymmetric membranes.

have identical separation and permeation rates. Without the complication of concentration polarization, three stacked membranes may be equivalent to a membrane whose thickness is three times as large as, both in dense skin layer and porous sublayer, and selectivity is equal to an individual membrane, as shown in Figure 41b. Therefore, the membrane stack containing three membranes will exhibit the same separation as, and one third of the permeation rate of, an individual membrane. Suppose that above analysis can be applied to a membrane stack made of more than three membranes. Then, when the number of stacked membranes increases from 3 to 6, the stack containing six membranes will have the same separation as, but one half of the permeation rate of, the stack containing three membranes.

In the present case, when the number of stacked membranes increased from 3 to 6, the mole fraction of ethyl alcohol inside membranes changed little, which indicated that the composition of the solution on the permeate side would change little, either. As for the permeation rate, the permeation rate for the stack containing three membranes was 0.15 g/h. One half of that rate would be 0.075 g/h. The observed rate of 0.05 g/h for the stack containing six membranes was only slightly lower than the latter value. If concentration polarization had been significant in Region III, a reduced separation and a lower permeation rate would have been observed. Therefore, it can be concluded that concentration polarization played little role when the number of stacked membranes increased from 3 to 6.

The results and discussions so far are based on experimental measurements, which clearly demonstrates that ethyl alcohol is sorbed more strongly by the cellulose acetate butyrate membrane and membrane material from the binary mixtures of ethyl alcohol and n-heptane. The following section presents the results of theoretical modelling.

4.2.1.4 Results of Liquid Sorption Calculated from Liquid Chromatography Data

Preferential sorption of liquid mixtures can be related to surface excess. The preferential sorption of a component *A* to a solid surface leads to accumulation of the latter component at the interface. To define surface excess, Atkins (1978) writes, "We can express this excess as an amount per unit area of the surface by introducing the surface excess". Surface excess may be either positive (accumulation of *A* at the interface) or negative (deficiency of *A* at the interface). By definition, positive surface excess of a component indicates accumulation or preferential sorption of that particular component to a solid surface.

For the binary mixtures of ethyl alcohol and n-heptane, the surface excess of ethyl alcohol, Γ_A, with respect to the cellulose acetate butyrate powder is generated from the liquid chromatography data using the method described in Section 2.2 of Theory and Methodology. In Figure 42, the surface excess of ethyl alcohol, Γ_A, is plotted against the mole fraction of ethyl alcohol in the bulk solution, $X_{\mu,A}$. The data in Figure 42 show that the surface excess of ethyl alcohol is positive in the entire range of ethyl alcohol mole fraction in the bulk solution. This means that ethyl alcohol is preferentially sorbed to the cellulose acetate butyrate polymer surface from the binary mixtures of ethyl alcohol and n-heptane regardless of the concentration of the bulk solution.

Figure 42 also indicates that the surface excess of ethyl alcohol has the highest value when the mole fraction of ethyl alcohol in the bulk solution is relatively small. For instance, the surface excess of ethyl alcohol, Γ_A, at 0.1 mole fraction of ethyl alcohol in the bulk solution is much greater than Γ_A at 0.9 mole fraction of ethyl alcohol in the bulk solution. This certainly indicates stronger sorption of ethyl

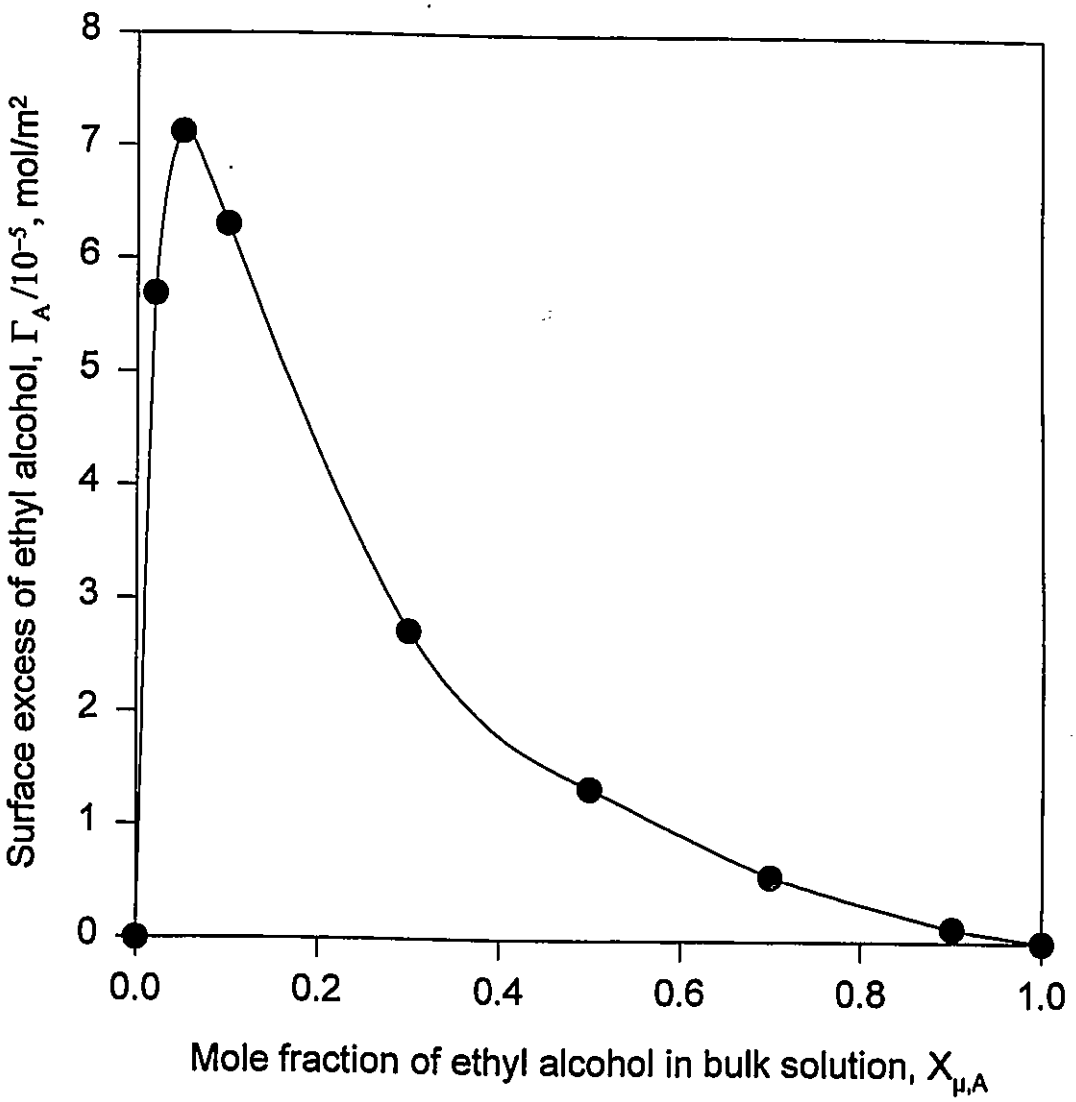

Figure 42 The surface excess of ethyl alcohol from ethyl alcohol/n-heptane solutions at the cellulose acetate butyrate (Eastman CAB-171-40) surface at 23°C.

alcohol to the cellulose acetate butyrate material when the concentration of ethyl alcohol in the bulk solution is low. This is consistent with an earlier observation that the intensity of the preferential sorption is weakened as the ethyl alcohol concentration in the bulk solution increases (Section 4.2.1.1).

Using Equation (15) in Section 2.2, $X_{K,A}$ was calculated using Γ_A as a function of $X_{\mu,A}^{o}$. The results are shown in Figure 43 as "calculated results". The curve indicates that the cellulose acetate butyrate material preferentially sorbs ethyl alcohol from the binary mixtures of ethyl alcohol and n-heptane.

The experimental sorption results given in Figures 37 and 38 are included in Figure 43, along with "calculated results" for comparison. The comparison of these curves shows that the calculated results agree well with the experimental results from the homogeneous membranes made from cellulose acetate butyrate, although the results from the cellulose acetate butyrate powders are below the other two curves. The difference between the results of the homogeneous membranes and those of the powders may be due to the difference in the polymer morphology of the homogeneous membranes and that of the powders. The homogeneous membranes were prepared by dissolving the polymer powder in a solvent and then evaporating the solvent completely. When a dense homogeneous membrane is prepared from polymer powder, the polymer chains become more densely packed. Therefore, the alignment of polymer chains in a dense homogeneous membrane becomes different from that in powder. It is possible that the structural difference between a homogeneous membrane and polymer powder may lead to different sorption characteristics.

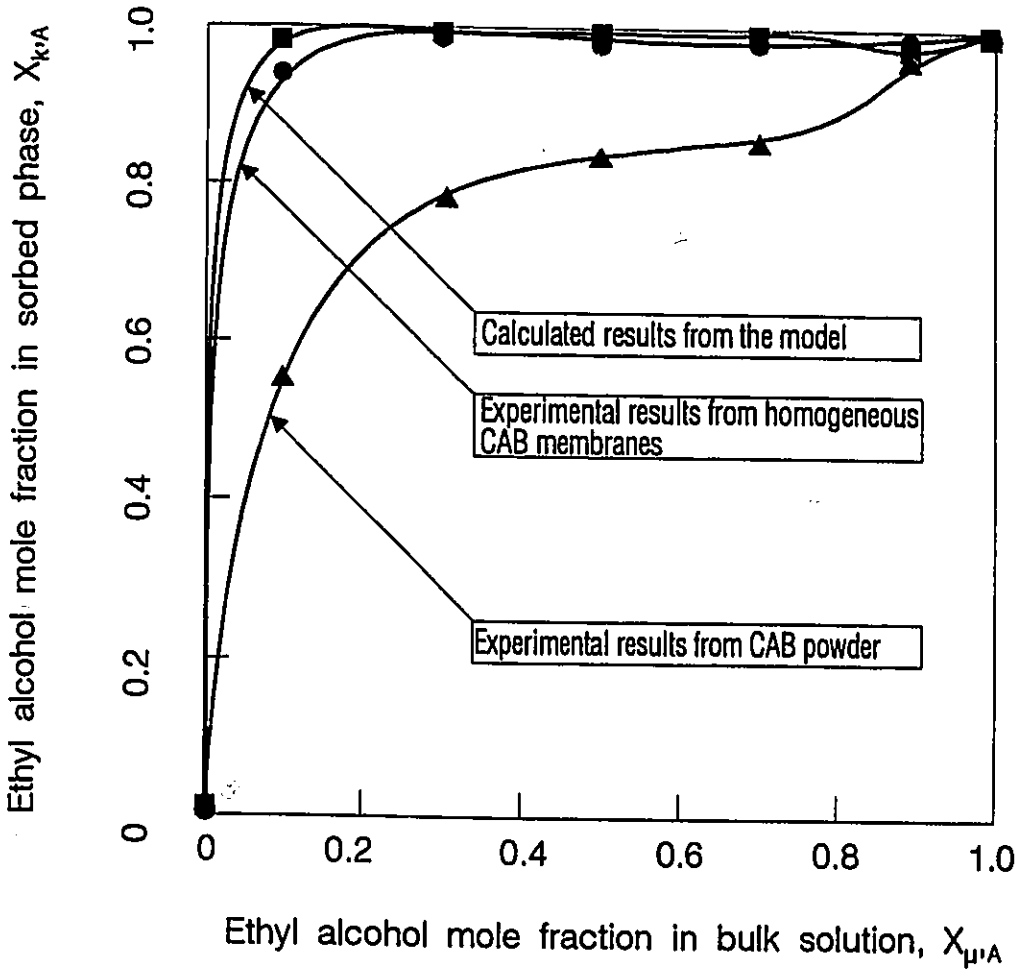

Figure 43 The agreement of calculated and experimental values of liquid sorption data for the cellulose acetate butyrate (CAB) membrane material/ethyl alcohol/n-heptane system at 23°C. Legend: ■, calculated results; ●, experimental results from the homogeneous CAB membrane; ▲, experimental results from the CAB powder.

4.2.2 Results of Reverse Osmosis Transport Study

The interaction between feed molecules and a membrane is a dominant factor in the transport of feed liquids in the reverse osmosis process. As described in Section 2.3.3, the interfacial interaction force constant can be used to characterize the interaction between a feed component and a membrane. For the cellulose acetate butyrate/ethyl alcohol/n-heptane system, the interfacial interaction force constant, $\underline{B}_A$, was generated using the method described in Section 2.3.3 for various feed mole fractions and the results are shown in Table 16. A positive force constant indicates attraction between the feed molecule and the membrane while a negative constant indicates repulsion between the two. The force constants for ethyl alcohol are positive numbers which indicates that ethyl alcohol molecules are attracted to the cellulose acetate butyrate membrane.

Using the transport equations in Section 2.3 of Theory and Methodology, the separation and permeation rate have been calculated for the reverse osmosis separation of ethyl alcohol and n-heptane by a cellulose acetate butyrate membrane. The calculated results are shown in Figure 44, which predict the enrichment of ethyl alcohol in the permeate.

The experimental results for the same system, i.e., asymmetric cellulose acetate butyrate membrane/ethyl alcohol/n-heptane, are also presented in Figure 44 (Fang et al., 1992). Both experimental and calculated results were obtained for the same conditions. The results show that ethyl alcohol is concentrated in the permeate. The previous discussion has shown the preferential sorption of ethyl alcohol by the cellulose acetate butyrate membrane. The flow of the sorbed fluid through the membrane results in the enrichment of ethyl alcohol in the permeate.

Table 16 The interfacial interaction force constant for the cellulose acetate butyrate membrane/ethyl alcohol/n-heptane system

$X_{\mu A}$	$\underline{B}_A \times 10^{30}$, m^3
0.00	0.00
0.025	164.99
0.05	154.45
0.10	139.47
0.20	116.99
0.30	99.85
0.40	84.99
0.50	70.89
0.60	56.22
0.70	39.81
0.80	22.06
0.90	8.02
1.00	0.00

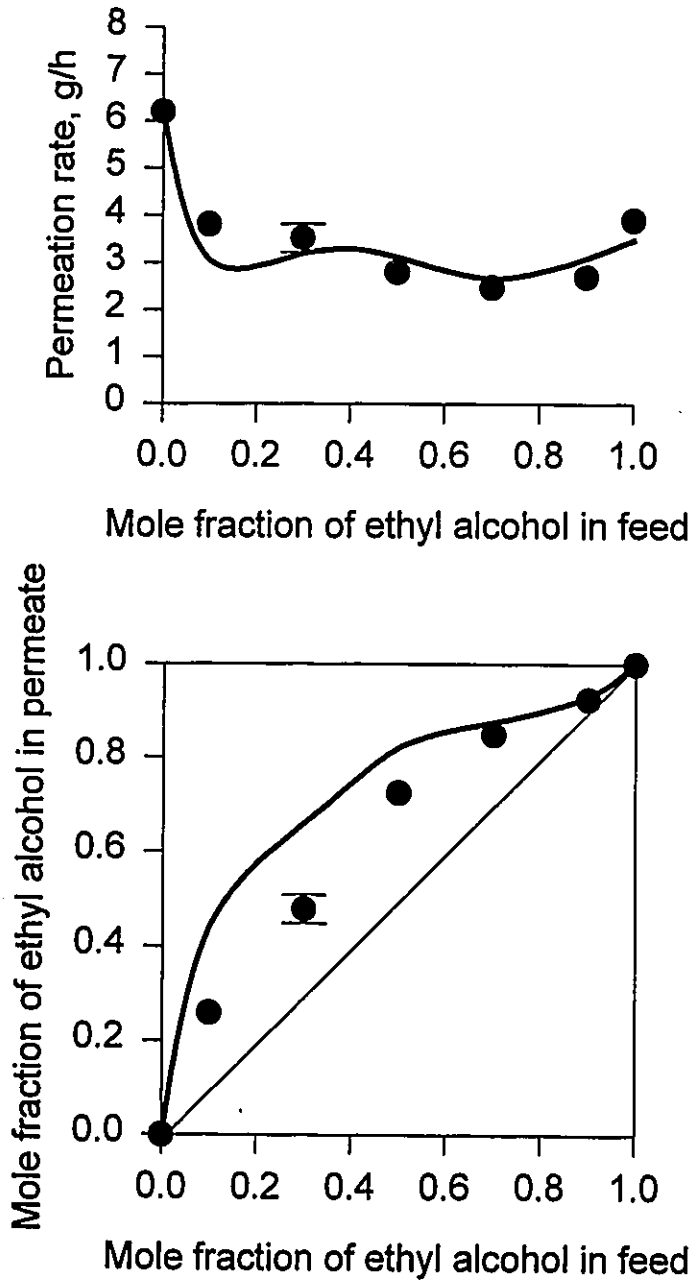

Figure 44 The experimental and calculated values for reverse osmosis separation of ethyl alcohol and n-heptane by the cellulose acetate butyrate membrane. Reverse osmosis conditions: 3448 kPa g (500 psig) and 23°C. Membrane area, 9.6×10^{-4} m^2. ●, the experimental values; The curve, the calculated values for $R_b = 6.5\times10^{-10}$ m.

Another factor that also favors the preferential permeation of ethyl alcohol is that ethyl alcohol has a mobility higher than heptane due to the smaller molecular size of ethyl alcohol.

When the calculated values are compared with the experimental ones, the agreement is reasonable. As for the separation shown in Figure 44, the experimental results are lower than the calculated values, although both results show the enrichment of ethyl alcohol in the permeate.

Some factors may contribute to the deviation in separation in Figure 44. 1) The pore size on the membrane surface may change when the feed composition changes because a bulk solution with a different composition may swell the CAB membrane to a different extent. Consequently, the swollen membrane has a lower separation. The transport equations used in the calculation do not take the swelling effect into consideration. 2) The pores on the membrane surface may not have a uniform pore size. It is more reasonable to assume that the pores on the membrane surface have a distribution. As a result of the pore size distribution, the presence of larger pores can reduce the separation. In general, the calculated results represent the separation under ideal conditions, such as without swelling effect and with a uniform pore size distribution, while the experimental results reflect the separation achieved under more realistic conditions.

Despite some differences observed between the calculated and experimental results, the calculated values represent the experimental results reasonably well. Therefore, the transport equations used in the study offer a valuable means to predict the separation and the permeation rate in reverse osmosis of the binary mixtures of ethyl alcohol and n-heptane.

The following conclusions are drawn from the above results and discussion.

1. The liquid sorption experiments show that both cellulose acetate butyrate powder and homogenous membrane preferentially sorbed ethyl alcohol from the binary mixtures of ethyl alcohol and n-heptane. It was also found that sorption properties of cellulose acetate butyrate powder and those of homogenous membranes were different.

2. The new method to determine the preferential sorption in binary mixtures based on liquid chromatography is presented. Sorption data can be calculated based on the liquid chromatography data. The calculated values are well in line with the data from the homogeneous CAB membrane. The good agreement between the two indicates the validity of the proposed approach.

3. Liquid chromatography can be a useful means to provide information on interaction between the membrane material and the feed solution. The interfacial interaction force constant can be generated from the liquid chromatography results.

4. The binary liquid mixtures of ethyl alcohol and n-heptane can be separated by reverse osmosis.

5. The reverse osmosis performance data can be calculated using the transport equations based on a pore model. The calculated data represent the experimental ones reasonably well. Thus, the approach proposed in this study can be considered as a valuable one.

4.3 Comparison Between Reverse Osmosis and Pervaporation

The results of reverse osmosis and pervaporation experiments are compared for two cases. The first case is the cellulose acetate butyrate membrane/ethyl alcohol/n-heptane system. The separation experiments cover the whole feed composition range. The second one deals with the separation of a vinyl acetate/hexane mixture at a particular feed concentration by four different membranes.

4.3.1 The First Case: Comparison Between Reverse Osmosis and Pervaporation for Cellulose Acetate Butyrate Membrane/Ethyl Alcohol/n-Heptane System

Comparison between reverse osmosis and pervaporation is made using the cellulose acetate butyrate membrane/ethyl alcohol/n-heptane system. The membrane preparation was described in the experimental section 3.2 in detail. Results of reverse osmosis and pervaporation experiments are shown in Figures 45 and 46.

The pervaporation results in Figure 45 show that, in the entire range of the feed concentration, ethyl alcohol is enriched in the permeate for both membranes that have been prepared with solvent evaporation periods of 30 and 60 seconds. As shown in Figure 45a, the ethyl alcohol concentration in the permeate is much higher for the membrane with 60-second solvent evaporation than that for the membrane with 30-second solvent evaporation. For example, when the mole fraction of ethyl alcohol in the feed is 0.1, the mole fraction of ethyl alcohol in the permeate is 0.9 for the former membrane and 0.39 for the latter membrane. From the discussion in Section 4.2.1, one knows that ethyl alcohol is preferentially adsorbed to cellulose acetate butyrate polymer. A longer solvent evaporation period results in a smaller pore size on the membrane surface, which enhances the flow

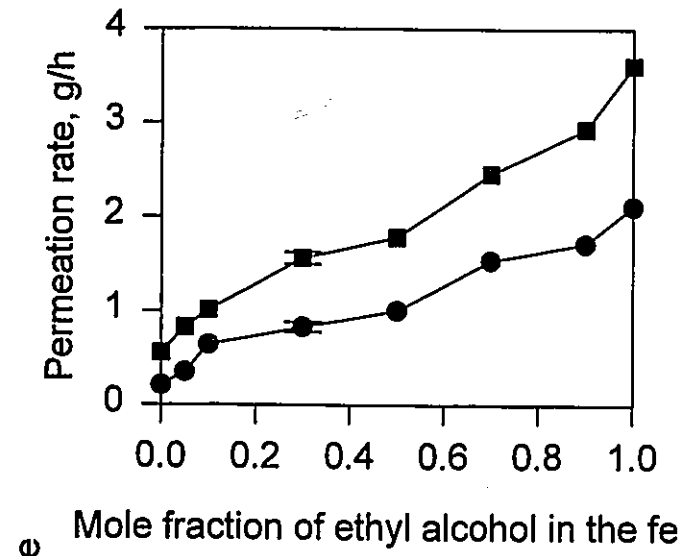

(b)

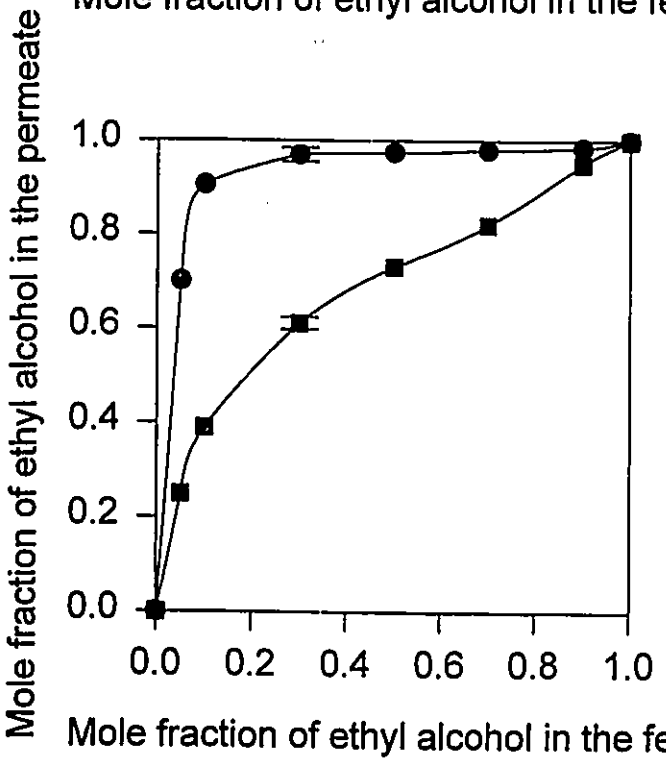

(a)

Figure 45 Results of pervaporation experiments for cellulose acetate butyrate membrane/ethyl alcohol/n-heptane system. Downstream pressure: 400 Pa (3 mmHg). Effective membrane area: 9.6×10^{-4} m^2, ■, 30-second solvent evaporation; ●, 60-second solvent evaporation.

of the preferentially sorbed component. Ethyl alcohol is preferentially sorbed in the present case. Further, for a given pore radius, Stokes' radius offers a measure of the mobility of the component molecule (Sourirajan and Matsuura, 1985). The smaller Stokes' radius is, the higher the mobility. Stokes' radii of ethyl alcohol and n-heptane are 1.2 and 2.5 Å, respectively. Therefore, the mobility of ethyl alcohol is higher than that of heptane. Both factors, i.e., the preferential adsorption and higher mobility of ethyl alcohol, favor the enrichment of ethyl alcohol in the permeate. The smaller pore size of the membrane with a 60-second solvent evaporation period is reflected in its smaller permeation rate, as shown in Figure 45b.

It is interesting to note that the permeate is made of almost pure ethyl alcohol (ethyl alcohol mole fraction ≥0.98) when the mole fraction of ethyl alcohol in the feed is 0.3 or more. It is also clear from Figure 45a that the cellulose acetate butyrate membrane can easily break the azeotrope of ethyl alcohol/n-heptane, whose composition is 0.67 mole fraction of ethyl alcohol (Perry and Green, 1984). This clearly demonstrates the unique applicability of pervaporation in the separation of azeotropic mixtures.

The results of reverse osmosis experiments for the membrane with a 60-second solvent evaporation period are plotted in Figure 46 together with those of pervaporation experiments for the same membrane. The reverse osmosis results show that fractionation of the mixture does take place and ethyl alcohol is preferentially transported through the cellulose acetate butyrate membrane. When the pervaporation results are compared with the reverse osmosis results, ethyl alcohol is enriched in the permeate in both cases, while the degree of enrichment and the permeation rate are different. For the same feed concentration, the mole fraction of ethyl alcohol in the permeate is much higher in pervaporation than in

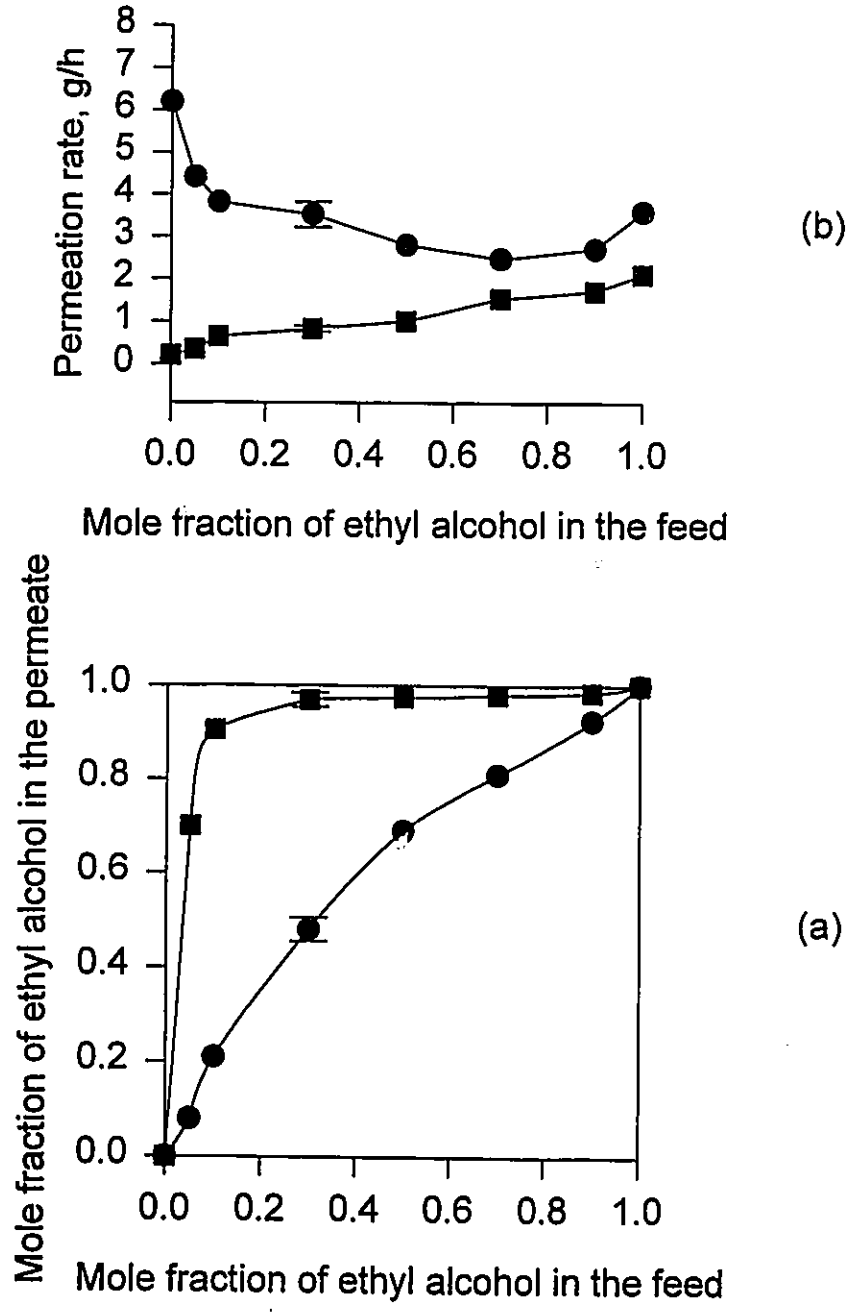

Figure 46 Comparison of the results of reverse osmosis and pervaporation experiments for the cellulose acetate butyrate membrane/ethyl alcohol/n-heptane system. Effective membrane area: 9.6×10^{-4} m^2. Temperature: 23°C. ■, pervaporation results under 400 Pa (3 mmHg); ●, reverse osmosis results under 3448 kPa g (500 psig).

reverse osmosis as indicated in Figure 46a. However, Figure 46b shows that the permeation rate of pervaporation is much less than that of reverse osmosis.

To understand the mechanism for the performance difference between reverse osmosis and pervaporation processes, one may consider the approach described by Okada and Matsuura (1991). The approach starts from the assumption that, in pervaporation, there is a bundle of straight cylindrical pores penetrating across the active surface layer of the membrane perpendicular to the membrane surface. Furthermore, it is assumed that the entire membrane is in an isothermal condition. As shown schematically in Figure 47, a part of the pore is filled with liquid, and the rest of the pore is filled with vapor. Therefore, the approach views the transport of the permeant to consist of three steps: (1) the permeant flows first by liquid transport in the liquid-filled portion of the pore; (2) evaporation occurs at the liquid-vapor phase boundary; and (3) the permeant flows by vapor-phase transport in the vapor-filled portion of the pore. By comparison, in reverse osmosis, the entire pore is filled with liquid. Hence, the permeant flows by only liquid transport.

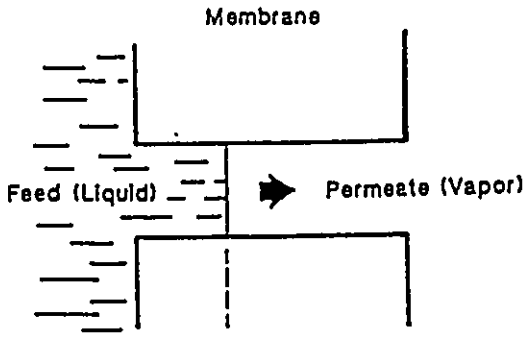

Figure 47 Schematic representation of pervaporation occurring in a membrane pore (Matsuura, 1994).

To explain the higher degree of separation exhibited by pervaporation than reverse osmosis, one may keep the above transport mechanism in perspective. Matsuura and co-workers (Deng et al., 1994) suggest that the membrane that is in contact with the feed liquid mixture is highly swollen and contributes little to the membrane selectivity, whereas the membrane on the downstream side is dry and governs the membrane's selectivity. When a dry membrane is compared with a highly swollen membrane, the dry one appears to have a smaller pore size.

The same principle may apply to interpret the data in Figure 46 that show a higher degree of separation in pervaporation than in reverse osmosis. Suppose the liquid transport through the swollen part of the membrane exhibits the same extent of separation in pervaporation as in reverse osmosis. Then, in pervaporation the vapor transport comes into play. Since the vapor transport portion of the membrane is on the downstream side, it remains dry and has a smaller pore size. When a membrane has a smaller pore size, a higher separation occurs. In the present case, the higher separation is reflected in the greatly enhanced enrichment of ethyl alcohol in the permeate in pervaporation.

From the above discussion, it becomes clear that it is the smaller pore size of the membrane involved in the vapor-phase transport that causes the significantly higher separation of the ethyl alcohol/heptane mixture by pervaporation.

On the other hand, the lower permeation rate in pervaporation than in reverse osmosis can be understood using the same approach. According to Okada and Matsuura (1991) and Bai et al. (1994), an increase in the upstream pressure increases the flux linearly in pervaporation. One also knows that an increase in downstream pressure leads to a lower flux. Figure 48 illustrates these effects of

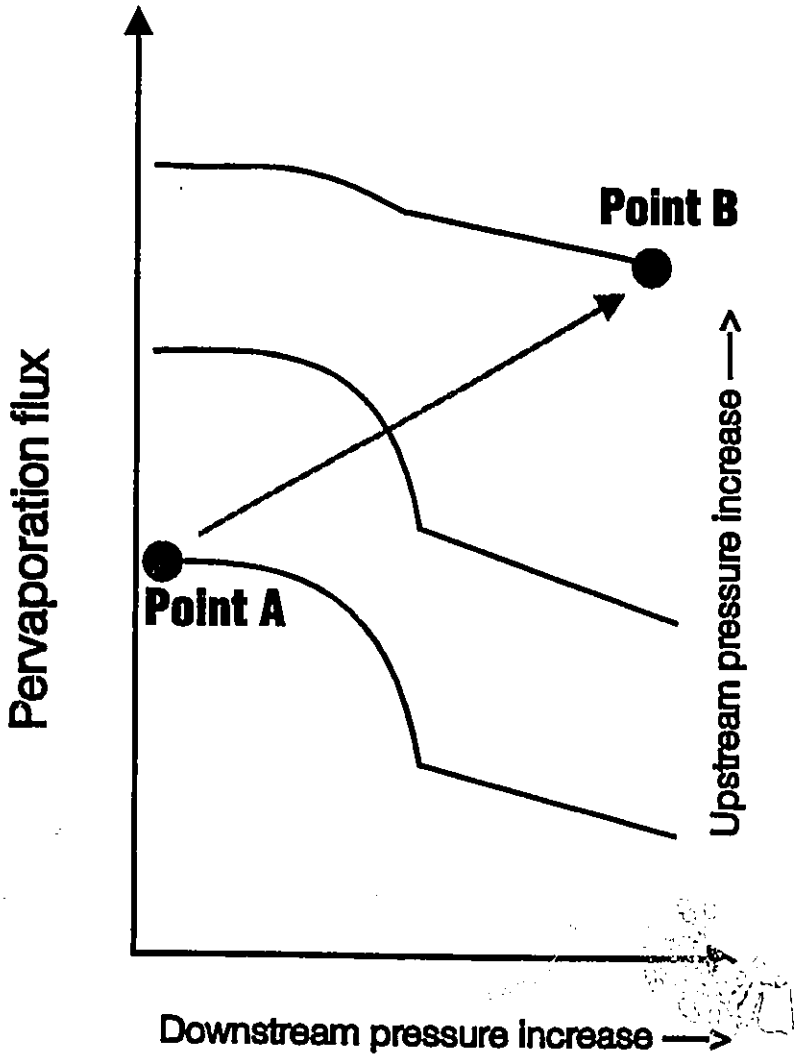

Figure 48 Schematic illustration of the effect of upstream and downstream pressures on the flux in pervaporation (based on Okada and Matsuura (1991) and Bai et al., 1994). Point A: lower upstream and downstream pressures; Point B: higher upstream and downstream pressures.

pressure changes on the changes in flux. Therefore, it is inferred that when both downstream and upstream pressures are increased, the flux increase resulting from the upstream pressure increase may be more significant than the flux decrease resulting from the downstream pressure increase. This scenario is depicted in Figure 48 as Point A moving to Point B. Consequently a net increase in flux occurs.

The above principle may help to explain the flux pattern of pervaporation and reverse osmosis. When the upstream pressure increases from 1 atmosphere to 34 atmosphere (500 psig) and downstream pressure increases from a few mmHg to 1 atmosphere, the combined effect of the pressure increases in upstream and downstream pressures may well generate a net increase in flux. When the aforementioned kind of pressure increases in upstream and downstream occur, a pervaporation process becomes a reverse osmosis process *de facto*. Therefore, the flux in reverse osmosis can be higher than that in pervaporation. This is the reason why for the ethyl alcohol/heptane mixture, the permeation rate in pervaporation is higher than in reverse osmosis as shown in Figure 46. Other approaches to explain the different permeation rate between reverse osmosis and pervaporation are discussed by Brass and Meares (1982), Rautenbach and Albrecht (1989), Mulder and Smolders (1991), and Rautenbach and Knauf (1995). The above discussion also illustrates that the reverse osmosis and pervaporation are two closely related processes in liquid separation in terms of both separation and flux.

In brief, the first case study indicates (1) that for the ethyl alcohol/heptane mixture, ethyl alcohol is enriched in the permeate in both reverse osmosis and pervaporation by the cellulose acetate butyrate membrane; (2) that pervaporation is more effective than reverse osmosis to enrich ethyl alcohol in the permeate using the cellulose acetate butyrate membrane, but it has lower permeation rate than reverse osmosis.

4.3.2 The Second Case: Comparison Between Reverse Osmosis and Pervaporation for Vinyl Acetate/Hexane Mixture by Four Different Membranes

Four different kinds of polymeric membranes, namely, a cellulose acetate butyrate membrane (laboratory made), an aromatic polyamide membrane (laboratory made), an aromatic polyamide composite membrane (commercial) and a silicone rubber membrane (commercial), were tested for the separation of a vinyl acetate/hexane mixture by reverse osmosis and pervaporation processes at room temperature. The vinyl acetate/hexane mixture contained 10 wt % of vinyl acetate, which was of industrial interest (Matsuura, 1992). The description of the membrane preparation is given in the experimental section.

Table 17 shows the permeation data of reverse osmosis of a vinyl acetate/hexane mixture by four kinds of membranes. It shows that the concentration of vinyl acetate in the permeate, depending on the membranes used, varies from 11.2 to 18.1 wt %, and the permeation rate varies from 0.10 to 30.04 g/h. The permeation data in Table 17 indicate that separation takes place for all the membranes used. They also show that vinyl acetate permeates preferentially through the CAB membrane and the PA membrane. As for FT-30 and silicone rubber membranes, vinyl acetate is only very slightly concentrated in the permeate.

Table 18 shows the experimental data of pervaporation of a vinyl acetate/hexane mixture by four kinds of membranes. It shows that the vinyl acetate concentration in the permeate, depending on the membranes used, varies from 13.5 to 49.0 wt %, and the flux varies from 1.61 to 34.15 g/h. The experimental data in Table 18 clearly indicate that separation takes place for all the membranes used. In the case of the laboratory made aromatic polyamide (PA) membrane, significant separation

Table 17 Reverse osmosis results for the separation of vinyl acetate/hexane with four different membranes

Membrane	Vinyl acetate in feed, wt %	Vinyl acetate in permeate, wt %	Permeation rate g/h*
CAB [1]	10.0	18.1	10.07
PA [2]	10.0	15.4	0.10
FT-30[3]	10.0	11.3	4.51
Silicone rubber [4]	10.0	11.2	30.04

* Effective membrane area: 9.6×10^{-4} m^2; operating pressure: 3448 kPa g (500 psig)†.

[1] CAB=cellulose acetate butyrate membrane (laboratory made)†.

[2] PA=aromatic polyamide membrane (laboratory made)†.

[3] FT-30=aromatic polyamide composite membrane, (commercial code: FT-30-SW30-8040, from Dow Chemical Co.)†.

[4] Silicone rubber membrane, polydimethylsiloxane (commercial code: MEM-100, from General Electric Co.)†.

† The description of membrane preparation is given in the experimental section 3.2.

occurs. As shown in the table, the concentration of vinyl acetate in the permeate is 49 wt % when the feed concentration is 10 wt %. They also show that vinyl acetate permeates preferentially through the CAB, PA, FT-30 and silicone rubber membranes, although vinyl acetate is only slightly concentrated in the permeate for FT-30 and silicone rubber membranes.

Table 18 Pervaporation results for the separation of vinyl acetate/hexane with four different membranes

Membrane†	Vinyl acetate in feed, wt %	Vinyl acetate in permeate, wt %	Permeation rate g/h*
CAB [1]	10.0	20.5	15.41
PA [2]	10.0	49.0	2.77
FT-30 [3]	10.0	14.5	1.61
Silicone rubber [4]	10.0	13.5	34.15

† Membranes are specified in Table 17.

* Effective membrane area is 9.6×10^{-4} m^2.

[1] Downstream pressure: 900 Pa (6.75 mmHg).

[2] Downstream pressure: 700 Pa (5.25 mmHg).

[3] Downstream pressure: 2000 Pa (15.00 mmHg).

[4] Downstream pressure: 1100 Pa (8.25 mmHg).

Table 19 shows the experimental data for the pervaporation of the same vinyl acetate and hexane mixture with two laboratory made aromatic polyamide (PA) membranes. These two membranes were cast from the same casting solution but they had different solvent evaporation period, PA 1 membrane being 10 minutes and PA 2 membrane being 8 minutes. The data in Table 19 show that when the evaporation period was increased from 8 minutes to 10 minutes, the concentration of vinyl acetate in the permeate increased from 22 wt % to 49 wt %, while the permeation rate was reduced from 56.75 g/h to 2.77 g/h. This clearly indicates that membranes with significantly different performance can be prepared depending on

the conditions of membrane preparation. This also suggests that a membrane of a high separation together with a reasonable flux is achievable by proper adjustment of preparation conditions.

Table 19 Pervaporation results for the separation of vinyl acetate/hexane with two laboratory made aromatic polyamide membranes

Membrane	Vinyl acetate in feed, wt %	Vinyl acetate in permeate, wt %	Permeation rate† g/h
PA 1‡	10.0	49.0	2.77
PA 2‡	10.0	22.0	56.75

† Effective membrane area: 9.6×10^{-4} m^2; downstream pressure for PA 1 and PA 2 membranes: 700 Pa (5.25 mmHg) and 800 Pa (6.00 mmHg), respectively.

‡ PA 1 and PA 2 membranes have the same composition of the casting solution. The solvent evaporation period of PA 1 and PA 2 membranes: 10 and 8 minutes, respectively.

To better understand the above results, Stokes' radius was calculated, and the solubility parameter of the components involved was obtained. The results are listed in Table 20.

Since the liquid component that has the solubility parameter closer to the solubility parameter of the polymeric material is attracted preferentially to the polymeric material, the component preferentially attracted to the polymer is indicated in column 2 of Table 21.

Table 20 Solubility parameters for the components in vinyl acetate/hexane/polymer system

Component	Solubility parameter, $MPa^{1/2}$	Stokes' radius*, Å
Vinyl acetate	18.5[a]	1.69
Hexane	14.9[b]	2.07
Cellulose acetate butyrate	23.5[c]	—
Aromatic polyamide	32.5[d]	—
Silicone rubber	15.5[e]	—

* Calculation of Stokes' radius is shown in Appendix H.

[a] Source: Barton, "CRC Handbook of Solubility Parameters and Other Cohesion Parameters", CRC Press (1991), p. 137. Details of the reference are given in the reference section.

[b] Source: Barton (1991), p. 131.

[c] Source: Matsuura, "Synthetic Membranes and Membrane Separation Processes", CRC Press (1994), p.22. Details of the reference are given in the reference section.

[d] Source: Matsuura (1994), p. 23.

[e] Source: Barton (1991), p. 406.

Table 21 Preferential attraction and the relative mobility of the vinyl acetate/hexane/polymer system

Membrane polymer	Component of preferential attraction	Component of higher mobility	Component expected to be enriched
Cellulose acetate butyrate	Vinyl acetate	Vinyl acetate	Vinyl acetate
Aromatic polyamide	Vinyl acetate	Vinyl acetate	Vinyl acetate
Silicone rubber	Hexane	Vinyl acetate	Vinyl acetate/hexane*

* indicates the component which is expected to be enriched can be either of them.

Since the size of the vinyl acetate molecule is significantly smaller than that of the hexane molecule as indicated by Stokes' radius in Table 20, the size effect always enhances the preferential permeation of vinyl acetate. Therefore, one can expect a synergistic effect of attraction and mobility on the preferential permeation of vinyl acetate when the membrane material is either cellulose acetate butyrate or aromatic polyamide. This is indicated in column 4 of Table 21. The results of reverse osmosis and pervaporation in Tables 17 and 18 confirm that vinyl acetate permeates preferentially through these membranes. For the silicone rubber membrane, the preferential adsorption (a thermodynamic factor) favors the preferential permeation of hexane, while the mobility (a dynamic factor) favors the preferential permeation of vinyl acetate. In other words, these two factors compete with each other and the result of the competition determines which component is to be enriched in the permeate. In the present case, results in Tables 17 and 18 show that vinyl acetate is slightly enriched in the permeate.

It is interesting to compare the experimental data of pervaporation with those of reverse osmosis. Data in Tables 17 and 18 show that the vinyl acetate concentration in the permeate is higher in pervaporation than in reverse osmosis. As has been discussed before, in pervaporation, the permeant undergoes a vapor transport step. The pervaporation membrane on the downstream side is considered to be dry and has a smaller pore size than the membrane on the upstream side which is swollen by the feed liquid. The smaller pore size usually leads to higher separation. The enhanced separation during the vapor-phase transport is reflected in the higher vinyl acetate concentration in the permeate in pervaporation than in reverse osmosis. As for the permeation rate, there is no clear pattern. For the FT-30 membrane, the permeation rate is higher in reverse osmosis than in pervaporation. For the cellulose acetate butyrate membrane, laboratory made polyamide membrane and silicone rubber membrane, the permeation rate is lower in reverse osmosis than in pervaporation.

In short, this part of the study suggests that

1. Separation takes place in reverse osmosis for all the four different membranes tested. Vinyl acetate permeates preferentially through the laboratory made cellulose acetate butyrate membrane and aromatic polyamide membrane, although vinyl acetate is only very slightly concentrated in the permeate for FT-30 and silicone rubber membranes.

2. Separation takes place in pervaporation for all the four different membranes tested. Vinyl acetate permeates preferentially through the cellulose acetate butyrate membrane, aromatic polyamide membrane, and silicone rubber membrane, although vinyl acetate is only slightly concentrated in the permeate for FT-30 and silicone

rubber membranes. Significant separation occurs for the laboratory made aromatic polyamide membrane.

3. Higher separation is achievable in the separation of the vinyl acetate/hexane mixture by a change of membrane preparation parameters, in this case, the solvent evaporation period.

4. Pervaporation tends to have a higher separation than reverse osmosis.

To conclude, which component is to be enriched in the permeate may be determined under the careful consideration of the factors such as the permeant's size and preferential attraction to the membrane material. A pervaporation process may enhance the extent of separation exhibited by a reverse osmosis process, as indicated by the two cases presented, namely, the separation of ethyl alcohol/n-heptane and of vinyl acetate/hexane. The results are discussed and interpreted using the pore model. The first case illustrates the process difference between reverse osmosis and pervaporation for the separation of ethyl alcohol/n-heptane. The second case demonstrates the importance of membrane material selection for the separation of vinyl acetate/hexane. Both membrane material and process selection are crucial in liquid separation by membranes.

5. Conclusions

The following statements summarize the findings based on the research performed.

● Chloroform is strongly preferentially adsorbed, in comparison to water, to the PES material in the vapor phase and only slightly preferentially adsorbed in the liquid phase.

● Polyethersulfone membrane is water selective in pervaporation separation of the chloroform/water mixture. A longer evaporation period leads to a higher separation and a lower permeation rate for the mixture.

● Asymmetric membranes can be prepared from polyethersulfone solutions containing SMM. Membranes with different structures can be obtained by varying the solvent evaporation period.

● Adding SMM in the casting solution significantly increases both the advancing and the receding contact angles of water on the surface of PES/SMM membranes. The PES/SMM membrane has a more hydrophobic surface than the PES membrane.

● The fluorine concentration is much higher at the membrane surface than in the bulk. The membrane surface is covered by a layer of SMM and the fluorine tail of the SMM molecule is oriented upwards at the membrane surface.

● Conclusions 4 and 5 confirm that adding SMM to a membrane casting solution leads to fluorine-containing SMM migrating to and accumulating at the membrane-air interface.

● Only a small amount of SMM is needed to cover the membrane surface completely.

● Polyethersulfone membranes containing SMM have a superior performance for pervaporation separation of chloroform/water.

● It takes longer time for a PES membrane to reach a stable separation and a stable permeation rate for pervaporation separation of chloroform/water than for a PES/SMM membrane.

● For a PES membrane, a higher chloroform concentration in the feed leads to a higher chloroform concentration in the permeate and a higher permeation rate; while for a PES/SMM membrane, a higher chloroform concentration in the feed leads to a lower chloroform concentration in the permeate and no particular trend of the permeation rate for pervaporation separation of chloroform/water.

● For a PES membrane without SMM, a higher PVP concentration in the casting solution results in a lower separation and a higher permeation for pervaporation separation of chloroform/water. For a PES/SMM membrane, a higher PVP concentration in the casting solution leads to a higher permeation rate and changes the membrane from water selective to chloroform selective.

● When compared with a PES membrane, a PES/SMM membrane increases the permeation rate of n-heptane, and lowers the permeation rate of ethyl alcohol for pervaporation separation of ethyl alcohol/n-heptane mixtures.

● Both CAB powder and homogenous membranes preferentially sorb ethyl alcohol from binary mixtures of ethyl alcohol and n-heptane. It was also found that sorption

properties of CAB powder and those of homogenous membrane were different.

● Sorption data can be calculated based on the liquid chromatography data. Calculated values are in line with the data from the homogeneous CAB membrane. The good agreement between the two indicates the validity of the new method .

● The interfacial interaction force constant can be generated from liquid chromatography results.

● The binary liquid mixtures of ethyl alcohol and n-heptane can be separated by reverse osmosis.

● Reverse osmosis performance data can be calculated using the transport equations based on a pore model. The calculated data represented the experimental ones reasonably well. Thus, the approach proposed in this study can be considered as a valuable one.

● Separation takes place in reverse osmosis for all the four different membranes tested, namely, the laboratory made CAB membrane, the laboratory made aromatic polyamide membrane, the FT-30 membrane and silicone rubber membranes. Vinyl acetate permeates preferentially through the laboratory made CAB membrane and aromatic polyamide membrane, although it is only slightly concentrated in the permeate for FT-30 and silicone rubber membranes.

● Separation takes place in pervaporation for all the four different membranes tested. Vinyl acetate permeates preferentially through the CAB membrane, aromatic polyamide membrane, and silicone rubber membrane, although it is only slightly

concentrated in the permeate for FT-30 and silicone rubber membranes. Significant separation occurs for the laboratory made aromatic polyamide membrane.

- Higher separation is achievable in the separation of vinyl acetate/hexane mixture by the change of membrane preparation parameters, in this case, the solvent evaporation period.

- Pervaporation tends to have a higher separation than reverse osmosis in the separation of the vinyl acetate/hexane mixture.

6. Recommendations

The following recommendations are general suggestions concerning possible future extensions for the research.

1. Calculate surface free energy by measuring contact angles corresponding to different PVP concentration and SMM concentration. Correlate surface free energy or the reduction of surface free energy with membrane pervaporation data.

2. Prepare a homogeneous SMM membrane and determine its selectivity for pervaporation of aqueous/nonaqueous and nonaqueous/nonaqueous mixtures.

3. Examine the effect of solvent evaporation temperature on separation and flux. Change gelation media by introducing high-boiling co-solvents such as ethylene glycol, since they tend to dramatically improve wetting performance by promoting molecular mobility and by orientating polymer surfactants (Schmidt et al., 1994).

4. Study PES/SMM membrane morphology using an atomic force microscope. Use plasma ablation to determine the SMM layer's thickness. Correlate membrane thickness, SMM layer's thickness with membrane selectivity for water or for organics.

5. Investigate the mechanism of SMM's migration. Find out the determinant of SMM's migration. Develop models relating surface composition to bulk composition.

6. Extend the approach to prepare PES/SMM membranes to the formation of membranes used in other membrane processes in addition to pervaporation.

7. References

Adam, W. J., B. Luke and P. Meares, "The Separation of Mixtures of Organic Liquids by Hyperfiltration", J. Membrane Sci. **13**, 127-149 (1983).

Adamson, A. W., "Physical Chemistry of Surfaces", John Wiley & Sons, Inc., New York, New York (1990), 5th ed., Chap. III-3, "Orientation at Interfaces", pp. 69-71.

Alger, M. S. M., "Poly-(*N*-Vinylpyrrolidone)", in "Polymer Science Dictionary", M. S. M. Alger, Ed., Elsevier Science Publishers, New York, NY (1989), p. 390.

Andrade, J. D., L. M. Smith and D. E. Gregonis, "The Contact Angle and Interface Energetics", in "Surface and Interfacial Aspects of Biomedical Polymers", J. D. Andrade, Ed., Plenum Press, New York, NY (1985), p. 278.

Aptel, P., N. Challard, J. Cuny and J. Néel, "Application of the Pervaporation Process to the Separation of Azeotropic Mixtures", J. Membrane Sci. **1**, 271-287 (1976).

Asaeda, M. and S. Kitao, "Separation of Molecular Mixtures by Inorganic Porous Membranes of Ultra Fine Pores", in "Proceedings of the Second Int. Conf. on Inorganic Membranes", A. J. Burggraaff, J. Charpin and L. Cot, Eds., Trans Tech Publications, Zürich (1991), pp. 295-300.

Atkins, P. W., "Physical Chemistry", W. H. Freeman and Company, San Francisco, CA (1978), p. 238.

Bai, J., A. E. Fouda, T. Matsuura and J. D. Hazlett, "A Study on the Preparation and Performance of Polydimethylsiloxane-Coated Polyetherimide Membranes in Pervaporation", J. Appl. Polym. Sci. **48**, 999-1008 (1993).

Bai, J., A. E. Fouda and T. Matsuura, "Effect of Upstream Pressure on the Flux of Single Permeant in Pervaporation", Polym. J. **26**, 1100-1110 (1994).

Baig, F., personal communication (1996).

Bajzer, W. X. and Y. K. Kim, "Fluorine Compounds, Organic", in "Kirk-Othermer Encyclopedia of Chemical Technology", 4th Ed., Vol. 11, Wiley-Interscience Publishers, New York, NY (1994), pp. 467-482 and pp. 722-729.

Baker, R. W., "Analysis of Research Needs", in "Membrane Separation Systems - - Recent Developments and Future Directions", R. W. Baker, E. L. Cussler, W. Eykamp, W. J. Koros, R. L. Riley and H. Strathmann, Noyes Data Corp., Park Ridge, NJ (1991), pp. 58-59.

Bao, S., S. Sourirajan, F. D. F. Talbot and T. Matsuura, "Gas and Vapor Adsorption on Polymeric Materials by Inverse Gas Chromatography", in "Inverse Gas Chromatography", D. R. Lloyd, T. C. Ward and H. P. Schreiber, Eds., ACS Symposium Series 391, American Chemical Society, Washington, DC (1989), pp. 59-76.

Barrer, R. M. and K. Ueberreiter, "Diffusion and Permeation in Heterogeneous Media" (Chap. 6) and "The Solution Process" (Chap. 7), in "Diffusion in Polymers", J. Crank and G. S. Park, Eds., Academic Press, London (1968), pp. 165-257.

Barton, A. F. M., "CRC Handbook of Solubility Parameters and Other Cohesion Parameters", 2nd ed., CRC Press, Boca Raton, FL (1991), p. 131 (for hexane), p. 137 (for vinyl acetate) and p. 406 (for polydimethylsiloxane).

Bengtson, G. and K. W. Böddeker, "Pervaporation of Low Volatiles from Water", in "Proceedings of Third Int. Conf. on Pervaporation Processes in the Chem. Ind.", Bakish Materials Corp., Englewood, NJ (1988), pp. 439-448.

Binning, R. C. and F. E. James, "Now Separate by Membrane Permeation", Petroleum Refiner **37**, 214-215 (1958a).

Binning, R. C. and F. E. James, "Permeation, a New Way to Separate Mixtures", Oil Gas J. **56**, 104-105 (1958b).

Binning, R. C., R. J. Lee, J. F. Jenning and E. C. Martin, "Separation of Liquid Mixtures by Permeation", Ind. Eng. Chem. **53**, 45-50 (1961).

Bitter, J. G. A. , J. P. Haan and H. C. Rijkens, "Solvent Recovery Using Membranes in the Lubeoil Dewaxing Process", in "Membrane Separations in Chemical Engineering", AIChE. Symp. Ser. **85**, No. 272, A. E. Fouda, J. D. Hazlett, T. Matsuura and J. Johnson, Eds., AIChE., New York, NY (1989), pp. 98-100.

Black, L. E. and H. A. Boucher, "Separating Alkylaromatics from Aromatic Solvents and the Separation of the Alkylaromatic Isomers Using Membranes", Eur. Pat. Appl. EP 160,140, Chem. Abstr. 104:129598w (1986).

Bitter, J. G. A. and J. P. Haan, "Process for Separating a Fluid Mixture Containing Hydrocarbons and an Organic Solvent", Eur. Pat. Appl. EP 254,359 26, Chem. Abstr. 108:134750b (1988).

Black, L. E., "Interfacially Polymerized Membranes, and Reverse Osmosis Separation of Organic Solvent Solutions Using them", Eur. Pat. Appl. EP 421,676; Chem. Abstr. 115:95291a. (1991).

Blume, I. and R. Baker, "Separation and Concentration of Organic Solvents from Water Using Pervaporation", in "Proceedings of Second Int. Conf. on Pervaporation Processes in the Chem. Ind.", Bakish Materials Corp., Englewood, NJ (1987), pp. 111-125.

Blume, I., J. G. Wijmans and R. W. Baker, "The Separation of Dissolved Organics from Water by Pervaporation", J. Membrane Sci. **49**, 253-286 (1990).

Böddeker, K. W. and G. Bengtson, "Selective Pervaporation of Organics from Water", in "Pervaporation Membrane Separation Processes", R. Y. M. Huang, Ed., Elsevier Science Publishers, New York, NY (1991), pp. 437-460.

Böddeker, K. W., "Pervaporation of Aqueous Phenol", in "Proceedings of Second Int. Conf. on Pervaporation Processes in the Chem. Ind.", Bakish Materials Corp., Englewood , NJ (1987), pp. 141-145.

Brady Jr, R. F., "Coming to an Unsticky End", Nature, **368**, 16-17 (1994).

Brass, I. J. and P. Meares, "Some Considerations Regarding the Hyperfiltration of Organic Liquids", in "Polymeric Separation Media", Polymer Science and Technology Series, Volume 16, A. R. Cooper, Ed., Plenum Press., New York, NY (1980), pp. 7-17.

Brun, J. P., C. Larchet, R. Melet and G. Bulvestre, "Modelling of the Pervaporation of Binary Mixtures through Moderately Swelling Non-Reacting Membranes", J. Membrane Sci. **23**, 257-283 (1985a).

Brun, J. P., C. Larchet, G. Bulvestre and B. Auclair, "Sorption and Pervaporation of Dilute Aqueous Solutions of Organic Compounds through Polymer Membranes", J. Membrane Sci. **25**, 55-100 (1985b).

Brunauer, S., P. H. Emmett and E. Teller, "Adsorption of Gases in Multimolecular Layers", J. Amer. Chem. Soc. **60**, 309-319 (1938).

Brüschke, H. E. A., "State of Art of Pervaporation", in "Proceedings of Third Int. Conf. on Pervaporation in the Chem. Ind.", Bakish Materials Corp., Englewood, NJ (1988), pp. 2-11.

Brüschke, H. E. A., "State-of-Art of Pervaporation", in "Proc. Fifth Int. Conf. on Pervaporation Processes in the Chem. Ind.", R. Bakish, Ed., Bakish Materials Corp., Englewood, NJ (1991), pp. 2-6.

Cabasso, I., "Organic Liquid Mixtures Separation by Permselective Polymer Membranes, I. Selection and Characteristics of Dense Isotropic Membranes Employed in the Pervaporation Process", Ind. Eng. Chem. Prod. Res. Dev. **22**, 313-319 (1983).

Cadotte, J. E., "Interfacially Synthesized Reverse Osmosis Membrane and its Use in Removing Solute from Solute-Containing Water", U. S. Patent 4,277,344 (July 7, 1981).

Chang, Y. A., S. S. Kulkarni and E. W. Funk, "Membrane Separation of Hydrocarbons", US Patent 4,595,507 (1986).

Chen, M. S. K., G. S. Markiewicz and K. G. Venugopal, "Development of Membrane Pervaporation TRIM™ Process for Methanol Recovery from CH_3OH/MTBE/C4 Mixtures", in "Membrane Separations in Chemical Engineering", AIChE. Symp. Ser. **85**, No. 272, A. E. Fouda, J. D. Hazlett, T. Matsuura and J. Johnson, Eds., AIChE., New York, NY (1989), pp. 82-88.

Côté, P. and C. Lipski, "Mass Transfer Limitations in Pervaporation for Water and Wastewater Treatment", in "Proceedings of Third Int. Conf. on Pervaporation Processes in the Chem. Ind.", Bakish Materials Corp., Englewood, NJ (1988), pp. 449-462.

Deng, S., B. Shiyao, S. Sourirajan and T. Matsuura, "A Study of the Pervaporation of Isopropyl Alcohol/Water Mixtures by Cellulose Acetate Membranes", J. Colloid Interface Sci. **136**, 283-291 (1990).

Deng, S., S. Sourirajan and T. Matsuura, "A Study of Polydimethylsiloxane/ Aromatic Polyamide Laminated Membranes for Separation of Acetic Acid/Water Mixtures by Pervaporation Process", Separation Sci. Tech. **29**, 1209-1216 (1994).

Doghieri, F., A. Nardella, G. C. Sarti and C. Valentini, "Pervaporation of Methanol-MTBE Mixtures through Modified Poly (phenylene oxide) Membranes", J. Membrane Sci. **91**, 283-291 (1994).

Eustache, H. and G. Histi, "Separation of Aqueous Organic Mixtures by Pervaporation and Analysis by Mass Spectrometry or a Coupled Gas Chromatograph-Mass Spectrometer", J. Membrane Sci. **8**, 105-114 (1981).

Fang, Y., V. Pham, H. Mahmud, J. P. Santerre, R. Nabaitz, T. Matsuura, "Application of Surface Modifying Macromolecules for the Preparation of Membranes with High Surface Hydrophobicity to Extract Organic Molecules from Water by Pervaporation", in "Proceedings of Seventh International Conference on Pervaporation Processes in the Chemical Industry", R. Bakish, Ed., Bakish Materials Corporation, Englewood, NJ (1995), pp. 349-362.

Fang, Y., S. Sourirajan and T. Matsuura, "Reverse Osmosis Separation of Binary Organic Mixtures Using Cellulose Acetate Butyrate and Aromatic Polyamide Membranes", J. Appl. Polym. Sci. **44**, 1959-1969 (1992).

Fang, Y., V. Pham, T. Matsuura, P. Santerre, R. Nabaitz, "Effect of Surface Modifying Macromolecules and Solvent Evaporation Time on the Performance of Polyethersulfone Membranes for the Separation of Chloroform/Water Mixtures by Pervaporation", J. Appl. Polym. Sci. **54**, 1937-1943 (1994).

Farnand, B., "A Study of Reverse Osmosis Separations Involving Nonaqueous Solutions", Ph.D. Thesis, Department of Chemical Engineering, The University of Ottawa, Ottawa, ON (1983).

Farnand, B. A., C. Nader and H. Sawatzky, "Evaluation of Various Polymers as Membranes for the Reverse Osmosis Upgrading of Light Petroleum Distillates", Polym. Mater. Sci. Eng. **51**, 162-165 (1984b).

Farnand, B., F. D. F. Talbot, T. Matsuura and S. Sourirajan, "Reverse Osmosis Fractionation of Ethanol-Heptane Mixtures Using Membranes of Different Polymeric Materials", in "Proc. 5th Canadian Bioenergy Seminar", S. Hasnain, Ed., Elsevier Applied Science Publishers, New York, NY (1984a), pp. 195-200.

Farnand, B., F. D. F. Talbot, T. Matsuura and S. Sourirajan, "Reverse Osmosis Separation of Organic and Inorganic Solutes in Methyl Alcohol Solutions", in "Proc. 4th Bioenergy R & D Seminar", National Research Council Canada, Ed., Ottawa, ON (1982), pp. 535-539.

Farnand, B. A. and H. Sawatzky, "Reverse Osmosis Fractionation of Petroleum and Synthetic Crude Distillates", Energy, Mines, Resource Canada, Report Canmet-84-54TR (1989), pp. 1-14.

Farnand, B., F. D. F. Talbot , T. Matsuura and S. Sourirajan, "Reverse Osmosis Separations of Alkali Metal Halides in Methanol Solutions Using Cellulose Acetate Membranes", in "Proc. 2nd Bioenergy R & D Seminar", National Research Council Canada, Ed., Ottawa, ON (1980), pp. 179-183.

Featherstone, W. and T. Cox, "Separation of Aqueous-Organic Mixtures by Pervaporation", Ind. Eng. Chem. Process Des. Dev. **16**, 817-819 (1971).

Fleming, H. L. and C. S. Slater, "Pervaporation", in "Membrane Handbook", W. S. W. Ho and K. K. Sirkar, Eds., Van Nostrand Reinhold Publishers, New York, NY (1992), pp. 148-152.

Fritsch, D., G. Bengtson and K. W. Böddeker, "Pervaporation of Aqueous-Organic and Organic-Organic Mixtures Using Elastomeric Polymer Membranes", in "Macromolecules 1992", J. Kahovec, Ed., VSP Publishers, Frankfurt (1993), pp. 485-497.

Hafez, M. M. and B. A Koenitzer, "Preswelling Regenerated Cellulose Membranes for Organic Separations and their Use", Eur. Pat. Appl. EP 137,698, Chem. Abstr. 103:23991h (1985).

Hamilton, R. J. and P. A. Sewell, "Introduction to High Performance Liquid Chromatography", Halsted Press, London (1978), pp. 14-15.

Hazlett, J. D., O. Kutowy, T. A. Tweddle and B. A. Farnand, "Processing of Crude Oils with Polymeric Ultrafiltration Membranes", in "Membrane Separations in Chemical Engineering", AIChE. Symp. Ser. **85**, No. 272, A. E. Fouda, J. D. Hazlett, T. Matsuura and J. Johnson, Eds., AIChE., New York, NY (1989), pp. 101-107.

Henis, J. M. S. and M. K. Tripodi, "Multicomponent Membranes for Gas Separations", U. S. Patent 4,230,463 (October 28, 1980).

Hennepe, H. J. C. T., D. Bargeman, M. H. V. Mulder and C. A. Smolders, "Pervaporation with Zeolite-filled Silicone Rubber Membranes", in "Proceedings of Second Int. Conf. on Pervaporation Processes in the Chem. Ind.", Bakish Materials Corp., Englewood, NJ (1987b), pp. 71-78.

Hennepe, H. J. C. T., D. Bargeman, M. H. V. Mulder and C. A. Smolders, "Alcohol-Water Separation with Zeolite-filled Silicone Rubber Membranes", Abstracts of the 1987 International Congress on Membranes and Membrane Processes, ICOM'87, Tokyo (1987a), pp. 484-485.

Hu, C. B. and C. S. P. Sung, "Surface Chemical Composition-Depth Profile of Polyether Poly (urethane ureas) as Studied by FT-IR and ESCA", USA Government Report No. **AD-A078240** (1979), pp.1-18.

Huang, R. Y. M. and M. Fels, "Separation of Organic Liquid Mixtures by the Permeation Process with Graft Copolymer Membranes", Chem. Eng. Progr., Sympos. Ser. **65**, 52 (1969).

Huang, R. Y. M. and V. J. C. Lin, "Separation of Liquid Mixtures by Using Polymer Membranes. I. Permeation of Binary Organic Liquid Mixtures through Polyethylene", J. Appl. Polym. Sci. **12**, 2615-2631 (1968).

Huang, R. Y. M. and J. W. Rhim, "Separation Characteristics of Pervaporation Membrane Separation Processes", in "Pervaporation Membrane Separation Processes", R. Y. M. Huang, Ed., Elsevier Science Publishers, New York, NY (1991), pp. 111-180.

Huber, J. F. K. and R. G. Geritse, "Evaluation of Dynamic Gas Chromatography Methods for the Determination of Adsorption and Solution Isotherm", J. Chromatogr. **58** (2), 137-158 (1971).

Ishihara, K. and K. Matsui, "Pervaporation of Ethanol-Water Mixture through Composite Membranes Composed of Styrene-Fluoroalkylacrylate Graft Copolymers and Cross-linked Polydimethylsiloxane Membrane", J. Appl. Polym. Sci. **34**, 437-440 (1987).

Johnson, R. E., Jr. and R. H. Dettre, "Wettability and Contact Angles", in "Surface and Colloid Science", Volume 2, E. Matijevic, Ed., Wiley-Interscience, New York, NY (1969), p. 109.

Jonsson, G and C. E. Boesen, "Water and Solute Transport through Cellulose Acetate Reverse Osmosis Membranes", Desalination **17**, 145-165 (1975).

Karch, K., S. Sebestian, I. Halász and H. Engelhardt, "Optimization of Reversed-Phase Separations", J. Chromatography **122**, 171-184 (1976).

Kaschemekat, J., J. G. Wijmans, R. W. Baker and I. Blume, "Separation of Organics from Water Using Pervaporation", in "Proceedings of Third Int. Conf. on Pervaporation Processes in the Chem. Ind.", Bakish Materials Corp., Englewood, NJ (1989), pp. 405-412.

Kasemura, T., Y. Oshibe, H. Uozumi, S. Kawai, Y. Yamada, H. Ohmura and T. Yamamoto, "Surface Modification of Epoxy Resin with Fluorine-Containing Methacrylic Ester Copolymers", J. Appl. Polym. Sci. **47**, 2207-2216 (1993).

Kashiwagi, T., K. Okabe and K. Okita, "Separation of Ethanol from Ethanol-Water Mixtures by Plasma-polymerized Membranes from Silicone Compounds", J. Membrane Sci. **36**, 353-362(1988).

Kedem, O. and A. Katchalsky, "Thermodynamic Analysis of the Permeability of Biological Membranes to Non-electrolytes", Biochimica et Biophysica Acta **27**, 229-246 (1958).

Kesting, R. E., "Synthetic Polymeric Membranes -- A Structural Perspective", 2nd Ed., John Wiley & Sons, New York, NY (1985), pp. 277-281.

Knox, J. H. and R. Kaliszan, "Theory of Solvent Disturbance Peaks and Experimental Determination of Thermodynamic Dead-Volume in Column Liquid Chromatography", J. Chromatography **349**, 211-234 (1985).

Kober, M. and B. Wesslén, "Amphiphilic Segmented Polyurethanes as Surface Modifying Additives", J. Polym. Sci. Part A: Polym. Chem. **30**, 1061-1070 (1992).

Koops, G. H. and C. A. Smolders, "Estimation and Evaluation of Polymeric Materials for Pervaporation Membranes", in "Pervaporation Membrane Separation Processes", R. Y. M. Huang, Ed., Elsevier Science Publishers, New York, NY (1991), pp. 253-278.

Kopecek, J. and S. Sourirajan, "Equisorptic Compositions in Reverse Osmosis", Can. J. Chem. **47**, 3467-3469 (1969).

Kopecek, J. and S. Sourirajan, "Performance of Porous Cellulose Acetate Membranes for the Reverse Osmosis Separation of Mixtures of Organic Liquids", Ind. Eng. Chem. Process. Des. Dev. **9**, 5-12 (1970).

Kuk, M. S., R. J. Hron, Sr. and G. Abraham, "Reverse Osmosis Membrane Characteristics for Partitioning Triglyceride-Solvent Mixtures", J. of the American Oil Chemists' Society **66**, 1374-1380 (1989).

Kulkarni, S. S., E. W. Funk and N. N. Li, "Hydrocarbon Separations with Polymeric Membranes", in "Recent Advances in Separation Techniques-III", AIChE. Symp. Ser. 250, Vol. 82, N. N. Li, Ed., AIChE., Washington, DC (1986), pp. 78-84.

Laatikainen, M. and M. Lindström, "Separation of Methanol-Ethanol and Ethanol-n-Heptane Mixtures by Reverse Osmosis and Pervaporation", Acta Polytechnica Scandinavica, Chemical Technology and Metallurgy Series No. 175, Helsinki, 1-61 (1986).

Lee, Y. T., K. Iwamoto and M. Seno, "Pervaporation of Water-Alcohol Mixtures with Chemically Modified Porous Glass Membranes", Maku (Membrane Jap.) **13**, 171-176 (1988).

Lee, Y. M., D. Bourgeois and G. Belfort, "Selective Organic Transport through Polyvinylidenefluoride (PVDF) for Pervaporation", in "Proceedings of Second Int. Conf. on Pervaporation Processes in the Chem. Ind.", Bakish Materials Corp., Englewood, NJ (1987), pp. 249-265.

Lipski, C. and P. Côté, "The Use of Pervaporation for the Removal of Organic Contaminants from Water", Environmental Progress **9**, 254-261 (1990).

Long, V. T., B. S. Minhas, T. Matsuura and S. Sourirajan, "Gas Chromatographic Method for the Measurement of Gas Sorption on Polymeric Materials", J. Colloid Interface Sci. **125**, 478-483 (1988).

Lonsdale, H. K., U. Merten and R. L. Riley, "Transport Properties of Cellulose Acetate Osmotic Membrane", J. Appl. Polymer Sci. **9**, 1341-1362 (1965).

Martin, E. C., R. C. Binning, L. M. Adams and R. J. Lee, "Diffusive Separation", US Patent 3,140,256 (1964).

Masuoka, T., K. Mizoguchi, Y. Suda and O. Hirasa, "Separation Membranes for Ethanol-Water Mixture by Plasma-Polymerization", Abstracts of the 1987 International Congress on Membranes and Membrane Processes, ICOM'87, Tokyo (1987), pp. 590-591.

Masuoka, T., K. Mizoguchi, O. Hirasa and A. Yamauchi, "Ethanol Permselective Membranes Prepared by Plasma-Polymerization", in "Proceedings of Third Int. Conf. on Pervaporation Processes in the Chem. Ind.", Bakish Materials Corp., Englewood, NJ (1989), pp. 143-149.

Matsui, K., K. Ishihara, I. Shinohara, H. Nishide and R. Kogure, "Copolymer, Separating Membrane Made Thereof, and Method for Separating Charge Transfer Interactive Substance from a Liquid Mixtures Containing it", Eur. Pat. Appl. EP 190,647, Chem. Abstr.105:210114c (1986).

Matsuura, T. and S. Sourirajan, "Reverse Osmosis Transport through Capillary Pores under the Influence of Surface Forces", Ind. Eng. Chem. Process Des. Dev. **20**, 273-282 (1981).

Matsuura, T., Y. Taketani and S. Sourirajan, "Interfacial Parameters Governing Reverse Osmosis for Different Polymer Material-Solution Systems through Gas and Liquid Chromatography Data", J. Colloid Interface Sci. **95**, 10-22 (1983).

Matsuura, T., personal communication (1992).

Matsuura, T., "Synthetic Membranes and Membrane Separation Processes", CRC Press, Boca Raton, FL (1994), p. 393.

McCormick, R. M. and B. L. Karger, "Distribution Phenomena of Mobile-Phase Components and Determination of Dead Volume in Reversed-Phase Liquid Chromatography", Anal. Chem. **52**, 2249-2257 (1980a).

McCormick, R. M. and B. L. Karger, "Role of Organic Modifier Sorption on Retention Phenomena in Reversed-Phase Liquid Chromatography", J. Chromatography **199**, 259-273 (1980b).

Mehdizadeh, H. and J. M. Dickson, "Theoretic Modification of the Surface Force-Pore Flow Model for Reverse Osmosis Transport", J. Membrane Sci. **42**, 119-145 (1989).

Mehdizadeh, H. and J. M. Dickson, "Modelling of Reverse Osmosis in the Presence of Strong Solute-Membrane Affinity", AIChE. J. **39**, 434-445 (1993).

Merten, U., "Transport Properties of Osmotic Membranes", in "Desalination by Reverse Osmosis", U. Merten, Ed., M.I.T. Press, Cambridge, MA (1966), pp. 15-54.

Miyano, T., T. Matsuura and D. J. Carlsson, "Retention of Polyvinylpyrrolidone Swelling Agent in the Poly (ether p-phenylenesulfone) Ultrafiltration Membrane", J. Appl. Polym. Sci. **41**, 407-417 (1990).

Miyata, T., T. Iwamoto and T. Uragami, "Characteristics of Permeation of Separation for Propanol Isomers through Poly(vinyl alcohol) Membranes Containing Cyclodextrin", J. Appl. Polym. Sci. **51**, 2007-2014 (1994).

Mohlin, U.-B and D. G. Gray, "Gas Chromatography on Polymer Surfaces: Adsorption on Cellulose", J. Colloid Interface Sci. **47**, 747-754 (1974).

Mohr, J. M., D. R. Paul, Y. Taru, T. E. Mlsna and R. J. Lagow, "Surface Fluorination of Composite Membranes, Part II. Characterization of the Fluorinated Layer", J. Membrane Sci. **55**, 149-171 (1991).

Mulder, M., "Basic Principles of Membrane Technology", Kluwer Academic Publications, Dordrecht, The Netherlands (1991), pp. 281-288.

Mulder, M. H. V. and C. A. Smolders, "Mass Transport Phenomena in Pervaporation Processes", Separation Sci. Tech., **26**, 85-95 (1991).

Nakagawa, T. and S. Yamada, "Permeation and Separation of Alcohol-Water Solution by Copolymer Membranes Composed of Hydrophilic and Hydrophobic Monomer", Abstracts of the 1987 International Congress on Membranes and Membrane Processes, ICOM'87, Tokyo (1987), pp. 586-587.

Nakamura, M., S. Samejima and T. Kawasaki, "Liquid Separation With Fluorinated Polymer Membranes", J. Membrane Sci. **36**, 343-351(1988).

National Research Council, "Recovering Substances from Dilute Solutions", in "Separation & Purification--Critical Needs and Opportunities", National Academy Press, Washington, DC (1987), pp. 51-54.

Néel, J., "Introduction to Pervaporation", in "Pervaporation Membrane Separation Processes", R. Y. M. Huang, Ed., Elsevier Science Publishers, New York, NY (1991), pp. 1-109.

Nguyen, T. D., T. Matsuura and S. Sourirajan, "Effect of Nonsolvent Additives on the Pore Size and the Pore Size Distribution of Aromatic Polyamide RO Membranes", Chem. Eng. Commun. **54**, 17-36 (1987).

Nguyen, Q. T. and K. Nobe, "Extraction of Organic Contaminants in Aqueous Solutions by Pervaporation", J. Membrane Sci. **30**, 11-22 (1987).

Nijhuis, H. H., M. H. V. Mulder and C. A. Smolders, "Selection of Elastomeric Membranes for the Removal of Volatile Organic Components from Water", in "Proceedings of Third Int. Conf. on Pervaporation Processes in the Chem. Ind.", Bakish Materials Corp., Englewood, NJ (1989), pp. 239-251.

Ohya, H., H. Matsumoto, Y. Negishi and K. Matsumoto, "Concentration of Ethanol from its Aqueous Solution by Pervaporation Using Porous Polypropylene Hollow-Fiber Membrane", Maku (Membrane Jap.) **11**, 231-238 (1986b).

Ohya, H., H. Matsumoto, Y. Negishi and K. Matsumoto, "Concentration of Acetone and n-Butanol from Aqueous Solutions by Pervaporation Using Porous Polypropylene Hollow-Fiber Membrane", Maku (Membrane Jap.) **11**, 285-296 (1986a).

Okabe, K., T. Kashiwagi, K. Okita and K. Nomura, "Membrane Separation of Ethanol-Water Mixtures Using Electromagnetic Field as External Energy", Abstracts of the 1987 International Congress on Membranes and Membrane Processes, ICOM'87, Tokyo (1987), pp. 247-248.

Okada, T. and T. Matsuura, "Predictability of Transport Equations for Pervaporation on the Basis of Pore-flow Mechanism", J. Membrane Sci. **70**, 163-175 (1992).

Okada, T. and T. Matsuura, "A New Transport Model for Pervaporation", J. Membrane Sci. **59**, 133-150 (1991).

Park, I. J., S. Lee and C. K. Choi, "Surface Properties for Poly (perfluoroalkylethyl methacrylate) / Poly (*n*-alkyl methacrylate)s Mixtures", J. Appl. Polym. Sci. **54**, 1449-1454 (1994).

Perry, R. H. and D. Green, Perry's Chemical Engineers' Handbook, 6th Ed., R. H. Perry and D. Green, Eds., McGraw Hill Inc., New York, NY (1984), Section 13, p. 59.

Perry, R. H. and C. H. Chilton, Perry's Chemical Engineers' Handbook, 5th Ed., R. H. Perry and C. H. Chilton, Eds., McGraw Hill Inc., New York, NY (1973), Section 3, p. 229-233.

Perry, E. and W. F. Strazik, "Process for the Separation of Diene from Organic Mixtures", US Patent, 3,789,079 (1974).

Petersen, R. J. and J. E. Cadotte, "Thin Film Composite Reverse Osmosis Membranes", in "Handbook of Industrial Membrane Technology", M. C. Porter, Ed., Noyes Publications, Park Ridge, NJ (1990), pp. 307-327.

Petersen, R. J., "Composite Reverse Osmosis and Nanofiltration Membranes", J. Membrane Sci. **83**, 81-150 (1993).

Pham, V., Y. Fang, H. Mahmud, J. P. Santerre, R. Nabaitz, T. Matsuura, "New Surface Modifying Macromolecules and Their Effect on the Pervaporation Performance of Polyethersulfone Membranes", manuscript prepared to be submitted to J. Appl. Polym. Sci. 1995.

Pham, V. A., "Surface Modifying Macromolecules to Enhance the Pervaporation Performance", M. A. Sc., Thesis, The University of Ottawa, Department of Chemical Engineering, Ottawa, ON (1995) Canada.

Ratner, B. D., S. C. Yoon, A. Kaul and R. Rahman, "Control of Polyurethane Surface Structure by Synthesis and Additives: Implications for Blood Interactions", in "Polyurethanes in Biomedical Engineering II", H. Planck, G. Egbers and I. Syré, Eds., Elsevier Science Publishers, Amsterdam (1987), pp. 213-229.

Ratner, B. D. and R. W. Paynter, "Polyurethane Surfaces: the Importance of Molecular Weight Distribution, Bulk Chemistry and Casting Conditions", in "Polyurethanes in Biomedical Engineering", H. Planck, G. Egbers and I. Syré, Eds., Elsevier Science Publishers, Amsterdam (1984), p. 41-68.

Rautenbach R., S. Klatt and J. Vier, "State of the Art of Pervaporation -- 10 years of Industrial Pervaporation", in "Proceedings of Sixth Int. Conf. on Pervaporation Processes in the Chem. Ind., Bakish Materials Corp., Englewood, NJ (1992), pp. 2-15.

Rautenbach, R. and R. Knauf, "Comparison of Pervaporation and Reverse Osmosis with Respect to Mass-Transfer Resistances", in the section of "Membrane-Based Organic/Organic Separation", in "Proceedings of the North American Membrane Society 7th Annual Meeting", Portland, Oregon, May 20-24, 1995.

Rautenbach, R. and R. Albrecht, "Membrane Processes", John Wiley & Sons Ltd., New York, NY (1989). pp. 391-395.

Riedo, F. and E. Kováts, "Adsorption from Liquid Mixtures and Liquid Chromatography", J. Chromatography **239**,1-28 (1982).

Schmidt, D. L., C. E. Coburn, B. M. DeKoven, G. E. Potter, G. F. Meyer and D. A. Fischer, "Water-based Non-stick Hydrophobic Coatings", Nature, **368**, 39-41 (1994).

Shimidzu, T. and H. Okushita, "Selective Separation of Cyclohexane-Cyclohexanone-Cyclohexanol Mixtures through Poly-(N-vinylpyrrolidone-co-acrylonitrile) Membrane", J. Membrane Sci. **39**, 113-123(1988).

Sikonia, J. G. and F. P. M. Candless, "Separation of Isomeric Xylenes by Permeation through Modified Plastic Films", J. Membrane Sci. **4**, 229-241(1978).

Somorjai, G. A., "Composition of Surfaces: Thermodynamic Guidelines and Experimental Results", in "Chemistry in Two Dimensions: Surface", Cornell University Press, Ithaca, NY (1981), Chap. 3, pp. 100-125.

Sourirajan, S. and T. Matsuura, "Transport through Reverse Osmosis, Part I, II" in "Reverse Osmosis/Ultrafiltration Process Principles", National Research Council Canada, Ottawa, ON (1985), pp. 79-357.

Sourirajan, S. "Separation of Hydrocarbon Liquids by Flow under Pressure through Porous Membranes", Nature **203**, 1348-1349 (1964).

Sourirajan, S., Lectures on Reverse Osmosis, Division of Chemistry, National Research Council Canada, Ottawa, ON (1983), p. 39.

Spiegler, K. S. and O. Kedem, "Thermodynamics of Hyperfiltration (Reverse Osmosis): Criteria for Efficient Membranes", Desalination **1**, 311-326 (1966).

Strathmann, H., "Synthetic Membranes and Their Preparation", in "Handbook of Industrial Membrane Technology", M. C. Porter, Ed., Noyes Publications, Park Ridge, NJ (1990), pp. 45-46.

Suematsu, H., K. Harada and T. Kataoka, "Separation of Ethanol-Water Mixtures Using Silicone Rubber Membrane", Maku (Membrane Jap.) **12**, 95-100 (1987).

Suzuki, F., K. Onozato and H. Yaegashi, "Pervaporation of Organic Solvents by Poly[bis(2,2,2-trifluoroethoxy) phosphazene] Membrane", J. Appl. Polym. Sci. **34**, 2197-2204 (1987).

Tam, C. M., "Use of Liquid Chromatography in Membrane Material Characterization", M. A. Sc. Thesis, The University of Ottawa, Department of Chemical Engineering, Ottawa, ON (1989), Canada, pp. 16-18.

Tanigaki, M., M. Yoshikawa and W. Eguchi, "Selective Separation of Alcohol from Aqueous Solution through Polymer Membrane", in "Proceedings of Second Int. Conf. on Pervaporation Processes in the Chem. Ind.", Bakish Materials Corp., Englewood, NJ (1987), pp. 126-133.

Thompson, J. A., "Method for the Modification of Polycabonate Membranes, the Membranes Produced by Such Method and their Use", US Patent 4,715,960 (1987).

Tusel, G. F. and H. E. A. Brüschke, "Use of Pervaporation Systems in the Chemical Industry", Desalination **52**, 327-328 (1988).

Uragami, T., Y. Sugitani and M. Sugihara, "Studies on Syntheses and Permeabilities of Special Polymer Membranes. 26. Preparation and Permeation Characteristics of Cellulose Membranes", Separation Sci. Tech. **17**, 307-317 (1982).

Van Ness, H. C., C. A. Soczek and N. K. Kochar, "Thermodynamic Excess Properties for Ethanol-n-Heptane", J. Chem. Eng. Data **12**, 346-351 (1967).

Wan, W., "Modified Regenerated Cellulose Membrane for Nonaqueous Separations", Eur. Pat. Appl. EP 145,127, Chem. Abstr. 103:125261n (1985).

Ward, R. S., K. A. White and C. B. Hu, "Use of Surface-Modifying Additives in the Development of a New Biomedical Polyurethaneurea", in "Polyurethanes in Biomedical Engineering", H. Planck, G. Egbers and I. Syré, Eds., Elsevier Science Publishers, Amsterdam (1984), pp. 181-200.

Wernick, D. L., "Cellulose Acetate Membrane and its Use for Polar Solvent-Oil Separation", US Patent 4,541,972 (1985).

Wijmans, J. G., J. Kaschemekat, J. E. Davidson and R. W. Baker, "Treatment of Organic-Contaminated Wastewater Streams by Pervaporation", Environmental Progress **9**, 262-268 (1990).

Yamasaki, A. and K. Mizoguchi, "Preparation of PVA Membranes Containing β-Cyclodextrin Oligomer (PVA/CD membrane) and their Pervaporation Characteristics for Ethanol/Water Mixtures", J. Appl. Polym. Sci. **51**, 2057-2062 (1994).

Yanagishita, H., C. Maejima, D. Kitamoto and T. Nakane, "Preparation of Asymmetric Polyimide Membrane for Water/Ethanol Separation in Pervaporation by the Phase Inversion Process", J. Membrane Sci. **86**, 231-240 (1994).

Yoshikawa, M., M. Tanigaki and W. Eguchi, "Selective Separation of Aqueous Ethanol Solution through Synthetic Polymer Membranes", Abstracts of the 1987 International Congress on Membranes and Membrane Processes, ICOM'87, Tokyo (1987), pp. 594-595.

Yu, X. H., A. Z. Okkema and S. L. Cooper, "Synthesis and Physical Properties of Poly (fluoroalkylether) Urethanes", J. Appl. Polym. Sci. **41**, 1777-1795 (1990).

Zhou, Q. H., S. Sourirajan and T. Matsuura, "A Transport Model for Reverse Osmosis Separation of Binary Organic Liquid Mixtures", Chem. Eng. Commun. **104**, 177-208 (1991).

Zhu, C., L. Moe and X. Wei, "Separation of Ethanol-Water Mixtures by Pervaporation Membrane Separation Process", Desalination **62**, 299-313 (1987).

Zhu, C., C.-W. Yuang, F. R. Fried and D. B. Greenberg, "Pervaporation Membrane -- a Novel Separation Techniques for Trace Organics", Environmental Progress **2**, 132-143 (1983).

Appendix A Materials

All chemicals were from BDH Inc., Toronto, Ontario, except those stated below.

Cellulose acetate butyrate (CAB-171-40) was from Eastman Kodak Company, Rochester, New York. The code designation was explained by the following chart.

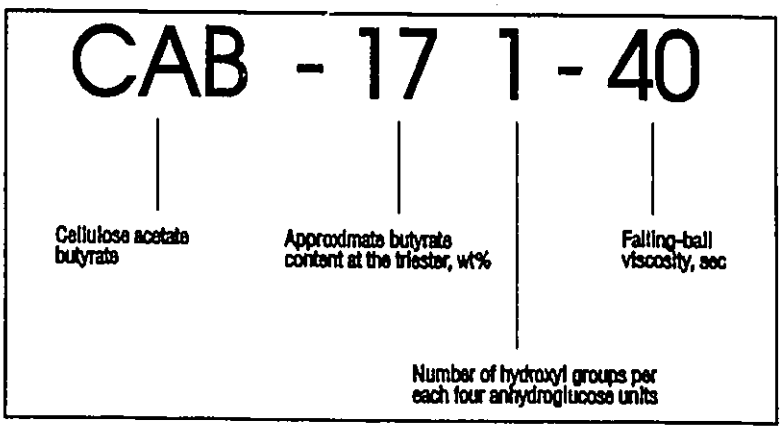

Code designation of cellulose acetate butyrate

Polyethersulfone (PES) was Victrex 4800P from ICI Advanced Materials Company, Billingham, Cleveland, England.

Polyvinylpyrrolidone (PVP) was from Sigma Chemical Company, St. Louis, Missouri.

Helium, nitrogen and compressed gas were supplied by Air Products Canada, Nepean, Ontario.

Deuterium oxide was from Aldrich Chemical Company, Inc., Milwaukee, Wisconsin.

The materials used for the synthesis included methylene bis-phenyl diisocyanate (MDI) (obtained from Eastman Kodak, Rochester, NY), polypropylene diol of average molecular weight 425 (PPO) (Aldrich Chemical Company, St. Louis, MO), fluorotelomer intermediate (Zonyl BA-L™) (Dupont Chemical, distributed by Van Waters & Roger in Montreal, Quebec) and for solvent N,N-dimethylacetamide (DMAc) (99%) (Aldrich Chemical Company, St. Louis, MO).

Prior to use, MDI was vacuum distilled at 0.025 mmHg. PPO was degassed for 24 hours at 0.5 mmHg. Fluorotelomer intermediate was vacuum distilled to yield three major fractions. The fraction used in the synthesis was a colourless liquid, with boiling temperature range from 50 to 55°C at pressure of 0.025 mmHg.

Appendix B Synthesis of Surface Modifying Macromolecules (SMM)

The surface modifying macromolecules were synthesized using a two-step solution polymerization. The polymerization was carried in a Labconco controlled atmosphere glove box containing dried nitrogen gas. The reaction solvent was distilled at 0.5 mmHg within 24 hours of the synthesis. The synthesis procedure is summarized as follows.

Polypropylene diol of average molecular weight 425 (PPO) was dissolved in 100 mL of N,N-dimethylacetamide (DMAc) (0.08 wt/wt) and transferred into the reaction vessel, then 50 mL of a methylene bis-phenyl diisocyanate (MDI)-DMAc solution (0.13 wt/wt) was added at once into the reaction vessel. Once the MDI addition was completed, the reacting solution temperature was kept at 40-50°C for 3 hours. Stirring and heating were accomplished using a Thermix™ Magnetic Stirring Hotplate model 210T with the following parameters: magnetic stirring bar length: 2", stirrer setting: 2 and periodic heating at low setting to keep the temperature range. After two and a half hours, the reacting solution was allowed to cool gradually, so at the end of the three hours period the temperature would be about 35°C, then 50 mL of the fluorotelomer intermediate (Zonyl BA-L™)-DMAc solution (0.13 wt/wt) was added at once to the reaction vessel. This reaction step was carried out for about 15 hours at room temperature. After the reaction was complete, the macromolecule solution was precipitated in distilled water, and then was washed five more times with distilled water to remove solvent and unreacted components. The macromolecules were then dried in a 50°C oven for two days to remove all water and trace solvent. The last step consisted of reducing the size of the macromolecules and washing three times with 1,1,2-trichloro-trifluoroethane. This step was necessary to remove all unreacted fluorotelomers. The washed

materials were then dried in a 50°C oven for three days to evaporate trace amount of 1,1,2-trichloro-trifluoroethane. Complete macromolecule nomenclature, reaction stoichiometry, description and relative molecular weight are provided in Table 1.

Table 1: Reaction stoichiometry and macro-characteristics of the surface modifying macromolecules (SMM)

Fluoropolymer: MDI / PPO(425) / BA-L (Low)		
MDI	PPO	BA-L
3 moles	2 moles	2 moles
Number Average:1.1×10^4,	Weight Average: 1.7×10^4,	Polydispersity: 1.5
Description:	Dry white solids	

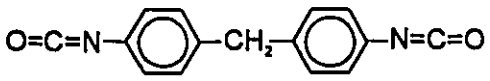

methylene bis-phenyl diisocyanate (MDI)

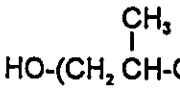

polypropylene diol (PPO)

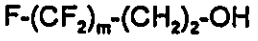

Zonyl BA-L™ fluorotelomer (BA-L)

Structures of chemicals for SMM synthesis.

Step 1 - The prepolymer reaction:

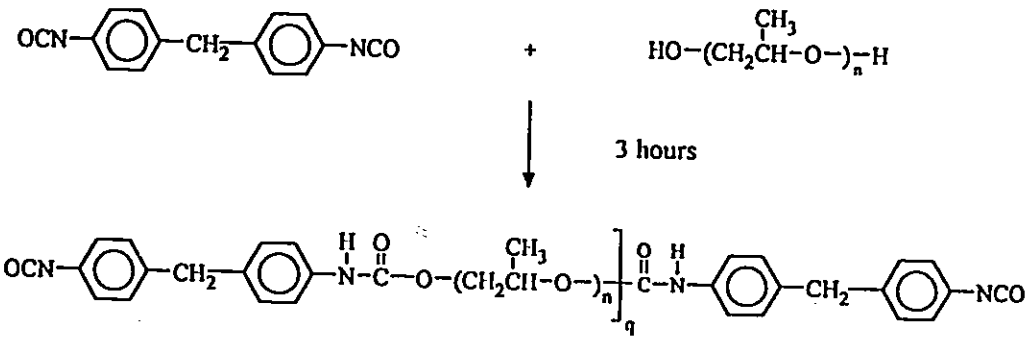

Step 2 - Reacting isocyanate-terminated prepolymer with fluorotelomer: +

2 moles of $F_3C-(-CF_2-)_m-CH_2-CH_2-OH$

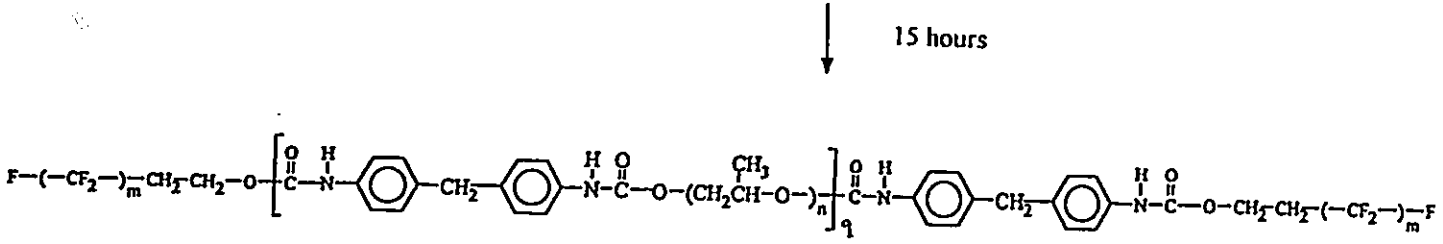

Steps of the synthesis.

Appendix C SMM code

SMM code used in this work	The equivalent code used by Mr. V. A. Pham
SMM40	MPB322HN
SMM41	MPB322LR
SMM58	MPB212HN
SMM44	MPB212LN

Appendix D A Description of Downstream Pressure Control in Pervaporation

The downstream pressure in pervaporation test was controlled by a system comprising a pressure transducer (MKS Instruments Canada, Ltd., Nepean, Ontario, Model 122AA-00100AB), an exhaust throttle valve (MKS Instruments Canada, Ltd., Model 253A-20-40-1), a pressure controller (MKS Instruments Canada, Ltd., Model 651), and a vacuum pump (Welch Vacuum Tech, Inc., Skokie, Illinois, Welch DuoSeal™ vacuum pump, Model No. 1400). A schematic diagram of the downstream pressure control system is given in the following figure.

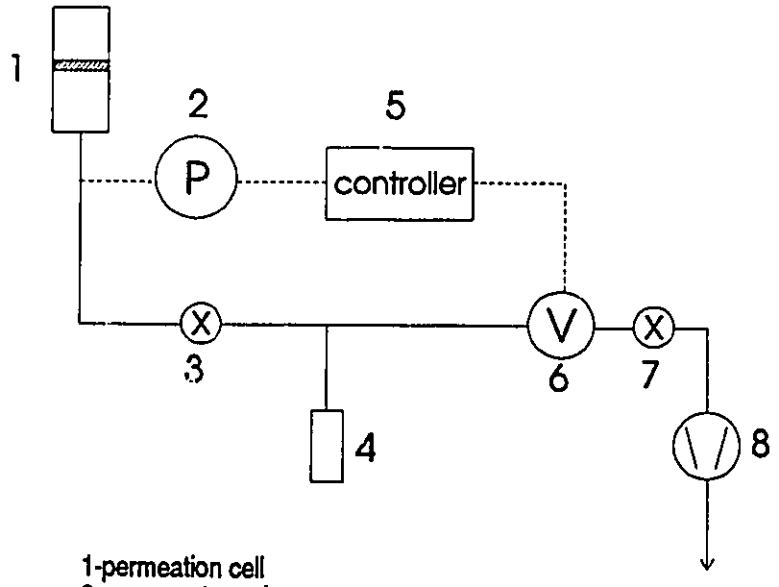

A schematic diagram of downstream pressure control in pervaporation.

The operation of the system is described as follows.

1. Start the pervaporation experiment.

2. Input the pressure setting, e.g., 3 torr, into the pressure controller and designate it as Setting A by pressing the "A" button on the instrument panel.

3. Press the "Learn" button and hold it for 3 seconds. This enables the pressure controller to "learn" the flow pattern of the permeate. Depending on the flow rate of the permeate, it takes about 2-5 minutes to finish this procedure. When the green light on the instrument panel showing "ready" is on, it means the procedure is successful and the controller is ready.

4. Activate the control system by pressing the "A" button on the instrument panel. The downstream pressure will gradually be adjusted to reach the set pressure. Typically it takes 5-15 minutes to reach the set pressure. If the set pressure can not be reached, repeat steps 3 and 4 several times until the set pressure is reached.

Appendix E Calibration curve for chloroform concentration

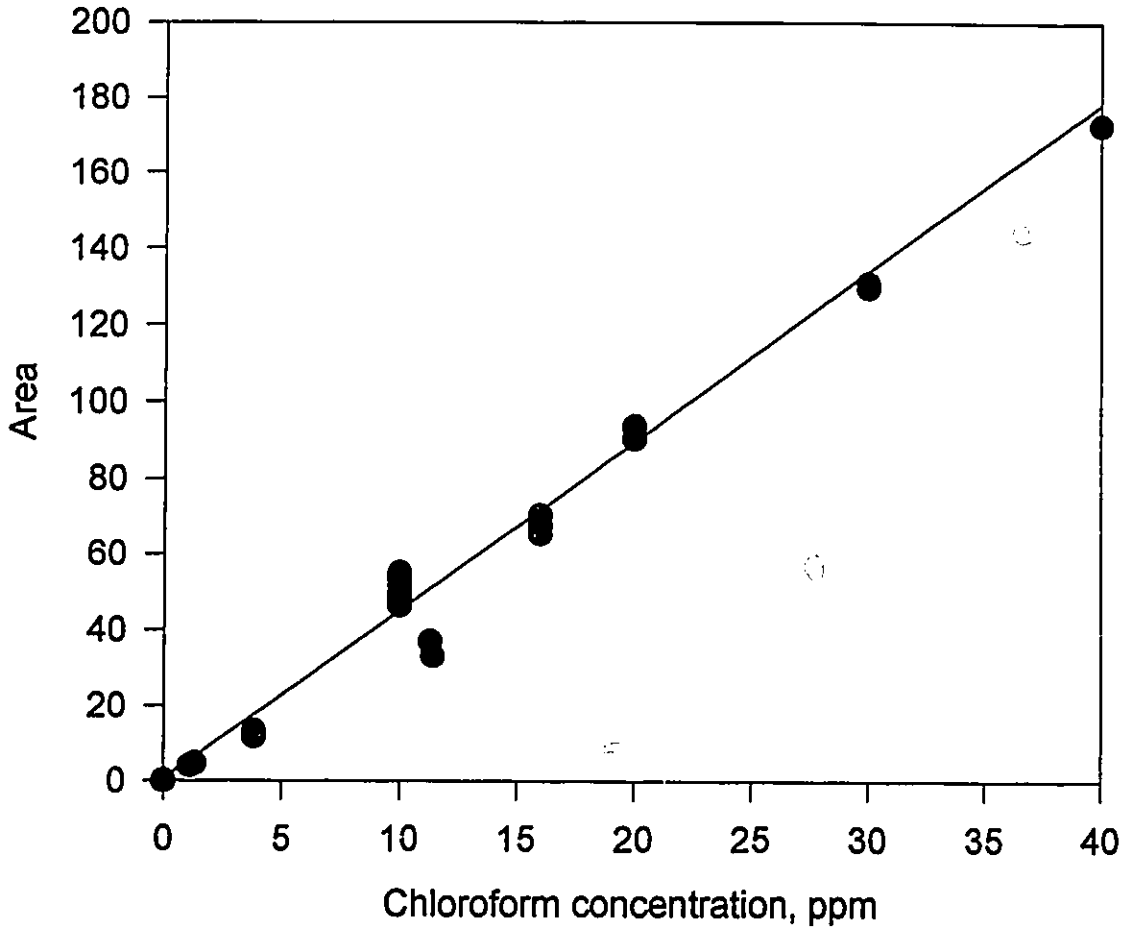

Appendix F Estimation of fluorine content in the dry membrane

Suppose 1.5 wt % SMM was added in the casting solution. Then, the membrane casting solution was made of following components (wt %):

polyethersulfone (PES):	25.0%
polyvinylpyrrolidone (PVP):	6.0%
SMM:	1.5%
dimethylacetamide:	67.5%

When the above solution was cast into a membrane and gelled in the water, dimethylacetamide as a solvent was supposed to leach out completely. Further, assume that PVP is retained inside the membrane, as Matsuura and co-workers (Miyano et al., 1990) indicated. Then, the dry membrane was considered to be made of PES, PVP and SMM. From the elemental analysis results, SMM had 19 wt % of fluorine element. Therefore, the fluorine wt % in the dry membrane was estimated by:

1.5 (SMM) × 19% (F% in SMM) ÷ [25 (PES) + 6 (PVP) +1.5 (SMM)] = 0.88%

That is to say, the dry membrane, corresponding to 1.5 wt % SMM added to the membrane casting solution, contains 0.88 wt % of fluorine in the dry membrane.

PES has the chemical formula $[-C_{12}H_8O_3S-]_n$
Weight of the repeat unit= 12C+8H+3O+1S=12×12.0+8×1.0+3×16.0+1×32.1=232.1
To calculate the elemental weights in 25 g of PES
C weight = C wt % × 25 = (12C/232.1)× 25 = (12×12.0/232.1) × 25 = 15.51 g
H weight = H wt % × 25 = (8H/232.1) × 25 = (8× 1.0/232.1) × 25 = 0.86 g
O weight = O wt % × 25 = (3O/232.1) × 25 = (3×16.0/232.1) × 25 = 5.17 g
S weight = S wt % × 25 = (1S/232.1) × 25 = (1×32.1/232.1) × 25 = 3.46 g

PVP has the chemical formula $[-C_6H_9ON-]_n$
Weight of the repeat unit = 6C+9H+1O+1N=6×12.0+9×1.0+1×16.0+1×14.0=111.0
To calculate the elemental weights in 6 g of PVP:
C weight = C wt % × 6 = (6C/111.0) × 6 = (6×12.0/111.0) × 6 =3.89 g
H weight = H wt % × 6 = (9H/111.0) × 6 = (9×1.0/111.0) × 6 =0.49 g
O weight = O wt % × 6 = (1O/111.0) × 6 = (1×16.0/111.0) × 6 =0.86 g

N weight = N wt % × 6 = (1N/111.0) × 6 = (1×14.0/111.0) × 6 =0.76 g

To calculate the elemental weights in 1.5 g of SMM:
C weight = C wt % × 1.5 = 51.31 %* × 1.5 =0.77 g
H weight = H wt % × 1.5 = 5.12 %* × 1.5 =0.08 g
O weight = O wt % × 1.5 =20.79 %* × 1.5 =0.31 g
N weight = N wt % × 1.5 = 3.78 %* × 1.5 =0.06 g
F weight = F wt % × 1.5 =19.00 %* × 1.5 =0.29 g

*determined by elemental analysis.

Thus,
Total C weight = 15.51+3.89+0.77=20.17 g
Total H weight = 0.86+0.49+0.08=1.43 g
Total O weight = 5.17+0.86+0.31=6.34 g
Total N weight = 0.76+0.06=0.82 g
Total S weight = 3.46 g
Total F weight = 0.29 g
Total mass = 25 g PES + 6 g PVP +1.5 g SMM = 32.5 g

Therefore,
C wt %=20.17/32.5=62.1%
H wt %=1.43/32.5=4.4%
O wt %=6.34/32.5=19.5%
N wt %=0.82/32.5=2.5%
S wt %=3.46 /32.5=10.6%
F wt %=0.29/32.5=0.89%

Using the procedure in Appendix G, fluorine wt % is converted to fluorine atomic % by

$$F\ atomic\ \% = \frac{\frac{0.89\%}{19.0}}{\frac{62.1\%}{12.0}+\frac{4.4\%}{1.0}+\frac{19.5\%}{16.0}+\frac{2.5\%}{14.0}+\frac{10.6\%}{32.1}+\frac{0.89\%}{19.0}} = 0.41\%$$

In the case that no PVP is retained in the membrane, similar calculations give:
Total C weight = 15.51+0+0.77=16.29 g

Total H weight = 0.86+0+0.08=0.94 g
Total O weight = 5.17+0+0.31=5.48 g
Total N weight = 0+0.06=0.06 g
Total S weight = 3.46+0=3.46 g
Total F weight = 0.29 g
Total mass = 25 g PES + 0 g PVP +1.5 g SMM = 26.5 g

Therefore,
C wt %=20.17/26.5=61.5%
H wt %=1.43 /26.5=3.5%
O wt %=6.34 /26.5=20.7%
N wt %=0.82/26.5=0.2%
S wt %=3.46 /26.5=13.0%
F wt %=0.29 /26.5=1.1%

Using the procedure in Appendix G, fluorine wt % is converted to fluorine atomic % by

$$F\ atomic\ \% = \frac{\frac{1.1\%}{19.0}}{\frac{61.5\%}{12.0}+\frac{3.5\%}{1.0}+\frac{20.7\%}{16.0}+\frac{0.2\%}{14.0}+\frac{13.0\%}{32.1}+\frac{1.1\%}{19.0}} = 0.56\%$$

Compared with a 0.44 atomic % assuming that PVP is fully retained, one knows that F atomic % is little affected by whether PVP is retained or not, for the composition involved.

Using the procedure given in Appendix G, the ratio F/C is calculated by:

$$\frac{F\,wt\%}{C\,wt\%}\times\left(\frac{C}{F}\right)$$

In the case of all PVP being retained,
the ratio F/C = (0.89%/62.1%) × (12/19) = 0.0091

In the case of no PVP being retained,
the ratio F/C = (1.1%/61.5%) × (12/19) = 0.011

Appendix G Conversion from fluorine wt % to fluorine atomic %

Elemental analysis results are expressed as a weight percentage (wt %), while XPS results show the atomic percentage (atomic %). Therefore, it is necessary to convert the wt % to the atomic % in order to compare these results. Following calculations show this conversion.

Elemental analysis of SMM44 shows the wt % of constituent elements as follows:

N 3.78 %

C 51.31 %

F 19.00 %

O 20.79 %

H 5.12 %

where N, C, F, O, H represent the nitrogen, carbon, fluorine, oxygen and hydrogen elements, respectively. The fluorine wt % is converted to atomic % by

$$F\ atomic\ \% = \frac{\frac{F\ wt\%}{F}}{\frac{N\ wt\%}{N} + \frac{C\ wt\%}{C} + \frac{F\ wt\%}{F} + \frac{O\ wt\%}{O} + \frac{H\ wt\%}{H}} \times 100$$

Substituting the elemental atomic weights into the above equation, then, 19 wt % of fluorine is converted into atomic % by:

$$F\ atomic\ \% = \frac{\frac{19.00\%}{19}}{\frac{3.78\%}{14} + \frac{51.31\%}{12} + \frac{19.00\%}{19} + \frac{20.79\%}{16} + \frac{5.12\%}{1}} \times 100 = 8.36\%$$

That is to say, 19 wt % of fluorine is equivalent to 8.36 atomic % of fluorine.

Similarly, we have

$$C\ atomic\ \% = \frac{\frac{C\ wt\%}{C}}{\frac{N\ wt\%}{N} + \frac{C\ wt\%}{C} + \frac{F\ wt\%}{F} + \frac{O\ wt\%}{O} + \frac{H\ wt\%}{H}} \times 100$$

Therefore, the atomic ratio of F/C can be calculated as

$$the\ ratio\ of\ \frac{F}{C} = \frac{\frac{F\ wt\ \%}{F}}{\frac{C\ wt\ \%}{C}} = \frac{F\ wt\ \%}{C\ wt\ \%} \times \left(\frac{C}{F}\right)$$

Substituting the numerical values, F wt %=19.00%, C wt %=51.31%, we have the ratio of F/C = (19.00%/51.31%) × (12/19) = 0.23

Appendix H Calculation of Stokes' Radius

To calculate Stokes' radius, the diffusivity term is first estimated by the Wilke-Chang equation (Perry, 1973) and then Stokes' radius is calculated from the Stokes' equation (Sourirajan 1983).

The Wilke-Chang equation is:

$$D_L\mu/T = 7.4 \times 10^{-8} (X \cdot M)^{0.5} / V_b^{0.6} \quad (37)$$

where D_L = diffusivity of solute at infinite dilution, cm^2/sec; μ=solution viscosity, centipoise; T=absolute temperature, K; X=association parameter; M=solvent molecular weight; V_b = molar volume of solute at normal boiling point, cm^3/mol.

Unit conversion factor used in the calculation is:

$1\ (cm^2)\ (cp)/\ (s \cdot K) = (1 \times 10^{-4}\ m^2)[1 \times 10^{-3}\ (N)(s)/m^2]/(s \cdot K) = 1 \times 10^{-7}\ N/K$

All physicochemical properties necessary for the calculation of diffusivity by Equation (37) are listed in the following table.

Property data for the Wilke-Chang equation (Perry, 1973)

Solvent	X	M (g/mole)	V_b
ethyl alcohol	1.5	46.07	59.2
n-heptane	1.0	100.20	162.8
hexane	1.0	86.17	140.6
vinyl acetate	1.0	86.09	99.8

The Stokes' equation is:

$$D_L = kT/ (6\pi\mu r_{AB}) \quad (38)$$

where k, T, μ and r_{AB} are the Boltzmann constant, absolute temperature, solvent viscosity and the solute radius, respectively.

Rearranging:

$$r_{AB} = k / [6\pi (D_L\mu/T)_{AB}] \quad (39)$$

For ethyl alcohol (A) in solvent heptane (B):

$M=M_{solvent}=100.20$, $V_b=(V_b)_{solute}=59.2$, X=1.0 (heptane is solvent).
From Equation (37):

$$(D_L\mu/T)_{A\ in\ B} = 7.4 \times 10^{-8} [(1.0)(100.20)]^{0.5}/ (59.2)^{0.6}$$
$$= 6.401\times 10^{-8}\ (cm^2)(cp)/(s\cdot K)$$
$$= 6.401\times 10^{-15}\ N/K$$

Substituting into Equation (39):
$r_{AB} = 1.38048 \times 10^{-23}\ J/K / [(6)(3.1416)\ (6.401\times 10^{-15}\ N/K)] = 1.1 \times 10^{-10}\ m$

For heptane (B) in solvent ethyl alcohol (A):

$M=M_{solvent}=46.07$, $V_b=(V_b)_{solute}=162.8$, X=1.5 (ethyl alcohol is solvent).
From Equation (37):

$$(D_L\mu/T)_{B\ in\ A} = 7.4 \times 10^{-8} [(1.5)(46.07)]^{0.5}/ (162.8)^{0.6}$$
$$= 2.897 \times 10^{-8}\ (cm^2)(cp)/(s\cdot K)$$
$$= 2.897 \times 10^{-15}\ N/K$$

Substituting into Equation (39):

$r_{BA} = 1.38048 \times 10^{-23}$ J/K / [(6)(3.1416) $(2.897 \times 10^{-15}$ N/K)] = 2.5×10^{-10} m

Similarly,

<u>for hexane (A) in solvent vinyl acetate (B):</u>

$(D_L\mu/T)_{A \text{ in } B} = 7.4 \times 10^{-8}$ [(1.0)(86.09)]$^{0.5}$/ $(140.6)^{0.6}$

$= 3.53 \times 10^{-8}$ $(cm^2)(cp)/(s \cdot K)$

$= 3.53 \times 10^{-15}$ N/K

$r_{AB} = 1.38048 \times 10^{-23}$ J/K / [(6)(3.1416) $(3.53 \times 10^{-15}$ N/K)] = 2.07×10^{-10} m

<u>for vinyl acetate (B) in solvent hexane (A):</u>

$(D_L\mu/T)_{B \text{ in } A} = 7.4 \times 10^{-8}$ [(1.0)(86.17)]$^{0.5}$/ $(99.8)^{0.6}$

$= 4.34 \times 10^{-8}$ $(cm^2)(cp)/(s \cdot K)$

$= 4.34 \times 10^{-15}$ N/K

$r_{BA} = 1.38048 \times 10^{-23}$ J/K / [(6)(3.1416) $(4.34 \times 10^{-15}$ N/K)] = 1.69×10^{-10} m

Appendix I Pervaporation data for PES membrane with various evaporation periods

Evaporation period	0 wt % SMM		1.0 wt % SMM	
minutes	$[CHCl_3]$,ppm	rate,g/h	$[CHCl_3]$,ppm	rate,g/h
1	500	2.40	750	1.12
3	280	0.03	38	0.07
5	27	0.27	19	0.23

Casting solution composition: see Table 9.

Feed: 1000 ppm chloroform/water.

Appendix J Pervaporation data for PES membrane with various SMM wt %

SMM wt %	$[CHCl_3]$, ppm	rate,g/h
0	58	0.046
0.5	N/D*	0.025
1	2.0	0.021
1.5	N/D	0.023
2	N/D	0.024
2.5	2.0	0.046
3	14	0.059

* N/D means not detected.

Casting solution composition: see Section 4.1.6.

Feed: 1000 ppm chloroform/water.

Appendix K Pervaporation performance versus running time

[SMM]=0%			[SMM]=0.5%			[SMM]=1.0%		
Hours	[$CHCl_3$] ppm	Rate g/h	Hours	[$CHCl_3$] ppm	Rate g/h	Hours	[$CHCl_3$] ppm	Rate g/h
9.7	30	0.034	9.4	N/D	0.018	9.4	1	0.029
19.1	50	0.042	19.9	N/D	0.018	19.9	5	0.025
29.6	60	0.047	29.9	N/D	0.025	29.9	2	0.021
39.6	58	0.046						

Casting solution composition: see Section 4.1.7.

Feed: 1000 ppm chloroform/water.

Appendix L Pervaporation data for PES membrane with various feed concentration

Feed conc.	0 % SMM		0.5 % SMM	
ppm	[$CHCl_3$],ppm	rate,g/h	[$CHCl_3$],ppm	rate,g/h
100	11	0.033	15	0.038
300	8	0.031	40	0.050
500	48	0.037	2	0.015
700	23	0.045	N/D	0.020
1000	58	0.046	N/D	0.025

Casting solution composition: see Section 4.1.8.

Appendix M Pervaporation data for PES membrane with various PVP wt %

	No SMM		1% SMM	
PVP %	[$CHCl_3$],ppm	rate,g/h	[$CHCl_3$],ppm	rate,g/h
0	N/D	0.021	5	0.085
1	3	0.016	N/D	0.075
2	N/D	0.022	11	0.22
3	13	0.029	2300	0.70
4	1	0.078	3900	0.39
8	33	0.133	4100	0.40

Casting solution composition: see Table 12.

Feed: 1000 ppm chloroform/water.

Appendix N Pervaporation data for PES/SMM membrane/Ethyl alcohol/heptane

	No SMM		1 % SMM	
EtOH mol % in feed	EtOH mol % in permeate	rate g/h	EtOH mol % in permeate	rate g/h
0	0	0.65	0	0.77
0.1	0.50	0.49	0.42	0.48
0.5	0.98	0.46	0.90	0.55
0.9	0.99	0.62	0.99	0.60
1	1	0.76	1	0.59

Appendix O Contact angle data for PES/SMM membrane

SMM%	Advancing contact angle (°)	Receding contact angle (°)
0	68.0	21.0
0.5	105.5	51.2
1	106.2	51.7
2	113.4	61.3

Casting solution composition: see Section 4.1.4.

Appendix P XPS data for PES membrane containing various SMM %

The ratio of $-CF_2-$ to $-CF_3$ fragment of an SMM in XPS measurements was obtained by deconvolution of the C1s XPS signal into several peaks.

[SMM]=0.5%			
Element	Atomic % at 90°	Atomic % at 45°	Atomic % at 15°
F	2.57	3.36	2.50
O	16.87	17.44	17.41
N	3.44	3.43	2.57
C	73.40	71.97	71.13
S	3.08	2.83	0.64
Si	0.63	0.96	5.74

[SMM]=1%			
Element	Atomic % at 90°	Atomic % at 45°	Atomic % at 15°
F	2.46	2.89	0.59
O	17.13	16.34	18.13
N	3.07	3.17	2.97
C	73.24	74.12	70.29
S	3.53	3.29	0.80
Si	0.56	0.17	7.22

[SMM]=1.5%			
Element	Atomic % at 90°	Atomic % at 45°	Atomic % at 15°
F	15.68	18.09	30.44
O	14.67	14.40	12.44
N	3.90	40.28	3.40
C	63.95	61.90	52.84
S	1.58	1.24	0.64
Si	0.22	0.09	0.25

[SMM]=2%			
Element	Atomic % at 90°	Atomic % at 45°	Atomic % at 15°
F	15.14	16.96	23.23
O	15.15	15.06	12.93
N	4.29	4.76	3.63
C	63.60	61.77	59.34
S	1.71	1.27	0.86
Si	0.10	0.17	0.00

[SMM]=2.5%			
Element	Atomic % at 90°	Atomic % at 45°	Atomic % at 15°
F	22.57	24.27	32.53
O	12.97	12.92	11.41
N	4.17	3.88	2.11
C	58.14	56.48	49.51
S	1.00	0.69	0.95
Si	1.14	1.75	3.48

[SMM]=3%			
Element	Atomic % at 90°	Atomic % at 45°	Atomic % at 15°
F	22.26	25.57	37.03
O	11.55	10.63	9.20
N	4.41	4.07	2.89
C	60.47	59.04	50.47
S	1.31	0.69	0.41
Si	0.00	0.00	0.00

[SMM]=3.5%			
Element	Atomic % at 90°	Atomic % at 45°	Atomic % at 15°
F	25.86	29.05	37.41
O	10.71	10.24	8.59
N	4.78	4.64	2.43
C	58.32	55.82	51.13
S	0.32	0.24	0.35
Si	0.00	0.00	0.08

Casting solution composition: see Section 4.1.4.

Appendix Q XPS data for PES membrane containing various PVP %

[PVP]=0%		
Element	Atomic % at 90°	Atomic % at 15°
F	15.18	37.05
O	16.13	10.58
N	3.51	1.47
C	64.36	49.88
S	0.33	0.14
Si	0.49	0.87

[PVP]=0.5%		
Element	Atomic % at 90°	Atomic % at 15°
F	12.02	29.48
O	16.69	13.75
N	3.90	2.40
C	64.71	50.39
S	1.03	0.43
Si	1.65	3.56

[PVP]=1.0%		
Element	Atomic % at 90°	Atomic % at 15°
F	13.10	31.60
O	15.61	11.70
N	4.03	2.45
C	66.04	52.90
S	0.77	0.25
Si	0.46	1.11

[PVP]=2.0%		
Element	Atomic % at 9[illegible]	Atomic % at 15°
F	6.45	20.07
O	19.97	15.61
N	2.19	2.23
C	67.63	59.23
S	2.89	1.25
Si	0.87	1.61

Casting solution composition: see Table 12 except PVP % as indicated in this appendix.